FROM CHRONIC OBSTRUCTIVE PULMONARY DISEASE TO LUNG CANCER: AN IMMUNOLOGIC APPROACH

Daniel Ramis Cabrer

UPF DOTORAL THESIS / 2019

Thesis director:

Dr. Esther Barreiro

Department of Experimental and Health Sciences

Universitat Pompeu Fabra Barcelona

“Most people say that it is the intellect which makes a great scientist. They are wrong: it is character”

Albert Einstein

A mi familia y amigos,
que aún en la distancia
han estado siempre tan cerca.

Y a todos aquellos
que han sido aquí tan gran apoyo.

TABLE OF CONTENTS

Page

ABSTRACT..... 1

RESUMEN..... 3

PREFACE..... 5

ABBREVIATIONS..... 7

INTRODUCTION..... 11
1. RESPIRATRY SYSTEM..... 13
1.1. Structure and anatomy..... 13
1.2. Physiology and measurements..... 17
2. LUNG CANCER..... 19
2.1. Epidemiology..... 19
2.2. Etiologic factors..... 20
2.3. Diagnosis..... 22
2.3.1. Histopathological subtypes..... 22
2.3.2. Staging of LC..... 23
2.4. Therapeutic strategies in LC..... 25
2.4.1. Surgery..... 25
2.4.2. Chemotherapy..... 25
2.4.3. Biological therapies..... 26
2.4.3.1. Tyrosine kinase inhibitors..... 27
2.4.3.2. Immune checkpoint inhibitors..... 28
2.5. Prognosis and survival in LC..... 30
2.5.1. Survival prediction and early detection markers... 30
3. CHRONIC OBSTRUCTIVE PULMONARY DISEASE..... 33
3.1. Epidemiology..... 33
3.2. Etiologic factors..... 33
3.3. Pathophysiology..... 34
3.4. Clinical symptoms and manifestations..... 35
3.5. Classification of COPD..... 36
4. RELATIONSHIPS BETWEEN LC AND COPD..... 37
4.1. Epidemiology..... 37

4.2. Etiology..... 40
4.3. Pathophysiology..... 41
5. PATHOPHYSIOLOGIC MECHANISMS OF LC DEVELOPMENT..... 42
5.1. Nitrosative and oxidative stress..... 42
5.2. Tumor microenvironment..... 44
5.3. Inflammation..... 47
5.4. Immune system..... 49
5.4.1. Tertiary lymphoid structures..... 49
5.5. Cell growth and proliferation..... 51
5.6. Apoptosis..... 52
5.7. Autophagy..... 53
6. MURINE MODELS OF LC..... 55
6.1. Syngeneic models..... 56

HYPOTHESIS..... 59

OBJECTIVES..... 63
STUDY 1..... 65
STUDY 2..... 66

METHODS..... 67
1. STUDY 1..... 69
1.1. Study design and ethics..... 69
1.2. Clinical assessment..... 70
1.3. Sample collection and preservation..... 70
1.4. Identification of T and B cells, Treg cells, plasmatic cells and TLSs in the lung specimens..... 71
1.5. Identification of GCs in TLSs of lung specimens..... 74
1.6. Identification of NK cells in lung specimens..... 75
1.7. Statistical analyses..... 76
2. STUDY 2..... 77
2.1. Animal experiments..... 77
2.1.1. Tumor development..... 77
2.1.2. Experimental design..... 77
2.1.3. Ethics..... 79
2.1.4. In vivo measurements conducted on the animals.. 79
2.1.5. Sacrifice and sample collection..... 80
2.2. Molecular biology analyses..... 80
2.2.1. Immunoblotting of 1D electrophoresis..... 80
2.2.2. Histological analyses of the tumor..... 83

2.3. Statistical analyses..... 85

RESULTS..... 87
1. STUDY 1..... 89
1.1. Clinical characteristics..... 89
1.2. Number and area of TLSs and GCs in lung specimens..... 90
1.3. Number of T and B cells in lung specimens..... 90
1.4. Number of Treg and NK cells in lung specimens..... 91
1.5. IgG and IgA secreting plasmatic cells in lung specimens..... 91
2. STUDY 2..... 102
2.1. Monoclonal antibodies administration reduces tumor burden and increases body weight in mice..... 102
2.2. Immunomodulators increase immune cell levels in the tumor microenvironment..... 102
2.3. Immunomodulators enhances oxidative stress in the tumor microenvironment..... 102
2.4. Increased levels of apoptosis and autophagy in response to immunomodulation..... 103

DISCUSSION..... 113
Differential immune profile between LC patients and LC patients underlying COPD..... 115
Altered TME in LC-bearing mice after immunomodulatory monoclonal antibodies administration..... 126

CONCLUSIONS..... 141

FUTURE PERSPECTIVES..... 145

REFERENCES..... 149

ABSTRACT

It is well established that a subset of cancer patients debuts with immune infiltrates, which organize into aggregates in the tumor niche and its vicinity. These lymphoid structures develop in response to inflammatory *stimuli* through a tightly regulated process. Besides the prognostic value of TLSs, they also may represent a novel avenue for therapeutic strategies, but it is currently still in its early stages. In contrast with the immune activator role of TLSs, in certain cancers, its effect may point towards tumor progression as a consequence of highly tumor-mediated immunosuppressive conditions present in the tumor niche. Preliminary data provided by the current investigation suggests that a differential immune profile may be present between LC patients and LC patients underlying COPD. This fact could present a potential impact in the prognosis and therapy of these patients. Moreover, crucial markers targeting different signaling pathways involved with oxidative stress, apoptosis, and autophagy were found to be overexpressed in response to immunomodulators administration in the current thesis. These data puts into manifest the interest of additional immunity-related mechanisms that could be targeted in order to assist immunity against cancer.

Keywords: lung cancer, COPD, immunosuppression, oxidative stress, autophagy

RESUMEN

Se ha establecido que un subconjunto de pacientes con cáncer debuta con infiltrados inmunes que se organizan en agregados en el nicho tumoral y sus alrededores. Estas estructuras linfoides se desarrollan en respuesta a estímulos inflamatorios a través de un proceso estrechamente regulado. Además de su valor pronóstico, las TLSs pueden representar una nueva vía para las estrategias terapéuticas, pero actualmente se encuentra en etapas iniciales. En contraste con el papel en la activación inmune de las TLSs, en ciertos tumores, su efecto puede apuntar hacia la progresión tumoral como consecuencia de las condiciones altamente inmunosupresoras mediadas por las células malignas presentes en el nicho tumoral. Los datos preliminares proporcionados por la siguiente investigación sugieren que los pacientes con cáncer de pulmón podrían presentar un perfil inmunitario diferencial respecto a estos mismos que además subyacen EPOC. Este hecho podría presentar un impacto potencial en el pronóstico y la terapia de estos pacientes. Por otra parte, resultados procedentes de la actual investigación también revelan que ciertos marcadores cruciales presentes en diferentes vías de señalización involucradas con el estrés oxidativo, la apoptosis y la autofagia podría sobre expresarse en respuesta a la administración de inmunomoduladores. Estos datos ponen de manifiesto el interés de mecanismos adicionales relacionados con la inmunidad que podrían ser manipulados para asistir a la inmunidad contra el cáncer.

Palabras clave: cáncer de pulmón, EPOC, inmunosupresión, estrés oxidativo, autofagia

PREFACE

Scientific collaborations

In the present thesis, the investigations have been performed in the Muscle Wasting and Cachexia in Chronic Respiratory Diseases and Lung Cancer Research group, Hospital del Mar Medical Research Institute (IMIM), Barcelona, Spain.

Research was conducted in collaboration with the Pulmonology Department, the Thoracic Surgery Department and the Pathology Department at Hospital del Mar, Parc de Salut Mar, Barcelona, Spain.

Funding

The different investigations that are included in the current thesis have been supported by: CIBERES (Instituto de Salud Carlos-III), FIS 14/00713 (FEDER), FIS 18/00075, SEPAR 2016, SEPAR 2018, FUCAP 2016, and Unrestricted grant from Menarini SA 2018 (Spain).

Acknowledgements

I would like to manifest my deepest greetings to Dr. Esther Barreiro, Dr. Víctor Curull, Dr. Lara Pijuán, Dr. Mercè Mateu-Jiménez, Ms. Anna Salazar-Degracia, Ms. Josune Alonso, Ms. Judit Prat-Duran, Ms. XueJie Wang, Ms. Jun Tang, and Ms. Liyun Qin for their respective contributions.

ABBREVIATIONS

ACP: american college of physicians
ACCP: american college of chest physicians
AICD: activation-induced cell death
ALK: anaplastic lymphoma kinase
AP: phosphatase alkaline
ATS: American thoracic society
Bax: B-cell lymphoma associated X protein
Bcl2: B-cell lymphoma 2
BMI: body mass index
BRAF: v-Raf murine sarcoma viral oncogene homolog B
Breg: B regulatory
BSA: bovine serum albumin
CAFs: cancer associated fibroblasts
CCL: C-C motif ligand
CD: cluster of differentiation
CDKN2A: cyclin-dependent kinase inhibitor 2A
COPD: chronic obstructive pulmonary disease
COX2: cyclooxygenase-2
Cre: Carbapenem-resistant Enterobacteriaceae
CRP: c-reactive protein
CS: cigarette smoking
CTLA-4: cytotoxic T-lymphocyte-associated protein 4
CCL: C-C motif ligand
CCR: CC chemokine receptor
CXCL: C-X-C motif ligand
Da: dalton
DAB: 3,3'-Diaminobenzidine
DC-Lamp: dendritic cell-lysosomal-associated membrane protein
DCs: dendritic cells
DDR2: discoidin domain receptor 2
DL_{CO}: carbon monoxide transfer
DNA: deoxyribonucleic acid
EGFR: epidermal growth factor receptor
ECM: extracellular matrix
EDTA: ethylenediamine tetraacetic acid
ELISA: enzyme-linked immunosorbent assay
EMT: epithelial-mesenchymal transition
ERK: extracellular-regulated kinase
ERS: european respiratory society
FAP: fibroblast activation protein
FasL: fas ligand
FEV_1: forced expiratory volume in the first second
FGF: fibroblast growth factor
FGFR1: fibroblast growth factor receptor 1
Flp: flippase
FOXP3: forkhead box P3
FVC: forced vital capacity

GAPDH: glyceraldehyde-3-phosphate dehydrogenase
GCs: germinal centers
GESEPOC: spanish COPD guideline
GITR: glucocorticoid-induced tumor necrosis factor receptor-related protein
GOLD: global initiative for chronic obstructive lung disease
G: gram
GSV: globular sedimentation velocity
HEPES: 4-(2-hydroxyethyl)-1-piperazineethanesulfonic acid
HER2: human epidermal growth factor receptor 2
HEV: high endothelial venules
HGF: hepatocyte growth factor
HIF-1α: hypoxia-inducible factor-1 alpha
HRP: horseradish peroxidase
ICAM: intracellular adhesion molecule
ICD: immunogenic cell death
IDO: indoleamine 2,3-dioxygenase
Ig: immunoglobulin
IL: interleukin
INFγ: interferon gamma
iNOS: inducible nitric oxide synthase
JKN1: c-Jun N-terminal kinase 1
K_{CO}: Krogh transfer factor
KRAS: Kirsten rat sarcoma viral oncogene homolog 11
L: liter
LC: lung cancer
LCC: large cell carcinoma
LC3: microtubule-associated protein 1A/1B-light chain 3
LDH: lactate dehydrogenase
LN: lymphoid nodes
LPR: liquid permanent red
LTα: lymphotoxin alpha
M: meter
mAbs: monoclonal antibodies
MHC: major histocompatibility complex
MAdCAM1: mucosal vascular addressin cell adhesion molecule 1
MDA: malondialdehyde
MDSC: myeloid-derived suppressor cells
MEF_{50}: maximal expiratory flow at 50% of the forced vital capacity
MEM: minimal essential medium
miRNA: microRNA
MMP-2: matrix metalloproteinase-2
MW: molecular weight
M1: macrophages type 1
M2: macrophages type 2
N: number
NADPH: nicotinamide adenine dinucleotide phosphate hydrogen
NCR1: natural cytotoxicity receptor 1
NICE: national institutes of health and care excellence
NIH: national institutes of health
NK: natural killer

NOX: NADPH oxidase
NSCLC: non-small cell lung cancer
NT: nitrotyrosine
PARP: poly (ADP-ribose) polymerase
PBS: phosphate buffered saline
PD-1: programmed cell death protein 1
PDGF: platelet-derived growth factor
PD-L1: programmed death-ligand 1
PEF: peak expiratory flow
PI3K: phosphatidylinositol 3-kinase
PMSF: phenylmethylsulfonyl fluoride
PNAd: peripheral node addressin
Pred: predicted
PTEN: phosphatase and tensin homolog 10
PVDF: polyvinylidene difluoride
ROS: reactive oxygen species
ROS1: ROS proto-oncogene 1
RNA: ribonucleic acid
RNS: reactive nitrogen species
RV: residual volume
SCC: squamous cell carcinoma
SCLC: small cell lung cancer
SDS-PAGE: sodium dodecyl sulphate-polyacrylamide gel electrophoresis
SEPAR: Spanish society of pneumology and thoracic surgery
SIRT1: sirtuin-1
SLOs: secondary lymphoid organs
SOD: superoxide dismutase
STAT3: signal transducer and activator of transcription 3
TCR: T cell receptor
TFG-β: tumor growth factor beta
Th: T helper
TL_{CO}: transfer factor of the lung for carbon monoxide
TLSs: tertiary lymphoid structures
TMB: tetramethylbenzidine
TME: tumor microenvironment
TNF-α: tumor necrosis factor alpha
TNFR: tumor necrosis factor receptor
TNM: tumor, nodes, metastasis
TP53: tumor protein 53
TRAIL: TNF-related apoptosis-inducing ligand
Treg: T regulatory
V_A: alveolar volume
VC: vital capacity
VCAM1: vascular cell adhesion molecule 1
VEGF: vascular endothelial growth factor

INTRODUCTION

1. RESPIRATORY SYSTEM

The respiratory system is an organized system conformed by specific organs and structures designated to the oxygen and carbon dioxide exchange between air and blood in a process known as ventilation (1,2). Breathing or ventilation allows the entry and exit of air to and out of the lungs (1,2). As a result, the entry of inspired air, rich in oxygen, supplies the other tissues of the organism and allows the exit of carbon dioxide, as a waste product of cells, through the expired air in a process known as gas exchange (1–3). Gas exchange between the air and blood occurs by diffusion through the lung tissue (1,2,4). The lungs have a large and thin surface in order to optimize gas diffusion (2).

1.1. Structure and anatomy

The lungs are two soft and spongy organs separated by the mediastinum that occupy the thoracic cavity and rest on the diaphragm (2,4). The lungs are composed of lobes: three in the right, and two in the left, in order to leave space for the heart (3). In addition, the lobes are conformed by lobules and trabeculae (4). Lungs are coated by a serous membrane known as visceral pleura and above of this membrane is located the parietal pleura (2). Additionally, the space in between these membranes is known as pleural space, a liquid layer that assists the ventilation process (4). Lungs are perfused by the pulmonary and bronchial arteries. The pulmonary artery carries venous (deoxygenated) blood, whereas bronchial arteries carry arterial (oxygenated) blood (1,4).

Introduction

The respiratory airways are formed by the nose, sinus cavities, pharynx, larynx, trachea, bronchi, bronchioles, alveolar ducts, alveolar sacs and alveoli (2). The trachea branches into primary bronchi at the carina, and the bronchi are sequentially subdivided into different generations until the terminal alveolar sacs (4). Before reaching the alveolar levels, the terminal bronchioles are branched into several generations of respiratory bronchioles, where some gas exchange starts taking place (2). In addition, distal bronchioles are interconnected by canals of Lambert while pores of Kohn connect alveoli (4).

As shown in **Figure 1**, the respiratory apparatus is divided into two major areas: 1) the conducting zone, and 2) the respiratory zone (1,2).

The conducting zone of the respiratory system includes all the anatomical structures that allow the entry of air into the respiratory zone. This region is responsible for the warming, humidification and filtration of the inspired air (4). The anatomical structures involved in this process consists of the respiratory airways and all the successive subdivisions up to the terminal bronchioles (2–4). Trachea and bronchi are lined with a ciliated pseudo-stratified epithelium rich in goblet cells that secrete mucous into the lumen of the airways (4). Above the basement membrane, mucous secreting glands are surrounded by smooth muscle fibres (4). The main function of the mucous secreted consists to trap small particles and filter the air inhaled (1,2). The particles trapped in the mucous are moved towards the pharynx

by action of the cilia projected from the epithelial cells to be them swallowed or expectorated (2).

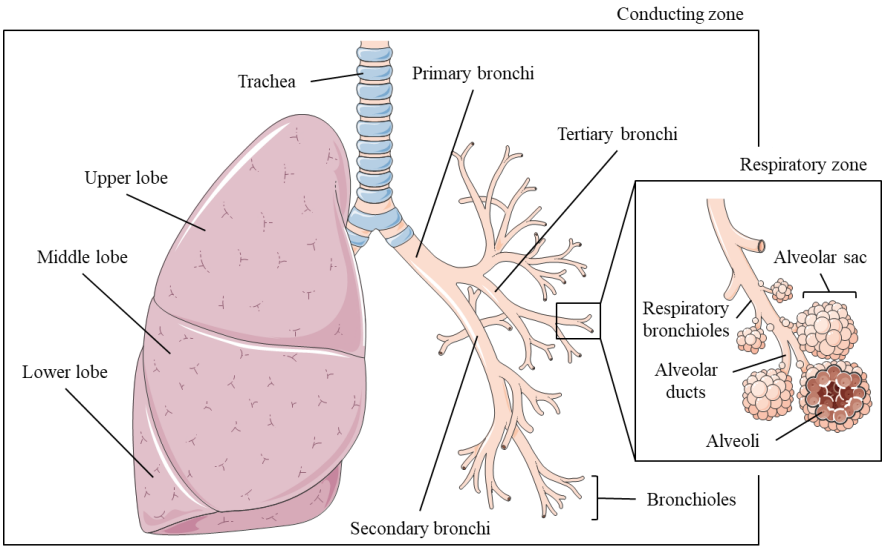

Figure 1. The conducting and respiratory zones of the respiratory system. The conducting zone consists of airways responsible to conduct the inspired air to the respiratory zone, which is the area designated to gas exchange. Figure was produced with image bank supply from Servier Medical Art (http://www.servier.com). Source from Netter FH and Stuart I (1,2).

Apart from the ciliated epithelial cells, the epithelia of bronchi is composed of basal cells, which are responsible to differentiate into other cells (1,2,4). Neuroendocrine cells, are also present in the airways and secrete compounds such as serotonin, bombesin, and calcitonin, in order to regulate the ventilation physiological response (4). Furthermore, neuroendocrine cells aggregate in clusters known as neuroepithelial bodies (4). As bronchi branch into successive generations, cartilaginous rings are replaced by cartilaginous plates (1,4). At the level of bronchioles, cartilage is progressively replaced

by smooth muscle fibres (4) and goblet cells are retrieved by Clara cells, responsible to secrete glycosaminoglycan to protect the luminal surface of the bronchioles (1,2,4).

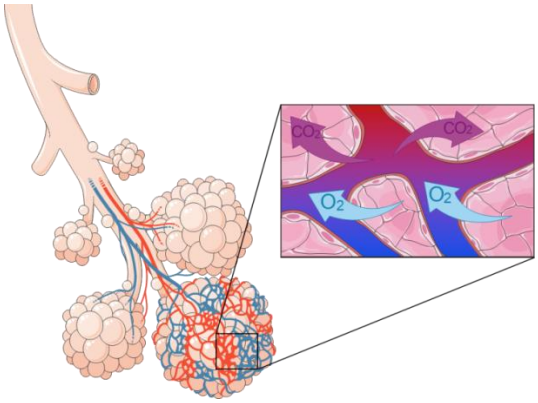

Figure 2. Representative figure of alveolar sacs architecture and gas exchange. Figure was produced with image bank supply from Servier Medical Art (http://www.servier.com). Source from Netter FH (1).

The respiratory zone is the region where gas exchange occurs (**Figure 2**). This region includes the respiratory bronchioles, alveolar ducts, alveolar sacs, and alveoli (2,4). The surface of respiratory bronchioles is built up by cubic epithelium and a thin collagenous layer with elastic fibres and smooth muscle cells (4). Alveolar ducts culminate through the atria in alveolar sacs, where alveoli are aggregated and interconnected by tiny pores (2,4). These structures are rich in capillaries that assist gas diffusion. Type I and II epithelial or alveolar cells conform the alveoli (2,4). Type I alveolar cells are the most abundant (95-97% of the surface) and with endothelial cells conform the surface for gas exchange (4). The main function of type

II alveolar cells consists to secrete surfactant to coat the alveolar surface for protection and fluid accumulation prevention (2,4).

In order to grant the integrity of alveoli, abundant levels of type IV collagen are present in the capillaries and alveolar walls (2). Furthermore, resident macrophages in the alveoli, also called alveolar phagocytes or dust cells, assist in the integrity of alveoli by removing the inspired noxious particles that were not trapped in the mucous produced in upper stream airways (2,4).

1.2. Physiology and measurements

As early mentioned, pulmonary ventilation is the main physiological mechanism of the lungs and consists in the movement of air into and out of the lungs. Pulmonary ventilation is driven by atmospheric, alveolar, and intrapleural pressure. The difference in pressures drives pulmonary ventilation as air flows from an area of higher pressure to an area of lower pressure. Pulmonary function assessment plays an essential role in the monitoring of patients with respiratory disease. Indeed, a lung function test can be used to diagnose a lung disease and assess whether a treatment for disease is improving health. There are different tests to measure lung or pulmonary function and the tests commonly used include spirometry, lung volume and gas transfer measurements, and exercise testing. These tests measure the amount of oxygen inhaled and the amount of carbon dioxide exhaled during breathing. Hence, the results obtained in these types of tests must be interpreted under the context of respiratory physiology and the history of patients.

Introduction

Spirometry test is non-invasive, readily, low-cost, and the most reproducible and sensible measurement for pulmonary function (5,6). A spirometer allows the measurement of several parameters. For instance, the most relevant parameters that express the physiological status of the conducting zone are: the volume of air exhaled after a deep inspiration or forced vital capacity (FVC) to maximal expiration or residual volume (RV) and the volume of air exhaled at the end of the first second during the test known as forced expiratory volume in one second (FEV_1) (5–7). The quotient between these two parameters (FEV_1/FVC) is another measure widely used (5–7). Whereas, the physiological parameters that express the function of the respiratory zone are: the carbon monoxide transfer (DL_{CO}), which represents the carbon monoxide diffusion capacity in a single-breath, and the Krogh transfer factor (K_{CO}) that measures the capacity of lung diffusion, are also important pulmonary function parameters (3,7,8). The transfer factor of the lung for carbon monoxide (TL_{CO}), alveolar volume (V_A) maximal expiratory flow at 50% of the forced vital capacity (MEF_{50}), vital capacity (VC), and peak expiratory flow (PEF) parameters are reported as the most relevant for discriminating chronic obstructive pulmonary disease (COPD) from asthma (9).

Lung function varies widely according to the anthropometrical characteristics of the study populations. These characteristics includes the following variables: age, height, weight, and gender (5,6,10). Hence, usefulness of any test depends on the availability of suitable standards and reference values must be interpreted during lung function assessment (11–13).

Moreover, spirometry should also be performed after previous bronchodilator administration to reduce test variability and also discard the diagnostic of asthma (5,6).

2. LUNG CANCER

Lung cancer (LC) is a disease that arises in the lung tissue by uncontrolled growth of abnormal cells with the capacity to break through the basement membrane and spread into distant organs (14). Lung tumors usually arise from basal epithelial cells that line the airways (15). These cells experience driver mutations in oncogenes and tumor suppressor genes that trigger malignant cell proliferation leading to tumor formation through the modulation of different pathways that display a relevant role in cell growth, cell division, DNA repair and cell death (15).

2.1. Epidemiology

LC is the third most prevalent type of cancer, after breast and prostate cancer, and remains as the major cause of cancer-related mortality worldwide, with only a 15% in men and 21% in women of 5-year total survival rate after primary diagnosis (14,16,17). Due to absence of screening and clinical manifestations, patients are not diagnosed until advanced stages, when the availability of therapeutic alternatives is reduced. The most frequent clinical features include dyspnoea, cough, and haemoptysis (14,18). But also difficulty to breath, swallow or speak properly, fatigue, chest pain, appetite or weight loss, and face or neck swelling (14). Symptoms can be produced by local tumor, locoregional spread, metastatic disease, or

paraneoplastic syndromes (18). The most frequent targets of metastasis in LC are lymph nodes, liver, bones, brain, and adrenal glands (14,19,20).

Not much symptoms are found in early-stage LC. For this reason, only 20% of patients have localized disease at initial diagnosis, 25% have regional metastasis, and 55% distant spread of disease (21). LC is diagnosed in asymptomatic patients (7-10% of cases) when a chest radiograph is performed for other reasons (21).

2.2. Etiologic factors

Several factors are involved in LC etiology but cigarette smoking (CS) is still the main cause (17,22). Exposure to toxic components of cigarettes triggers carcinogenic events that cause around 90% of LC deaths in men and almost 80% in women (23,24). The smoke of cigarettes is composed of gaseous and particulate compounds such as nicotine and tar, which seems to be the highest contributors to LC risk (15). Many potential carcinogens are found in CS, including polycyclic aromatic hydrocarbons, aromatic amines, N-nitrosamines, benzene, arsenic, and chromium (15). Some of them are dependent of metabolic activation in order to become carcinogenic and metabolic detoxification can take place. This phenomena provides a balance between activation and detoxification that accounts for individual cancer risk (15). CS carcinogens covalently bind to DNA, so repair processes will be effected in order to remove them, but the failure of the repairment machinery could lead to permanent mutations (25).

Apart from the exposure to noxious agents present in the CS, occupational exposure to other environmental agents such as air pollution, second-hand smoke, arsenic, asbestos, and certain metals may increase the risk of suffering from LC (26–28). In addition, radioactive materials, such as radon, bismuth, and polonium are also present in CS (15). Other risk factors include long-term use of hormone replacement therapy for menopause and a history of lung disease such as COPD or tuberculosis (15). Although, a history of LC events in the close family members accounts as an important risk factor, relatives that develop LC are current smokers, so it is unclear whether the raised risk is a result of genetic alterations or smoke exposure (15).

Environmental and genetic factors are major contributors to develop LC. Genetic factors or mutations can be somatic or germinal, which means that are acquired or inherited. Critical oncogenes and tumor suppressor genes are modulated by the action of carcinogenic agents (25). Tumor protein p53 (*TP53*), epidermal growth factor receptor (*EGFR*), and Kirsten rat sarcoma viral oncogene homolog 11 (*KRAS*) genes are usually mutated in LC (29). Mutations in *TP53* tumor suppressor gene disables the entrance on cell cycle arrest and further apoptosis in aberrant cells, while mutations in the *EGFR* or *KRAS* oncogenes lead to constant proliferation signals that trigger tumor formation (30).

Mutations in many other genes are common in LC (29,31). For instance, phosphatidylinositol 3-kinase (*PI3K*), v-Raf murine sarco-

ma viral oncogene homolog B (*BRAF*), cyclin-dependent kinase 2A (*CDKN2A*), anaplastic lymphoma kinase (*ALK*), human epidermal growth factor receptor 2 (*HER2*), ROS proto-oncogene 1 (*ROS1*), fibroblast growth factor receptor 1 (*FGFR1*), discoidin domain receptor 2 (*DDR2*), and phosphatase and tensin homolog 10 (*PTEN*) among others (32,33). Most of these genes are involved in the regulation of several mechanisms including: gene expression, apoptosis, cell proliferation, and differentiation.

2.3. Diagnosis

According to the cellular origin of the tumor and the microenvironment where is present, different specific lung tumor subtypes will grow (27). As lung tumor subtypes behave and respond to treatment in different ways, the therapeutic approach relies on the type of cell from which the cancer was raised.

2.3.1. Histopathological subtypes

Tumors are classified in different groups based upon the microscopic appearance of the tumor cells. There are two main types of primary LC: non-small cell lung cancer (NSCLC) and small cell lung cancer (SCLC). NSCLC represent about 80-85% of the diagnosed LC cases while 10-15% LC cases are SCLC and fewer than 5% are lung carcinoid tumors (34).

NSCLC is subdivided into three main subcategories that comprise adenocarcinoma, diagnosed in a 40% of cases, squamous cell carcinoma (SCC) in 25-30% of cases and large cell carcinoma (LCC)

in 10-15% of cases (34). Adenocarcinoma usually originates in distal sections of the lungs from mucus producer cells and SCC arises from squamous cells that cover the surface of the airways of proximal sections of the lungs (35). However, LCC arises from epithelial cells that line the airways of the lungs (30).

SCLC is a highly malignant pulmonary neoplasm that is thought to originate from smaller undifferentiated cells derived from neuroendocrine cells (15,27,34).

2.3.2. Staging of LC

The evaluation of LC staging uses the tumor-node-metastasis (TNM) classification, a globally recognised standard for the classification of the cancer spread extent using alphanumeric codes. Based on standardized criteria, the TNM classification is the most widely used cancer staging system as a tool for physicians to stage different types of cancer (37–39). This classification have been established in many solid tumors and some of them have their own TNM classification, except for hematologic and central nervous system cancers which do not share this classification (30,40).

The TNM staging system is based on three main descriptors: tumor extent (T), lymph nodes extent spread (N), and metastasis presence (M). Indeed, the T descriptor refers to the size and extent of the localized primary tumor and whether it has invaded nearby tissue. Moreover, it provides information about endobronchial location, distance from the carina, and the presence of satellite nodules (36,39).

Introduction

The N component is the nodal descriptor, which shows whether regional lymph nodes are involved, and the M component describes the invasion of distant tissues. The 8th edition of TNM (37) is currently being followed in clinical practice by medical professionals since January of 2018 in order to assess LC staging (**Table 1**).

Table 1. Eighth edition of TNM staging classification of LC. Adapted from Goldstraw P et al 2010 and Detterbeck FC et al 2017 (36,37).

Occult carcinoma	Tx	N0	M0
Stage 0	Tis	N0	M0
IA1	T1(mi)	N0	M0
	T1a	N0	M0
IA2	T1b	N0	M0
IA3	T1c	N0	M0
IB	T2a	N0	M0
IIA	T2b	N0	M0
IIB	T1a-c	N1	M0
	T2a	N1	M0
	T2b	N1	M0
	T3	N0	M0
IIIA	T1a-c	N2	M0
	T2a-b	N2	M0
	T3	N1	M0
	T4	N0	M0
	T4	N1	M0
IIIB	T1a-c	N3	M0
	T2a-b	N3	M0
	T3	N2	M0
	T4	N2	M0
IIIC	T3	N3	M0
	T4	N3	M0
IVA	Any T	Any N	M1a
	Any T	Any N	M1b
IVB	Any T	Any N	M1c

2.4. Therapeutic strategies in LC

2.4.1. Surgery

Surgery is the best option against LC in early stages but in most of cases the neoplasm is diagnosed in advanced stages with metastasis in distant organs. In these cases, surgery is no longer a therapeutic approach and alternative options must be applied. Patients with stage I-III tumors are usually candidates for resection but attention must be paid to the status of patients and whether they are able to overcome surgery. For instance, the age of patients and the presence of co-morbidities must be taken into account (41). The operability assessment of the tumor of a patient consists in imaging studies and biopsies (42). Patients can also benefit from adjuvant therapies by reducing the risk of cancer relapse (41,42). Adjuvant therapy includes radiation, chemotherapy, and targeted therapy in order to ensure total eradication of cancer cells after the surgical intervention (41,42).

2.4.2. Chemotherapy

The treatment against metastatic LC is applied systemically with cytotoxic agents and/or molecular-targeted therapies and radiotherapy (19,41,42). On these cases, the therapeutic approach depends on several factors which include the extent of disease, which organs are metastasized, and the response to therapy (42). Chemotherapy is very effective against SCLC since it is an aggressive cancer and in most of cases surgery is not an option but most of patients tend to relapse (43). The chemotherapy agent is comorbidity-dependent as platinum-based therapy is not compatible

with cardiovascular diseases, and cisplatin with renal dysfunction or neuropathy (43). Cisplatin and carboplatin are the standard agents but docetaxel, gemcitabine, paclitaxel or pemetrexed can also be found (44). Moreover, several agents are often applied in doublets or even triplets. The main disadvantage of chemotherapy apart from side-effects due to high toxicity is that tumors may become resistant (43). In case of treatment resistance, second-line therapy must be followed. Despite second-line treatment improves survival when patients develop resistance to first-line treatment, the following treatment is generally less effective than the initial (43). It is important to elucidate the trends in LC metastasis for the improvement of the clinical outcome of metastatic LC patients. For instance, some subtypes show preference for specific metastatic sites. NSCLC frequently metastasizes in the liver and SCLC in the brain (45).

2.4.3. Biological therapies

In regards to the significant advances in the treatment of LC over the last years, a range of molecularly targeted therapies and immunotherapy agents are under investigation and carried into the clinics (46). Molecular-targeted therapies modulate key signaling pathways in tumorigenesis such as angiogenesis (process recognized by the formation of new blood vessels for tumor supply), cell proliferation, motility, and survival through transmembrane receptors (41). Indeed, bevacizumab acts by blocking the signaling cascade produced through vascular endothelial growth factor (VEGF) (41). Cetuximab, erlotinib and geftinib bind to EGFR and inhibit the signal transduction cascade (41). In spite of the genetic alterations common-

ly affect a short group of oncogenic signaling pathways, different cancer-subtypes arise according to the genes mutated (32), and for this reason, the genotype screening of individual patients is an essential tool in LC therapy in order to assess the most accurate therapeutic treatments and ensure optimal outcome.

2.4.3.1. Tyrosine kinase inhibitors

Protein tyrosine kinases are enzymes that activate a downstream cascade of cellular signaling pathways which play a crucial role in signal transduction, cell proliferation, differentiation, death and other regulatory mechanisms (47–49).

Over the last years, several novel therapeutic agents that inhibit tyrosine kinase activity have been identified (48). In NSCLC, agents such as cetuximab, erlotinib and geftinib are used to inhibit the signal transduction cascade triggered from EGFR while bevacizumab and ramucirumab act against VEGF and crizotinib against ALK (42,48–53).

Mutation assessment is chief in order to screen and select patients that could benefit from therapy with targeted tyrosine kinase inhibitors (42). EGFR is a cell-surface tyrosine kinase receptor and its activation is associated with pathways that induce cell growth and proliferation (42). EGFR mutations produce uncontrolled cell division through constant activation in cancer (42). Hence, VEGF exerts its action through the interaction with tyrosine kinase receptors that are predominantly expressed in endothelial cells (50). VEGF binding to its cognate receptors induces the activation of several sig-

naling proteins that regulate angiogenesis, cell proliferation, survival, and migration (54). Moreover, a variety of environmental factors, growth factors, and genetic/epigenetic factors regulate the expression of VEGF in cancer (50). Finally, ALK gene rearrangements are found in NSCLC and represents an avenue for ALK kinase inhibitors such as crizotinib, a multitargeted small molecule tyrosine kinase inhibitor that induces entrance in cell cycle arrest and apoptosis (51–53).

2.4.3.2. Immune checkpoint inhibitors

Immune system is a natural barrier against cancer, and proliferation of cancer cells can be mitigated by empowering host immune surveillance through the different immune regulatory steps. Cell depletion strategies (55,56), tumor vaccines (57), and injection with agonistic and antagonistic antibodies (57,58) have been widely used in order to elicit immune-mediated elimination of cancer cells. Although LC was thought to be non-immunogenic (59), the favorable results obtained in several clinical trials have proven the effectivity of immunotherapy in this type of cancer and has restored the interest on the research conducted in the immunology field. Indeed, immune checkpoint blockade has become a standard treatment in several solid tumors including NSCLC (60,61).

Immune checkpoint inhibitors are monoclonal antibodies (mAbs) that bind to immunosuppressive receptors with an antagonistic effect and immunostimulatory receptors with an agonistic effect with the overall purpose to revert immune tolerance (62–64).

Checkpoint inhibitors targeting cytotoxic T-lymphocyte-associated protein 4 (CTLA-4), the programmed cell death protein 1 (PD-1), and programmed death-ligand 1 (PD-L1) have shown positive clinical responses with few toxicity events in several clinical trials in phase II and III (59). Nivolumab and pembrolizumab are humanized antagonistic mAb anti-PD1 approved by FDA for second-line treatment in NSCLC with a significant benefit in overall survival, durable clinical responses and manageable toxicity with good safety profile (65). Atezolizumab is an anti-PDL1 also approved by FDA for NSCLC treatment (65) and Ipilimumab is fully human IgG1 mAb anti-CTLA-4 approved for melanoma treatment and is under phase III clinical trial in NSCLC (66).

In addition, agonist antibodies against CD40, 4-1BB, glucocorticoid-induced tumor necrosis factor receptor-related protein (GITR), and OX-40 can also be used as enhancers for antigen-specific T cell responses (67). Agonistic mAbs anti-CD137 as Urelumab, are under investigation. Activation of CD137 is reported to promote dendritic cells (DCs), natural killer (NK) and T cells activity, as well as inhibit T regulatory (Treg) cells function (62).

Although the association between chemotherapy and immunotherapy or immunotherapy alone is an ongoing step in LC, more studies are needed to understand the optimal combination of the different therapeutic strategies. Indeed, immune response of LC is perplexing and significant variability exists in the response of patients (68).

2.5. Prognosis and survival in LC

Lung cancer prognosis is devastating. Over half of people diagnosed with LC pass away within one year after diagnosis and the 5-year survival rate is lower than 18% (42). In addition, patients who do not receive any treatment for their lung neoplasm live an average of 7 months (69) and around 85% of patients are diagnosed at an advanced stage (70,71). In terms of prognosis and survival, a significant variability is present between patients. For this reason, several specific factors with prognostic value may contribute to survival prediction as a relevant field in LC research (72). Moreover, the assessment of prognosis by the physicians in the clinics has a key role in decision-making (69). For this end, easily-measurable biologic markers with prognostic value are needed to stratify patients and select the most accurate treatment for optimal results in survival (73).

2.5.1. Survival prediction and early detection markers

Prognostic factors are used to predict survival of LC patients (70). For this reason, several factors have emerged as independent LC survival predictors in the recent decade (73). These prognostic factors can be segregated into four categories (72). Firstly, factors related to patient such as gender, age, smoking history, weight loss, body mass index (BMI), and comorbidities. Secondly, factors concerned to tumor like histological subtype, burden, invasion, and paraneoplastic syndromes. Thirdly, factors involved in treatment including the type

of therapeutic agent and response rate. Finally, other parameters that contribute to prognosis are serum lactate dehydrogenase (LDH), alkaline phosphatase, albumin, hemoglobin, leukocytosis, c-reactive protein (CRP), neutrophils-lymphocytes ratio, and thrombocytes-lymphocytes ratio.

Regardless CS in female population has increased (23); LC incidence is greater in men than women (16). Moreover, despite survival is greater in female than male, female patients seem to be younger and more sensitive to tobacco-mediated carcinogenesis (74). In addition, men are more likely to develop SCC while adenocarcinoma is more common in women (71). Another prognostic factor widely recognized among different cancers is age (70). Several studies have demonstrated the prognostic value of age (70). A cohort study showed that survival in elderly patients (>70 years) is lower than younger patients and elderly SCLC patients have a poor outcome when compared to NSCLC (70).

Comorbidities in terms of prognosis are controversial. The most frequent concomitant diseases found in men are cardiovascular and COPD, whereas in women cardiovascular, hypertension and COPD (75). Other studies revealed the prognostic value of weight loss in NSCLC patients, associating weight loss with aggressiveness and the smoking history with a negative impact (72,73).

Other relevant survival predictors may be found among tumor size, cell type, lymphatic and blood vessel invasion, rate of proliferation,

and extent of tumor necrosis (73). Lower survival rates are found in LCC patients compared to adenocarcinoma and SCC (72). Moreover, tumor grade is found to be associated with survival as well as carcinoma cells differentiation (70,73). In addition, another study showed that higher levels of LDH in serum are associated with poor prognosis (70). In addition, vitamin/mineral supplements are reported to modulate tumor growth and improve survival among LC patients (73).

The genomic approach in cancer research is significantly assisting in the identification of molecular markers with diagnostic, prognostic, and therapeutic value. In the past two decades, a vast number of studies on biological markers have been carried out in order to assess the usefulness of prognostic markers and to assist in patient management (76). For instance, mutations in *TP53* and *KRAS* are associated with poor prognosis (70).

Nevertheless, despite the efforts in the identification of molecular prognostic markers, its lack is notable in the clinical practice (77). However, PD-L1 has been identified as a predictive marker of a good response to immunotherapy but a poor prognostic indicator of overall survival (77).

Nevertheless, TNM stage remains as the main prognostic factor in predicting recurrence and survival, followed by tumor histology, gender, age, and performance status (77).

3. CHRONIC OBSTRUCTIVE PULMONARY DISEASE

COPD is a respiratory disorder that is characterized by obstructive ventilator alterations such as chronic airflow limitation caused by structural changes in the airways and lung parenchyma (5–7).

3.1. Epidemiology

In spite of COPD is a common, preventable and treatable disease, represents a progressive disease, which means that is irreversible or partially reversible (6,7). In addition, COPD is currently the fourth leading cause of death worldwide but prevalence and mortality of COPD is expected to rise, becoming the third major cause of death by 2020 due to increased age, exposure to harmful chemicals and reduced mortality from other common fatal diseases (6).

Morbidity from COPD includes other concomitant chronic conditions such as LC, cardiovascular disease, musculoskeletal impairment and diabetes mellitus but the most frequent symptoms in COPD patients are dyspnoea, chronic cough and sputum production among others (6).

3.2. Etiologic factors

Obstructive respiratory symptoms are originated from exposure to noxious particles or gases from CS, which is the main etiologic factor of COPD (5–7,78,79). Other factors that may contribute on top of CS are occupational or environmental exposure, genetic alterations, age,

gender and poor lung growth and development during childhood (5–7).

Exposure to noxious agents originated from CS is responsible to induce pro-inflammatory events in the airways of the lungs and that enhanced inflammatory response to inhaled particles or gases causes COPD (80,81). Despite the raise of inflammatory cells in the lung parenchyma in response to irritant agents present in the respiratory tract is not fully understood, some of the commonly increased inflammatory cells in COPD patients include macrophages, neutrophils, lymphocytes, and eosinophils (6). Furthermore, oxidative stress and proteolysis are known triggers of lung inflammation and inhalation of noxious particles may induce macrophages and neutrophils to produce oxidants (6). In addition, cigarette smoke contains free radicals that can increase the release of oxidants which are responsible of lung matrix damage through elastin and collagen degradation (82).

3.3. Pathophysiology

Airflow limitation is mainly driven through chronic inflammation of the airways (6,7,78,79). The pathogenic mechanisms that condition the histopathological changes of the respiratory system in COPD include chronic inflammation and lung parenchyma destruction (5). The inflammation in the airways is characterized by increased numbers of alveolar macrophages, neutrophils, lymphocytes, and T helper (Th) 1 cells recruited from the circulation. These cells and others such as endothelial cells and fibroblasts, secrete an array of cy-

tokines, chemokines, and growth factors that act as pro-inflammatory mediators (83–86). Chronic inflammation produces fibrosis and changes in the bronchi walls leading to airflow obstruction while destruction of the alveolar sacs and the adjacent capillary nests reduce elastic recoil (5).

Obstruction of the airways through bronchi walls dilatation due to cell infiltration and edema formation manifest persistent fibrosis, inflammation and airflow limitation as a consequence (5–7,79). Moreover, excessive mucus secretion and accumulation in the airways is a characteristic feature of this disorder (6,7,79). In fact, mucus hypersecretion is due to the presence of hypertrophic mucus secreting glands (7).

The destruction of the lung parenchyma implies the loss of alveolar attachments and capillary nests leading to a decline in lung elastic recoil (6,7). C5a-mediated stimulation of neutrophils by macrophages produces excessive amounts of elastase, an enzyme that degrades elastin, which is a major alveoli component (6,7). Moreover, collagen type IV impairment is also present and all together, represents a compromise for the integrity of alveolar walls (7).

3.4. Clinical symptoms and manifestations

COPD have different clinical manifestations which include chronic bronchitis and emphysema (5–7). Chronic bronchitis is characterized by structural changes in the architecture of bronchi (**Figure 3A**).

In order to establish the diagnosis of chronic bronchitis, symptoms must include cough and sputum production for at least three months each year for two years (6,7). Otherwise, emphysema (**Figure 3B**) is recognised by the destruction of alveolar structures that leads to terminal alveolar airspace enlargement (6,7,79).

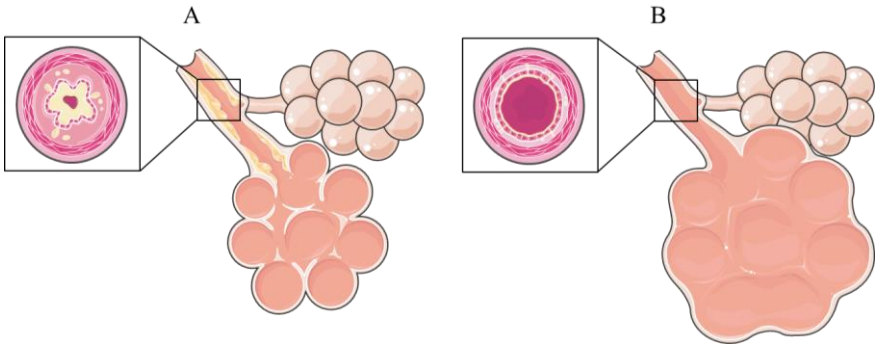

Figure 3. Representative figure of the airflow inflammation in obstructive bronchitis (**A**) and alveoli destruction in emphysema (**B**). Figure was produced with image bank supply from Servier Medical Art (http://www.servier.com). Source from West JB and Luks AM (7).

3.5. Classification of COPD

A variety of guidelines is used in clinical practice for the management of COPD. Global Initiative for Chronic Obstructive Lung Disease (GOLD) is the most widely recognized (6).

Regarding COPD diagnosis, patients must present a post-bronchodilator $FEV_1/FVC < 0.70$ so airflow limitation is stablished when the ratio is below 70% of the predicted value (5–7). The GOLD classification of COPD is based on the evaluation of symptoms, and exacerbations (**Table 2**).

Table 2. Classification of airflow limitation severity in COPD according to GOLD classification (6,87–90).

Stage	Severity	FEV_1	Symptoms	Exacerbations
I	Mild	$FEV_1 \geq 80\%$ pred	Chronic cough and sputum	0-1 per year
II	Moderate	$50\% \leq FEV_1 < 80\%$ pred	Dyspnoea	
III	Severe	$30\% \leq FEV_1 < 50\%$ pred	Worsened symptoms	
IV	Very severe	$FEV_1 < 30\%$ pred	Respiratory or heart failure	≥2 per year

Definition of abbreviations: FEV_1, forced expiratory volume in the first second; pred, predicted.

In order to determine the severity of COPD, several national and international guidelines are used in the world. The Spanish guideline of COPD (GESEPOC), the Spanish Society of Pneumology and Thoracic Surgery (SEPAR), the international GOLD, the technical standards of the European Respiratory Society (ERS) and American Thoracic Society (ATS), the guidelines of the National Institute of Health (NIH) and the National Institute of Health and Care Excellence (NICE), and the guidelines from the American College of Physicians (ACP) and American College of Chest Physicians (ACCP).

4. RELATIONSHIPS BETWEEN LC AND COPD

4.1. Epidemiology

The link between COPD and LC started to show up in epidemiological and case-control studies at the late 1980's. These studies suggested that the presence of airways obstruction could have

a strong correlation with an increased incidence of LC (91,92). Moreover, the presence of COPD was proven to be a better indicator of LC rather than age or the smoking history (91,92).

It has been stated that patients with airway obstruction have an 8.8% of probability to develop LC while patients with normal pulmonary function have a 2% of probability (92). Furthermore, it is also stated that LC patients debut with a 50% of COPD prevalence against 8% in control subjects (93). These data suggest that an early diagnosis of COPD may suppose a better prognosis for potential LC patients (94,95). Hence, supporting this statement, it has been found that decreased levels of FEV_1 may serve as a prognostic factor for increased LC risk (92). These studies give support in the use of FEV_1 and FEV_1/FVC as prognosis markers for LC apart from the smoking history.

Moreover, not only air obstruction but chronic bronchitis and emphysema are also considered as independent risk factors for the development of LC as it has been shown in several studies where an increased prevalence of LC was found in patients with emphysema or chronic bronchitis (93,96,97). In addition, LC patients with both chronic bronchitis and emphysema show worse prognosis and higher mortality (93,98–100). Indeed, the major cause of death in COPD patients is LC (98,100) and it has been also reported that smokers with COPD are more prone to develop LC than non-COPD smokers (99,101,102).

Moreover, the same feature is found in never-smokers (99). The results obtained in a cohort-based study suggested that COPD is prevalent and underdiagnosed in LC patients and patients with LC and COPD have greater comorbidities and lower K_{CO} (103).

Additionally, a prospective study showed that in mild COPD patients, heavy smokers had a higher probability to develop LC compared to light smokers and, interestingly, light smokers with severe COPD are less prone to develop LC than light smokers with mild COPD (104). Moreover, in severe COPD patients, differences were not found between light and heavy smokers in LC prevalence (104). All these data suggest that patients may debut with a differential susceptibility pattern to smoking.

It is also stated that the influence exerted by COPD in LC is depending on the degree of airway obstruction but there is a lack of information in that aspect and further studies are needed to elucidate this fact (104). For instance severe COPD patients were reported to have a higher LC risk compared to mild-to-moderate COPD patients in a study with smokers (99,105). Controversially, it was also found that GOLD stage IV COPD patients had increased LC prevalence compared to GOLD stage I COPD patients (106,107).

Another study evidenced that emphysema severity could be used as a predictor for tumor location in early-stage LC patients (108). Furthermore, the severity of COPD is correlated with the risk of LC mortality (109) and patients with LC have better survival rates than

patients with LC and COPD (99,110). Importantly, it is known that COPD patients tend to develop SCLC and SCC while a higher prevalence of adenocarcinoma is found in never-smokers and females but adenocarcinoma prevalence is increasing among smokers maybe due to a change in the composition of cigarettes (15,102,103,111). Indeed, the histological subtype of LC developed in COPD patients may also be COPD severity dependent due to the data shown in a study which revealed that GOLD stage I COPD patients were likely to develop adenocarcinoma while GOLD stage II and III develop SCC (106).

4.2. Etiology

Although COPD and LC are both mainly caused by environmental factors such as the smoke of cigarettes or air pollution, opposite roles are displayed between them. Indeed, COPD is associated with cell death, and matrix and blood vessels destruction, while LC is characterized by cell proliferation, cell death scape and the formation of new blood vessels (112,113). In spite of that, a high prevalence of COPD is found in patients with LC.

Currently, it is a well-known fact in the LC pathogenesis and many evidences suggest that there is a very tight relationship between COPD and LC. From date, a large amount of interventional trials, epidemiological, screening or population-based cohort studies have demonstrated the strong association between both diseases (94,114). Hence, it has been demonstrated that COPD accounts separately from cigarette smoking as an independent risk factor for LC (94,114).

4.3. Pathophysiology

LC and COPD involve common risk factors such as air pollution and CS as the main of them. These shared factors are triggers of analogous signaling pathways expressed in both diseases.

Noxious particles inhalation is known to induce mutations that lead to the dysregulation of several signaling pathways endangering tissue homeostasis. Several molecular mechanisms are involved in the pathophysiology of LC and COPD. For instance, CS-induced oxidative and nitrosative stress is known to trigger immune system activation and inflammation.

The over-inflamed tissue is likely to succumb to respiratory diseases such as COPD and when this chronic inflammation persists, LC may be developed. For this reason, elucidation of underlying biological mechanisms that may account for patients with chronic respiratory diseases to a higher influence of LC have gained a deep interest. Indeed, LC is a molecularly heterogeneous disease and the understanding of its biology is essential for the development of effective therapies (33).

In the current thesis, several signaling pathways that could link LC with COPD patients have been analyzed including cell growth (cell proliferation), cell death (apoptosis and autophagy), oxidative and nitrosative stress, inflammation, and immune system. In addition, a brief description of these mechanisms is found below.

5. PATHOPHYSIOLOGIC MECHANISMS OF LC DEVELOPMENT

5.1. Nitrosative and oxidative stress

Human beings are under constant oxidative stress which is originated from exogenous factors such as CS or ultraviolet rays, and endogenous factors derived from mitochondrial activity or production of nicotinamide adenine dinucleotide phosphate hydrogen (NADPH) by macrophages and neutrophils among others (115–117).

CS triggers chronic airway inflammation and activation of cells that produce high levels of reactive nitrogen species (RNS) and reactive oxygen species (ROS) which interact between them and thus produce other potentially carcinogenic reactive products (115,116). Moreover, oxidative stress can also arise from certain anticancer drugs under use in the clinics (116).

Healthy tissues own a natural system that allows the removal of ROS and RNS through different pathways and antioxidant systems including superoxide dismutase I (Cu-ZnSOD), superoxide sidmutase II (MnSOD) and catalase (118,119). When such oxidative stress levels cannot be countered by the natural oxidation-reduction system of the body, cell injury may arise through alterations in genes or transduction and transcription factors signaling (116). These alterations are translated into DNA damage and when is not possible to be restored, oncogenesis may take part (120).

Importantly, several pathways are affected by oxidative stress. Indeed, high levels of ROS and RNS are reported to promote cell proliferation through the activation of extracellular-regulated kinase 1/2 (ERK1/2), cell death evasion through PI3K/AKT activation, invasiveness by extracellular matrix (ECM) degradation or epithelial-mesenchymal transition (EMT) activation, and angiogenesis mediated by VEGF (115). Additionally, oxidative stress, produced by the imbalance between oxidants and antioxidants production, is linked to initiation, promotion and progression of carcinogenesis (22,121–123) but the role displayed remains controversial and may include tumor-suppressing and tumor-promoting effects, especially regarding the immune system (124,125). For instance, cancer cells contribute to increased oxidative stress levels by active oxygen production, as well as neutrophils and macrophages as early mentioned (116).

Furthermore, it is suggested that an association between the tumor stage and the oxidative stress levels may exist, and other evidences put into manifest an association between oxidative stress and drug resistance (116). On this basis, the oxidative stress status may play a crucial role in the patient clinical outcome, and for this reason oxidative stress markers are reported to have a prognostic value (115,116). Nevertheless the reliability of oxidative stress markers may be dependent of several factors, including the tumor type, tumor progression, and the patient status (116,124). Indeed, increased levels of oxidative stress and decreased levels of antioxidants are reported in advanced stage SCC patients (126).

Published data from our research group states that increased oxidative stress levels can be found in the normal bronchial epithelium of patients with LC with COPD respect LC patients without COPD and control subjects (121). Moreover, findings from our group suggest that predisposition of patients with COPD to LC may be influenced by oxidative stress (122). Increased nitrosative stress levels were also found in the tumor lesions compared with the non-tumor parenchyma in LC patients (120). Increased levels of nitrated and carbonylated proteins are found in the normal airways of LC patients compared to healthy controls, and those differences are exacerbated in patients when compared with patients with both LC and COPD (120). Moreover, oxidative stress-mediated EMT is reported in COPD smokers (127).

5.2. Tumor microenvironment

The cancer or tumor microenvironment (TME) is referred to the cellular niche in which the tumor arises and describes the non-cancerous cells present in the tumor including non-cellular components such as signaling molecules that support the growth of cancer cells known as ECM, the cells that conform the blood and lymphatic vascular networks, immune cells, inflammatory cells, neuroendocrine cells, adipose cells, fibroblasts, and myofibroblasts (128–130).

The tumor is permanently interacting with the surrounding environment thus generating a rich ambient for tumor growth by the secretion of factors that exert a promotion of proliferation and survi-

val and contribute to tumor plasticity, heterogeneity and aberrant tissue function (128–130). In fact, TME exerts an anti-tumor activity at first, but once it is pirated by neoplastic cells, it turns cancer-affiliated (129). For instance, tumor cells orchestrate modulations in the microenvironment by releasing several extracellular signals in order to promote neo-angiogenesis and peripheral immune tolerance (131,132).

In addition, TME can also act by favoring cell invasion and metastasis through EMT activation (133). Considering that immunity is influenced by a complex of tumor, host and environmental factors which modulate anti-cancer response (134), TME is reported to induce immune suppression, reduce chemotherapy efficacy, favor EMT in the airways, and also may play a relevant role in the study of the underlying biology that predisposes COPD patients to LC (22).

ECM is an entity that contains a complex set of molecules secreted by stromal cells (128). Despite the important role displayed by ECM in the maintenance of tissue architecture in normal conditions, the ECM role is opposed after the cancer is stablished and behaves favor of the tumor, but its modifications in presence of tumor cells are not fully understood (135). The main compounds found in the ECM are majorly collagen, elastin, fibronectin, periostin, and tenascin-C which are reported to display an important role in cancer cells proliferation and invasion but are also crucial for stroma development in a healthy state (128). Additionally, relevant ECM targets are being investigated as biomarkers and anti-cancer treatments (135).

Introduction

Cancer-associated fibroblasts (CAFs) are a sub-population of fibroblasts with a myofibroblastic phenotype which function is redirected towards carcinogenesis and remain permanently activated (129). Cancer cells activate CAFs in order to fuel tumor progression through growth factors, ROS, microRNA (miRNA) direct cell-cell communication, and adhesion molecules contacting with leukocytes (136–138). CAFs are able to remodel ECM with a deep impact through angiogenesis activation, inflammatory cells recruitment, and stimulation of cancer cell proliferation *via* mesenchymal-epithelial cell interactions, and growth factors and immune suppressive cytokines secretion (136,139).

A pivotal role is displayed in CAFs during carcinogenesis. Indeed, CAFs promote tumor growth and invasion through hepatocyte growth factor (HGF), fibroblast growth factor (FGF), transforming growth factor β (TGF-β), and platelet-derived growth factor (PDGF) (129). Furthermore, angiogenesis can be induced by CAFs through fibroblast growth factor 2 (FGF2) and VEGF expression (140). In addition, CAFs overexpress galectin-1, C–X–C motif ligand 12 (CXCL12), matrix metabolloproteinase-2 (MMP-2), and interleukin-22 (IL-22), which are important contributors to poor prognosis, and induce EMT, epithelial invasion, and cell invasion through signal transducer and activator of transcription 3 (STAT3) and extracellular signal-regulated kinases (ERK) signaling respectively (141–143). CAFs are also reported to modulate through TGF-β, among others, the action of neuroendocrine, inflammatory and immune cells towards carcinogenesis (144–146).

Regardless some difficulties are found in order to stablish selective markers for CAFs, a significant amount of markers represent useful targets in the treatment for LC (129). For instance, fibroblast activation into CAFs can be reversed through miRNA (142,144–146), and CAFs growth can be inhibited through PDGF, FGFR, and fibroblast activation protein (FAP) signaling impairment (147,148).

5.3. Inflammation

Inflammation is a crucial complex physiological process that functions in the maintenance of tissue homeostasis and takes place during protection through innate immunity against pathogens from infection and wound healing (63,68). Acute inflammation is a process tightly regulated by several intermediators but when inflammation is persistent and remains unsolved, it becomes chronic leading to the destruction of the healthy tissue (68). Otherwise, it is agreed that tumor initiation is connected to inflammation by extrinsic and intrinsic pathways (68).

In regards to extrinsic pathway, chronic inflammation increases the risk of LC and is thought to take part in all the stages of carcinogenesis, from initiation to invasion (68). Tumors raised in chronic inflamed areas show infiltration of immune cells, cytokines, chemokines, growth factors, and matrix-degrading enzymes (149). In addition, the immune component of the TME is mainly comprised of lymphocytes, DCs, and macrophages (68,150). All these components display either tumor-suppressing or tumor-promoting events.

Indeed, M2 macrophages are associated with tumor progression, but M1 macrophages can also contribute to tumorigenesis by releasing RNS, ROS and inflammatory cytokines promoting neoplastic transformation through genomic instability (151).

Regarding intrinsic pathway, it is reported that several oncogenes and tumor suppressor genes have a tight association with inflammation. These genes encode for inflammatory mediators that are able to induce tumor promoting features such as angiogenesis, ECM remodeling, induction of EMT and immune surveillance mis function (129,133,152,153). It is important to remark that in spite of extrinsic and intrinsic pathways represent distinct molecular mechanisms, both pathways converge in the TME through the activation of key transcription factors that coordinate inflammation (154,155). As previously mentioned, CS is a risk factor for chronic inflammation that leads to fibrosis and neoplasia but many controversies are found in the elucidation of the exact mechanisms through which inflammation promotes cancer (68). In addition, chronic inflammation induced from several cytokines can promote tumor initiation and malignancy, especially in patients with chronic respiratory conditions (22,68,149,156,157) and several chronic inflammatory events may represent a trigger for tumor development in patients with COPD (22), which are reported to present a pro-inflammatory pattern (158). Furthermore LC patients with COPD present a differential inflammation profile respect LC patients (121). For instance, release of several interleukins may influence key regulatory mechanisms such as apoptosis, autophagy, cell repair, an-

giogenesis and immune response, leading to tumor growth and metastasis (22). However, the mechanisms involved in tumor progression driven by inflammation are not clarified (68,149).

5.4. Immune system

Another chief component of the TME are immune cells. Briefly, the immune system is divided into adaptive immunity and innate immunity (129). Adaptive immunity includes thymus-dependent lymphocytes or T cells, and bursa-dependent lymphocytes or B cells, whereas innate immune cells consist of DCs, NK cells, and macrophages among others (159). T cells are subdivided into CD4+ T, known as helper T cells, and CD8+ T cells, known as effector or cytotoxic T cells (129). DCs express co-stimulatory molecules for T cells (160). Some types of immune cells have an immunosuppressive role (129). For instance, the main immunosuppressive cells are Treg cells, myeloid-derived suppressor cells (MDSC), and M2 macrophages (161).

5.4.1. Tertiary lymphoid structures

There is an increasing evidence of the presence of some structures, outside primary and secondary lymphoid organs, in which adaptive immune response is initiated (162,163). These structures are known as tertiary lymphoid structures (TLSs) and they could usually be found in inflamed tissues under pathological circumstances, including cancer, infectious diseases, rejection or autoimmunity (164). TLSs present a similar structure to lymphoid nodes (LN), suggesting that they may be formed *de novo* following similar orga-

nogenesis patterns (165). Indeed, it has been described that cytokines and molecules implicated in initiation, development and maintenance such as, lymphotoxin, C-C motif ligand (CCL)19 and CCL21 are shared (162,165). As occurs in LN, lymphocytes are congregated in two distinct and adjacent regions inside TLSs (105-109). First, there is a surrounding T-cell-rich area with clusters of T cells and mature DCs. Secondly, there is a B-cell-rich region termed germinal centers (GCs), which contains mostly B cells (mature and naïve), but also T cells, DCs, and macrophages. Both areas are encompassed by specific blood vessels termed high endothelial venules (HEV) which facilitate both the segregation and recruitment of cells (162).

Tumor-associated TLSs have been described in several different solid tumors (166,168–173). Even though the relationship between TLSs and patient outcomes depends on many parameters (including cancer type and stage), the presence of these structures in the tumor niche has been associated with favorable clinical prognosis (168,174). Patients with TLSs present better prognosis and survival compared to those without and the density of T cells and DCs in the tumor-associated TLSs correlates with better clinical outcomes (163). Moreover, the size and density of GCs, and the number of antibody-secreting plasma cells in tumor-associated TLSs correlates with a better clinical outcome (173,175). In fact, despite there are some aspects which remain unknown, it seems that TLSs act as primary initiation sites of antitumor immune responses, as they may work as functional sites where differentiation and activation of tumor-infiltrating cells take place (162,165).

5.5. Cell growth and proliferation

Cell proliferation is the mechanism by which an increase of the number of cells is produced as a result of cell growth and cell division and is defined by the balance between cell division and cell loss through cell death or differentiation. Cells of human body are constantly under division to further differentiate and die in a tightly regulated process in order to ensure tissue homeostasis maintenance. These growth regulatory mechanisms are crucial in certain situations (176). For example when aberrant cells arise, these mechanisms must be activated in order to avoid the proliferation of this kind of cells (177). A failure in this process will lead to malignity. Many molecules such as cytokines, transcription factors and miRNA are reported to regulate cell proliferation and growth in normal conditions and the same factors seem to be impaired in LC (178,179). Tumor proliferation assessment works as a tool for tumor growth measure. For this end, antigens associated with proliferation such as Ki-67 are commonly explored. Ki-67 is a nuclear protein expressed throughout the cell cycle in proliferating cells thus it is not expressed in quiescent cells (180). This proliferation marker is widely used by pathologists as a prognostic factor in many solid tumors (181–185). Tumor cell proliferation analyses describe tumor behavior and aggressiveness (180). Regarding NSCLC, tumor cells proliferation correlates with a worse outcome (186), and predicts recurrence (187,188) and survival after lung tumor resection (189). Importantly, Ki-67 should be used along with other parameters (180). Indeed, another study suggested that proliferation in adenocarcinoma is asso-

ciated with poor clinical outcome, in contrast with SCC which is associated with improved prognosis (180).

5.6. Apoptosis

Apoptosis is an orchestrated cellular process that takes place in physiological and pathological conditions (190). This programmed cell death process provides the capacity to eliminate damaged cells from tissues without inflammation in order to maintain tissue homeostasis (191–193). Several signals which include growth factors, interaction with neighbor cells, poor oxygen or nutrients supply, and cell damage can regulate apoptosis (194).

Apoptosis plays a crucial role in tumorigenesis as one of the hallmarks of cancer (192,195). Avoiding cell death allows the accumulation of sufficient oncogenic events to become malignant that otherwise would have been removed by apoptosis (195,196).

In cancer, a misbalance between cell division and cell death is produced (190). This situation can arise from any step of the apoptotic signaling pathway such as the downregulation of the tumor suppressor gene *TP53* (190). Mutations in the gene that encodes for p53 are linked to several cancers (197). This protein works as a sentinel for cellular stress (157). Stress caused by DNA damage, hypoxia or proliferative signals induces p53 to cause cells to undergo cell-cycle arrest and apoptosis (198). Cell-cycle arrest work as a checkpoint for oncogenic mutation prevention, and if cellular damage is unsolved, the apoptotic machinery must be activated (157).

Nevertheless, as one of the hallmarks of cancer, apoptosis can suppose a powerful therapeutic tool (196).

It is stated that apoptotic machinery disabling may contribute to tumor resistance against therapy (157). Hence, several studies have addressed the study of apoptosis in different subtypes of LC (193). SCLC cell lines compared to NSCLC, expressed higher levels of B-cell lymphoma 2 (Bcl-2) and the loss of several caspases (193), suggesting that tumorigenesis may arise from cell death evasion in SCLC by the silencing of pro-apoptotic genes by methylation (193). Moreover, activation or over-expression of anti-apoptotic pathways can be found along with pro-apoptotic pathways inactivation (193).

5.7. Autophagy

Autophagy is referred to a catabolic process involved in the degradation of cellular components for tissue homeostasis (199–201) but is also described as a non-apoptotic programmed cell death process (199). The activation of this pathway is suggested to induce cell survival through the supply of energy and the removal of dysfunctional components (199).

Cell death through autophagy, also termed macroautophagy or autophagic cell death is a controversial process (201,202) associated with absence of chromatin condensation, accumulated cytoplasmic vacuolization, LC3 lipidation and caspase-independent apoptosis (202). Moreover, it is reported to regulate apoptosis depending on the surrounding microenvironment (201).

Introduction

Prolonged stress conditions trigger autophagy and apoptosis within cells (202). Both pathways share common regulatory proteins such as Beclin-1, B-cell lymphoma associated X protein (Bax), and Bcl-2 (201), and several autophagy-related proteins (199). Indeed, cell death is a tightly regulated process. For example, the lack of nutrients activates c-Jun N-terminal protein kinase 1 (JNK1), which in turn phosphorylates Bcl-2, disabling its anti-apoptotic action produced after binding with Beclin-1, a promoter protein of both apoptosis and autophagy (203). However, extended starvation is reported to reverse this process (203). The same interaction is also observed between Bcl-2 and Bax. ROS are also involved in cell death (199). Several studies demonstrate the implication of autophagy in the degradation and formation of ROS (199). For instance, autophagy triggers catalase degradation, an antioxidant enzyme (199). Another study shows that stimulation of ROS induced by autophagy inhibition thus lead to NSCLC cells sensitization to cisplatin-mediated apoptosis (199). As a result, mitigation of proliferation in NSCLC cells was produced (199).

Autophagy is implicated in several diseases such as cancer (200). Initially, autophagy may act as an inhibitor of tumor development but then, as a promoter of tumor progression (200). Hence, it can play a positive and negative role in promoting apoptosis in NSCLC (201). This paradox in the role of autophagy in tumorigenesis may cope with the stress originated from hypoxia and increment resistance against therapeutic agents such as chemotherapy or radiotherapy (204).

In the context of cancer, autophagy is reported to be impaired by PI3K, AKT, Bcl-2, and p53 (200,201). This autophagy inactivation is known to lead to genomic instability (205,206) and mitigation of intracellular processes including differentiation (206), senescence (206), and metabolism (207) which in turn leads to Warburg effect activation. It is reported that decreased activity in autophagy is associated with excessive protein degradation prevention in starved or stressed tumor cells (201,204).

Low survival rates in LC patients are associated with resistance events against chemotherapy and radiotherapy due to defects in the autophagic and apoptotic interplay (204). On this basis, several cytotoxic agents that induce autophagy are carried in the clinics (199).

6. MURINE MODELS OF LC

A range of murine models that mimic human LC have been developed. These *in vivo* models are useful tools for understanding the tumor biology (either initiation or progression), the development and validation of new therapeutic strategies, and the identification of novel biomarkers for early diagnosis (208). Mouse models include chemically induced or spontaneous LC but genetically engineered are the most widely used and are also found to share better correlations with humans (209). Moreover, primary human LC tumors are implanted in the same original tissue of immunodeficient mice, these kind of animal models are known as xenografts (209,210). Carbapenem-resistant Enterobacteriaceae (Cre) and flippase (Flp) re-

combinase-mediated methods are widely used in order to develop LC in mice by inducing mutations in tumor-suppressor genes or by activating oncogenes (208,211). In order to induce Cre recombinase activity into pulmonary tissues, engineered adenovirus-Cre or lentivirus-Cre is intranasal or intratracheal administered (208,209). It is important to assess the reliability of the mice model according to the study that is intended to be carried out. For instance, immune deficient mice tumor xenografts derived from human cell lines are not valid models for the study of immunotherapeutic agents due to the lacking immune system in mice (210).

6.1. Syngeneic models

Syngeneic mouse models are widely used and consist of tumor tissues derived from the same genetic background as a given mouse strain, and once cancer cell lines are obtained, then are engrafted back into the same inbred immunocompetent mouse strain (208).

The advantages that feature this easy and economic model are that no tumor rejection is present and the immune system in mice is full. For this reason, it represents a perfect immunocompetent model for immunomodulation assays (210). In fact, in the current thesis, a syngeneic mouse model was used in order to study the immunomodulation exerted by monoclonal antibodies (mAbs) in LC. Briefly, it consists in the inoculation of LP07 lung adenocarcinoma cells in a BALB/c mice strain (212,213). The model used perfectly fits the interest of the research given that our immunocompetent model features full murine immunity and comprehensive stroma.

Moreover, syngeneic models are key tools for the study of immunotherapeutic strategies, particularly using immune checkpoint inhibitors. Furthermore is a long-time cancer cachexia model extensively used in our group and well validated (123,214–216).

HYPOTHESIS

Hypothesis

We hypothesized whether a differential immunologic profile may exist in the lung tumors of patients with lung cancer with and without COPD.

We also hypothesized whether biological mechanisms other than the immune system may also contribute to the reduced tumor burden attained by immunomodulators in mice with lung adenocarcinoma.

OBJECTIVES

STUDY 1

On the current thesis we focused on the study of individual immune patterns and how are influenced by several events such as the presence of COPD. Accordingly, this study aims to explore the relationships between LC-related biological conditions such as chronic respiratory diseases with the immune profile in lung tumors obtained from lung cancer patients with and without COPD who underwent pulmonary surgery for their lung neoplasm. The specific objectives are represented as follows:

1) To explore the immune profile in the lung tumor and non-tumor specimens of the study patients.
2) To analyze the clinical characteristics of the patients recruited for the study.
3) To assess potential correlations of biological markers with the prognosis of patients

STUDY 2

The aim of this study was to identify biological mechanisms other than the immune system involved in tumor regression after immunomodulators administration. In order to achieve this goal different objectives were defined:

1) To explore the impact of immunomodulators in tumor burden and body weight in mice with lung adenocarcinoma.
2) To assess differences in biological mechanisms involved in tumor regression such as oxidative stress, apoptosis and autophagy between the tumors of mice administered with immunomodulators and vehicle.

METHODS

1. STUDY 1

1.1. Study design and ethics

This was a cross-sectional, prospective study designed in accordance with the World Medical Association guidelines (Declaration of Helsinki, 2008) for research on human beings and approved by the institutional Ethics Committee on Human Investigation (*Hospital del Mar–IMIM*, Barcelona). All patients that were invited to participate in the study signed their informed consent.

Participants were consecutively recruited from the Lung Cancer Clinic of the Respiratory Medicine Department at *Hospital del Mar* (Barcelona, Spain). For this study, 133 patients with LC were recruited. Eligible patients that participated in the study were candidates for tumor resection that underwent pulmonary surgery before receiving any treatment for their lung neoplasm. LC diagnosis was confirmed through histological specimens and classified according to the guidelines for diagnosis and management of LC (217,218). Tumor clinical stage and histologic subtype were established by an expert pathologist. TNM staging was determined according to the 8th edition of the Lung Cancer Stage Classification (37,219). Individuals with signs of severe bronchial inflammation and/or infection (bronchoscopy), current or recent invasive mechanical ventilation and chronic oxygen, SCLC, and chronic cardiovascular, metabolic or clot system disorders were excluded from the study.

Specimens from the tumor and non-tumor lungs were obtained from all the study subjects. Patients were further subdivided *post-hoc* into two groups according to the presence of underlying COPD: 1) 40 patients with LC without COPD (LC group) and 2) 93 patients with LC and COPD (LC-COPD group).

1.2. Clinical assessment

In all patients, lung function parameters were assessed following standard procedures. COPD diagnosis and severity were defined using post-bronchodilator spirometry according to the current guidelines of GOLD (6,220,221).

Body composition evaluation included the assessment of BMI by bioelectrical impedance. In addition, nutritional parameters were also evaluated from all patients by conventional blood tests.

1.3. Sample collection and preservation

Lung specimens were obtained from tumor and surrounding non-tumor parenchyma following standard technical procedures by the specialized thoracic surgeons. In all cases, the lung pathologist expert selected specimens from the lung tumor and non-tumor surrounding parenchyma of approximately 10x10 mm^2 size from the fresh samples after a careful collection of the specimens required for diagnosis purposes. Non-tumor specimens were collected as far distal to the tumor margins as possible (>7 cm). Importantly, in the tumor specimens from all the study patients, a minimum amount of 50% of cancer cells was similarly identified. The remaining cell components

included inflammatory and stromal cells in all the analyzed tumors. A fragment of both tumor and non-tumor was formalin-fixed and paraffin-embedded until further use and another fragment was immediately snap-frozen in liquid nitrogen and stored at −80 °C. Part of the biological samples used in the current study were obtained from *Parc de Salut MAR* Biobank (MARBiobanc, Barcelona).

1.4. Identification of T and B cells, Treg cells, plasmatic cells and TLSs in the lung specimens

T and B cells, Treg cells, IgG and IgA immunoglobulins secreting plasma cells, and TLSs were identified on the three-micrometer lung tumor and non-tumor cross-sections with double-staining immunohistochemical assays (EnVision DuoFLEX Doublestain System, Dako North America Inc., Carpinteria, CA, USA) following the manufacturer's instructions and previous studies (222–225). T and B cells were identified through CD3 and CD20 expression respectively using appropriate antibodies (anti-CD3 antibodies and, anti-CD20, clone L26, Dako North America, Inc., CA, USA). Moreover, CD3 and forkhead box P3 (FOXP3) receptors were used to identify Treg cells using specific antibodies (anti-CD3 and anti-FOXP3, clone 236A/E7, Dako North America and Abcam, Cambridge, UK, respectively). Plasma cells were identified using CD138 and the corresponding immunoglobulins A and G (anti-CD138, clone MI15, anti-IgA, and anti-IgG, Dako North America). All reagents used in these experiments were part of the specific EnVision DuoFLEX Doublestain System kit. Before the start of the

assay, reagents were equilibrated to room temperature. Following deparaffinization, lung sample cross-sections were immersed into preheated antigen-retrieval solution (Dako high pH solution), incubated at 95ºC for 20 minutes to be then allowed to cool down to room temperature. Slides were washed over the following steps with wash buffer (Dako wash buffer solution). Endogenous peroxidase and phosphatase activity were blocked by 15-minute incubation in Dako endogenous dual enzyme block solution. Samples were incubated with the corresponding primary antibodies: anti-human CD3 rabbit polyclonal antibody or anti-human CD138 mouse monoclonal antibody for 40 minutes. Second incubation was performed for one hour with the corresponding antibody in each case (anti-human CD20 mouse monoclonal antibody, anti-human FOXP3 mouse monoclonal antibody, anti-human IgA or IgG rabbit polyclonal antibody). Dextran polymer (EnVision DuoFLEX, Dako) was used as secondary antibody. Samples were incubated for 20 minutes with horseradish peroxidase (HRP) for mouse monoclonal antibodies and alkaline phosphatase (AP) for rabbit polyclonal antibodies. Slides were gently washed and incubated for 10 minutes with diaminobenzidine (EnVision DuoFLEX DAB^{+}) as a chromogen for mouse monoclonal antibodies (brown reaction product; anti-CD20, anti-FOXP3 or anti-CD138 antibodies) and liquid permanent red (EnVision DuoFLEX LPR) as a chromogen for rabbit polyclonal antibodies (red reaction product; anti-CD3, anti-IgA or anti-IgG antibodies). All procedures were conducted at room temperature. Hematoxylin counterstain was performed for 2 minutes, and slides were mounted for conventional microscopy.

Images were captured under a light microscope (Olympus, Series BX50F3, Olympus Optical Co., Hamburg, Germany) coupled with an image-digitizing camera (Pixera Studio, version 1.0.4, Pixera Corporation, Los Gatos, CA, USA). The number of cells and total area (μm^2) was measured in each of the lung specimens (both tumor and non-tumor samples) using Image J software (National Institute of Health, Maryland, USA).

In each lung section, the total number of T cells (CD3-positively-stained), B cells (CD20-positively-stained), Treg cells (CD3 and FOXP3-positively-stained), plasma cells secreting IgA (CD138 and IgA-positively-stained) and plasma cells secreting IgG (CD138 and IgG-positively stained) were quantified blindly by two independent observers who were previously trained for that purpose. Data are presented as follows: 1) the percentage of either B or T cells separately in the measured area in both tumor and non-tumor lung specimens (% B cells/μm^2 and % T cells/μm^2, respectively); 2) the percentage of Treg cells in the measured area in both tumor and non-tumor lung specimens (% Treg cells/μm^2), and 3) the percentage of either IgA or IgG positive plasma cells in the measured area in both tumor and non-tumor lung specimens (% IgA plasma cells/μm^2 and % IgG plasma cells/μm^2).

The number of TLSs was also manually counted after identification of the cell types (T and B cells) forming these structures. Two independent observers who were previously trained for that purpose counted the number of TLSs. The total area (mm^2) was measured in

each of the lung specimens using Image J software (National Institute of Health). In addition, the area of each TLSs was also measured in both tumor and non-tumor specimens. Data are presented as follows: 1) the number of TLSs in the measured area in both tumor and non-tumor specimens (number of TLSs/mm^2) and 2) the total area of all the identified and counted TLSs (mm^2).

1.5. Identification of GCs in TLSs of lung specimens

Within the TLSs structures, the presence of GCs was specifically evaluated in each lung tumor and non-tumor specimens on the three-micrometer sections following standard procedures as previously described (172,226,227). Lung tumor and non-tumor specimens were stained with hematoxylin and eosin. Images of the stained lung sections (tumor and non-tumor) were captured using a light microscope (Olympus, Series BX50F3, Olympus Optical Co., Hamburg, Germany) coupled with an image-digitizing camera (Pixera Studio, version 1.0.4, Pixera Corporation, Los Gatos, CA, USA).

GCs were selected by the presence of two separate topographic zones: 1) one dark-stained area, which was characterized by a densely population of lymphocytes and 2) a light-stained area, which was characterized by a low-density lymphocyte site. Data are expressed as the absence or presence of GCs in the measured area in all study groups of patients (expressed as GCs/mm^2).

1.6. Identification of NK cells in lung specimens

NK cells were identified in the tumor and non-tumor lung specimens on the three-micrometer sections using immunohistochemical procedures as previously described (123,228). Following deparaffinization and alcohol battery hidratation, lung cross-sections were immersed into preheated antigen retrieval solution of ethylenediaminetertetraacetic acid (EDTA, pH 8), incubated at 95ºC for 20 minutes to be then allowed to cool down to room temperature. Slides were washed over the following steps with phosphate buffer saline (PBS). Endogenous peroxidase activity was blocked with 3% hydrogen peroxide for 30 minutes. Primary antibody incubation with anti-natural Cytotoxicity Triggering Receptor 1 (anti-NCR1, Abcam, Cambridge, UK) was performed for one hour. Slides were incubated with biotinylated universal secondary antibody for 30 minutes followed by 30-minute incubation with HRP-streptavidin and DAB for 5 minutes (kit LSAB+HRP Dako Cytomation Inc., Carpinteria, CA, USA) as a substrate. Hematoxylin counterstain was performed and slides were dehydrated and mounted for conventional microscopy. Images of the stained lung sections (tumor and non-tumor) were captured with a light microscope (Olympus, Series BX50F3, Olympus Optical Co., Hamburg, Germany) coupled with an image-digitizing camera (Pixera Studio, version 1.0.4, Pixera Corporation, Los Gatos, CA, USA). In addition, the number of NCR1-positively-stained cells was counted in the tumor and non-tumor lung specimens from all the study patients and the area of the lungs in which NK cells were identified (μm^2) was also measured in

both tumor and non-tumor specimens using Image J software (National Institute of Health). Data are expressed as the percentage of NK cells in the measured area in both tumor and non-tumor lung specimens (NK cells/μm^2).

1.7. Statistical analyses

All statistical analyses shown in the present study were performed using the software SPSS 22.0 (SPSS Inc, Chicago, IL, USA). Data are expressed as mean (standard deviation). The normality of the study variables was explored using Shapiro-Wilk test. Differences between the quantitative variables obtained in the study groups in the analyzed markers were assessed using one-way analysis of variance (ANOVA) and Tukey's *post-hoc* to adjust for multiple comparisons, whereas, differences between the qualitative variables (the number of GCs) in groups were explored using the Chi-square test. Differences between groups in clinical variables were assessed using the Student's T-test, whereas differences between study groups for qualitative variables (TNM staging, histological diagnosis, smoking history and body weight loss) were explored using the Chi-square test. Statistical significance was established at $P \leq 0.05$.

2. STUDY 2

2.1. Animal experiments

2.1.1. Tumor development

An animal model of LC was developed through the inoculation of malignant cells from LP07 stable cell line derived from the transplantable P07 lung tumor, an adenocarcinoma that appeared spontaneously in the lung of a BALB/c mouse (213). LP07 cell line was obtained *in vitro* after successive passages from primary culture of P07 cells in previous studies (212). Hence, both P07 and LP07 cell lines, show similar features regarding LC biology, which includes incidence, histology and paraneoplastic syndromes (212,213). Indeed, one month after inoculation of malignant cells, all mice developed lung metastasis, spleen enlargement, and severe cachexia without any other organ affectation as previously reported (212,213,229,230).

2.1.2. Experimental design

BALB/c female mice were obtained from *Harlan Interfauna Ibérica SL* (Barcelona, Spain) and kept under pathogen-free conditions with a 12: 12h light: dark cycle during all the study process in the animal house facility at the PRBB.

Experimental procedures conducted in mice along the study are illustrated in **Figure 4**. Indeed, eighteen female BALB/c mice received a subcutaneous inoculation of LP07 viable cells (4×10^5) resuspended in 0.2 mL of minimal essential medium (MEM) in the

left flank. After tumor transplantation at day 0, mice were studied for a period of 30 days and randomly divided into two independent groups (N=9/group) as follows: 1) LC-control group of mice administered with vehicle, and 2) LC-mAbs group of mice treated with a combination of mAbs.

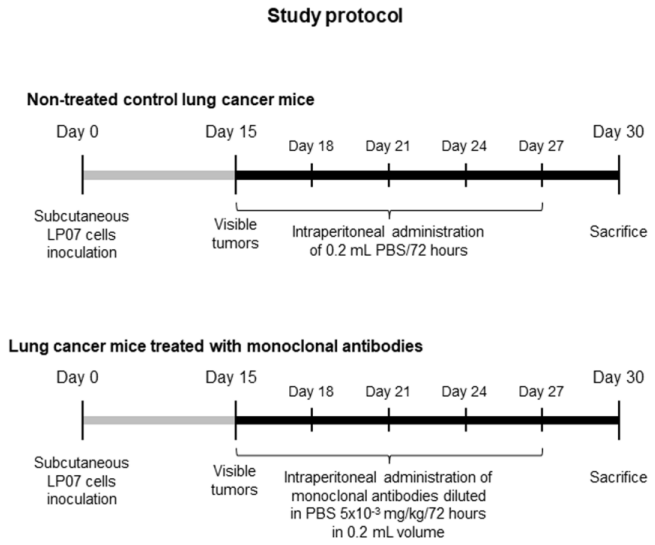

Figure 4. Graphical time-line representation of the control group of animals and group treated with mAbs.

The cocktail of mAbs was composed of selective immune checkpoint inhibitors reported to modulate different signaling pathways and reduce tumor burden through enhanced immunity (231). The immunomodulatory mAbs included in the cocktail were: 1) anti-programmed cell death-1 antibody (anti-PD-1 antibody; RMP1-14, Cat. #BE0146, BioXCell, New Hampshire, USA), 2) anti-cytotoxic T-lymphocyte associated protein-4 antibody (anti-CTLA-4 antibody;

9D9, Cat. #BE0164, BioXCell), 3) anti-TNF receptor superfamily member 9 antibody (anti-CD-137 antibody; LOB12.3; Cat. #BE0169, BioXCell), and 4) anti-B-lymphocyte antigen antibody (anti-CD19 antibody; 1D3, Cat. #BE0150, BioXCell).

Mice from LC-control group received an intraperitoneal administration of 0.2 mL of PBS, in contrast with animals from LC-mAbs group that were treated with the cocktail of mAbs (5×10^{-3} mg/kg of each antibody dissolved in PBS in a dose of 0.2 mL) intraperitoneally administered. In addition, both experimental groups respectively received their dose administration every 72 hours starting from day 15 after tumor transplantation at day 0 (**Figure 4**).

2.1.3. Ethics

This was a controlled study designed in accordance with the ethical regulations on animal experimentation of the European Community Directive 2010/63/EU, the Spanish Legislation (Real Decreto 53/2013, BOE 34/11370–11421) and the European Convention for the Protection of Vertebrate Animals Used for Experimental and Other Scientific Purposes (1986) at PRBB. All animal experiments were approved by the Animal Research Committee (Animal Welfare Department in Catalonia, Spain, # EBP-15-1704).

2.1.4. In vivo measurements conducted on the animals

From day 0, body weight and food intake were daily measured in all mice. In addition, tumor size was also daily measured with a caliper

from day 15 (when tumor injuries were visible) up until the end of the study period. Food and water were supplied *ad libitum* for the entire duration of the study.

2.1.5. Sacrifice and sample collection

At day 30 post-inoculation of LP07 cells, all mice from both experimental groups were euthanized 10 minutes after an intraperitoneal inoculation of 0.1 mL of sodium pentobarbital (60 mg/kg). In all animals, the pedal and blink reflexes were evaluated in order to verify total anesthesia depth. The subcutaneous tumors from all mice were collected and weight was measured in a high-precision scale. In all study samples, a fragment of the tumor specimens was immediately frozen in liquid nitrogen and stored at -80ºC afterwards. The remaining tumor specimen was immersed in an alcohol-formol bath to be then paraffin-embedded in blocks until further use. While frozen tissues were used to explore the expression levels of several molecular markers, the paraffin-embedded tissues were used for histological purposes.

2.2. Molecular biology analyses

2.2.1. Immunoblotting of 1D electrophoresis

Protein levels of the different molecular markers explored in the study were determined by immunoblotting 1D electrophoresis according to procedures applied in previous studies (232). In a brief, frozen tumor specimens extracted from mice of both experimental groups were homogenized in a specific buffer that contained 50 mM HEPES, 150 mM NaCl, 100 mM NaF, 10 mM sodium pyrophospha-

te, 5 mM EDTA, 0.5% Triton-X, 2 μg/mL leupeptin, 100 μg/mL PMSF, 2 μg/mL aprotinin and 10 μg/mL pepstatin A.

Protein concentration from each tumor homogenate was obtained from at least two nearly measurements by Bradford method. Equal amounts of total protein (30 μg) from tumor homogenates were always loaded onto the gels, as well as identical sample volumes/lane. In order to carry out the comparisons between the experimental groups, tumor homogenates were always run together in the same order in two fresh 10-well mini-gels for each of the antigens explored in the study. Proteins were then separated by electrophoresis, transferred to polyvinylidene difluoride (PVDF) membranes, blocked with 5% non-fat milk or with 1% bovine serum albumin (BSA), depending on the primary antibody and incubated with the corresponding selective primary antibodies overnight.

The following specific primary antibodies were used to detect the different molecular markers: anti-3-nitrotyrosine antibody (total protein tyrosine nitration, 1:1000, Invitrogen, Eugene, Oregon, USA), anti-malondialdehyde protein adducts antibody (MDA, 1:4000, Academic Bio-Medical Company, Inc. Houston, TX, USA), anti-catalase antibody (1:2000, Calbiochem, Darmstadt, Germany), anti-Mn-superoxide dismutase antibody (SOD2, 1:2000, Santa Cruz Biotechnology, Santa Cruz, CA, USA), anti-CuZn-superoxide dismutase antibody (SOD1, 1:2000, Santa Cruz), anti-light chain 3B antibody (LC3B, 1:1000, Cell Signaling Technology Inc. Massachusetts, USA), anti-Bax antibody (BAX; 1:1000, Santa Cruz),

anti-Bcl-2 antibody (BCL-2; 1:1000, Santa Cruz), sirtuin-1 antibody (SIRT1, 1:1000, Millipore, Massachusetts, USA) and anti-glyceraldehyde 3-phosphate dehydrogenase antibody (GAPDH; 1:2000, Santa Cruz). Antigens from all samples were detected using horseradish peroxidase (HRP)-conjugated secondary antibodies (Jackson ImmunoResearch Inc, West Grove, PA, USA) and a chemiluminescence kit (Thermo Scientific, Rockford, IL, USA). The specificity of the different antibodies was confirmed by the omission of the primary antibody and incubation of the membranes only with secondary antibodies. PVDF membranes were scanned with the Molecular Imager Chemidoc XRS System (Bio–Rad Laboratories, Hercules, CA, USA) using the software Quantity One version 4.6.5 (Bio–Rad Laboratories).

For each of the study antigens, PVDF membranes of samples from the different groups were always detected in the same picture under identical exposure times. Optical densities of specific proteins were quantified using the software Image Lab version 2.0.1 (Bio-Rad Laboratories). Final optical densities obtained in each experimental group of mice corresponded to the mean values of the different samples (lanes) of each of the study antigens. Values of total MDA-protein adducts and tyrosine nitration protein levels in a given sample were calculated by addition of optical densities (arbitrary units) of individual protein bands in each case. In order to validate equal protein loading across lanes, the glycolytic enzyme GAPDH was used as the protein loading control in all immunoblots.

Standard stripping methodologies were employed to detect the loading control GAPDH for each of the markers. Briefly, membranes were stripped of primary and secondary antibodies through incubation with a stripping solution [(25 nM glycine, pH 2.0, and 1% sodium dodecyl sulphate-polyacrylamide gel electrophoresis (SDS)] for 30 minutes followed by two consecutive washes containing phosphate buffered saline with tween (PBS-T) at room temperature for 10 minutes. Subsequently, membranes were blocked with either 5% non-fat milk or 1% BSA, depending on the primary antibody and incubated with primary and secondary antibodies following the procedures described above.

2.2.2. Histological analyses of the tumor

Immunohistochemical procedures were applied on the 3 µm paraffin-embedded tumor sections in order to explore expression levels of the proliferation marker Ki-67 following previous studies (229). Moreover, expression levels of CD3 and CD8 were assessed to identify T cells and cytotoxic T cells respectively. Briefly, tumor cross-sections were deparaffinized with heat, hydrated in an alcohol battery and antigen retrieval was carried out for 30 min by heating slides in a water bath in EDTA buffer pH 8 for Ki-67 and for 15 min by boiling using a pressure cooker in 0.1M citrate buffer (pH 6) for CD3 and CD8. Then, slides were washed in PBS and treated with 3% hydrogen peroxide for 30 minutes for Ki-67, and endogenous dual enzyme blocking solution (EnVision DuoFLEX, Dako) for CD3 and CD8. After the incubation with the corresponding Ki-67 primary antibody (anti-Ki67 antibody, Millipore Iberica, CA, USA) during 30

minutes, CD3 primary antibody (anti-CD3, 1:100, Dako), and CD8 primary antibody (anti CD8, 1:500, Abcam, Cambridge, UK). Slides were then washed and incubated for 30 minutes with biotinylated universal secondary antibody followed by incubation for 30 minutes with horseradish-conjugated streptavidin and DAB for 5 minutes (kit LSAB+HRP Dako Cytomation Inc., Carpinteria, CA, USA) as a substrate. Slides were counterstained with hematoxylin for 2 minutes, dehydrated and mounted for conventional microscopy. Images of the stained tumors were taken under a light microscope (Olympus, Series BX50F3, Olympus Optical Co., Hamburg, Germany) coupled with an image-digitizing camera (Pixera Studio, version 1.0.4, Pixera Corporation, Los Gatos, CA, USA). In addition, the number of positively stained nuclei for Ki-67 (marker of cell proliferation) was counted in tumors from all animal groups by using Image J software (National Institute of Health, Maryland, USA). Data are expressed as the percentage of positively-stained nuclei for each of the tumors in the two groups of mice.

In tumor paraffin-embedded sections, apoptotic nuclei were identified using the terminal deoxynucleotidyl transferase-mediated uridine 5'-triphosphate (UTP) nick-end labeling (TUNEL) assay (ApopTag® Peroxidase In Situ Apoptosis Detection Kit, Meck-Millipore, Darmstadt, Germany) in subcutaneous tumors from all study groups following the manufacturer's instructions and previously published studies (215,216). Briefly, tumor sections were fixed and permeabilized. Subsequently, they were incubated with the TUNEL reaction mixture that contains fluorescein-dUTP and termi-

nal deoxynucleotidyl transferase (TdT). During the incubation period, terminal TdT catalyzed the addition of fluorescein-dUTP at free 3'-OH groups in single- and double-stranded DNA. After several washes, the label incorporated at the damaged sites of the DNA was marked by an anti-fluorescein antibody conjugated with the reporter enzyme peroxidase. After washing to remove unbound enzyme conjugate, the peroxidase retained in the immune complex was visualized by a substrate reaction. Negative control experiments, in which addition of the reaction mixture was avoided, were also conducted. Apoptotic positively nuclei were stained (brown color) while negative nuclei were non-stained (blue color, hematoxylin counterstaining). TUNEL-positive nuclei were identified when clearly located within the tumor regions. In each tumor cross-section, the TUNEL-positive nuclei and the total number of nuclei were counted. On this basis, in each tumor preparation, data was expressed as the percentage of the TUNEL positively nuclei from the total number of counted nuclei following previously published methodologies (215,216). A minimum amount of 300 nuclei were counted in each tumor preparation. Final results corresponded to the mean value of the counts provided by the two independent observers (correlation coefficient 95%).

2.3. Statistical analysis

Statistical power was calculated using specific software (StudySize 2.0, CreoStat HB, Frolunda, Sweden). Tumor area and weight were both selected as the target variables on the basis of the T-test to estimate the statistical power between the two experimental groups:

Methods

LC-control mice and LC-mAbs mice treated with monoclonal antibodies. On the basis of a standard power statistics established at a minimum of 80% and assuming an alpha error of 0.05, the statistical power was sufficiently high to detect a minimum difference percentage of 700 and 0.6 points respectively between groups in the sample size (minimum N=9 respectively for tumor area and tumor weight variables). Normality of the study variables was assessed using Shapiro-Wilk test. Results are represented as mean (standard deviation) and the comparisons between study groups were analyzed using the Student's T-test. A significance level of $P \leq 0.05$ was established. Statistical analyses were performed using the Statistical Package for the Social Sciences (Portable SPSS, PASW statistics 22.0 version for Windows, SPSS Inc., Chicago, IL, USA).

RESULTS

1. STUDY 1

1.1. Clinical characteristics

Clinical and functional characteristics of all LC and LC-COPD patients that were recruited in the current thesis are shown in **Table 3**. The number of LC-COPD patients was higher than those with LC-only. Age and BMI did not significantly differ between LC-COPD and LC patients. The number of male patients among the LC-COPD group was significantly higher compared to LC group in contrast with the number of LC-COPD females that was significantly lower than LC females.

The number of current smokers, ex-smokers and the number of packs/year was greater in LC-COPD patients compared to LC patients. Otherwise, the number of never smokers in LC-COPD group was significantly lower than LC group. The functional parameters FEV_1, FEV_1/ FVC, DL_{CO} and K_{CO} in LC-COPD patients were significantly lower than LC patients. Moreover, the prevalence of LC-advanced stages was increased in the LC-COPD group compared to LC. Hence, increased prevalence of SCC and adenocarcinoma was found in LC-COPD patients compared to LC. In LC-COPD compared to LC patients, the blood levels of total leucocytes, neutrophils and lymphocytes were significantly increased. Moreover, the levels of albumin were significantly decreased and while total proteins, fibrinogen, c-reactive protein (CRP), globular sedimentation (GSV), and body weight loss did not differ.

1.2. Number and area of TLSs and GCs in lung specimens

The number of TLSs/mm^2 was significantly increased in the tumors compared to non-tumor specimens in LC patients, while no significant differences were found between the tumor and non-tumor specimens in LC-COPD patients (**Figures 5A** and **5B**). In addition, greater levels of TLSs/mm^2 were found in the tumor specimens of LC patients compared to LC-COPD patients (**Figures 5A** and **5B**).

The area of the TLSs (mm^2) identified was higher in the tumor lesions than in non-tumor specimens in both LC and LC-COPD groups of patients (**Figure 5A** and 5**B**). In contrast, the total area of these structures did not significantly differ between LC-COPD and LC patients in either tumor or non-tumor lungs (**Figures 5A** and **5B**).

Furthermore, the number of GCs/mm^2 was significantly increased in the tumors compared to non-tumor specimens in both LC and LC-COPD patients but any differences were found in the number of GCs between specimens from LC or LC-COPD patients (**Table 4** and **Figure 6**).

1.3. Number of T cells and B cells in lung specimens

Total numbers of B cells/μm^2 were significantly higher in the tumors compared to non-tumor lung specimens in both LC and LC-COPD patients (**Figure 7A** and 7**B**).

On the contrary, the number of T cells/μm^2 significantly decreased in the tumors compared to non-tumor lung specimens of LC patients while no differences were found between the lung specimens of LC-COPD patients (**Figure 7A** and 7**B**). Hence, no significant differences were found in the total number of T cells/μm^2 and B cells/μm^2 between LC-COPD and LC patients in either tumor or non-tumor specimens (**Figure 7A** and 7**B**).

1.4. Number of Treg and NK cells in lung specimens

Levels of Treg cells/μm^2 were significantly increased in the tumors compared to non-tumor specimens in both LC and LC-COPD patients (**Figure 8**). However, no differences were found in the levels of NK cells/μm^2 between the tumor and non-tumor lung specimens in either LC or LC-COPD patients (**Figure 9**). Additionally, no significant differences were found in the total numbers of Treg cells/μm^2 and NK cells/μm^2 between LC-COPD and LC patients in either tumor or non-tumor specimens (**Figures 8** and **9**).

1.5. IgG and IgA secreting plasmatic cells in lung specimens

Levels of IgG+ plasmatic cells/μm^2 significantly decreased in the tumors of both LC and LC-COPD patients compared to respective non-tumor specimens (**Figure 10**). However, any differences were found in the levels of IgA+ plasmatic cells/μm^2 between tumor and non-tumor lung specimens in either LC or LC-COPD patients (**Figure 11**). No significant differences were found in the total num-

bers of IgG+ plasmatic cells/μm^2 and IgA+ plasmatic cells/μm^2 between LC-COPD and LC patients in either tumor or non-tumor specimens (**Figures 10** and **11**).

Table 3. Clinical and functional characteristics of the study patients.

Anthropometric variables	**LC**	**LC-COPD**
Age, years	64 (12)	68 (8)
Male, N / Female, N	15 / 25	80 / 13 ***
BMI, kg/m^2	26 (4)	26 (4)
Smoking history		
Current: N, %	21, 20	44, 47 ***
Ex-smoker: N, %	8, 20	44, 47 ***
Never smoker: N, %	20, 50	5, 6 **
Pack-years	17 (21)	56 (26) ***
Lung function testing		
FEV_1, % pred	90 (12)	67 (9) ***
FEV_1/FVC, % pred	76 (6)	61 (9) ***
DLCO, % pred	84 (14)	68 (18) ***
KCO, % pred	85 (11)	69 (17) ***
TNM staging		
Stage 0: N, %	2, 5	3, 3
Stage IA: N, %	15, 38	27, 29
Stage IB: N, %	11, 28	17, 19
Stage IIA: N, %	1, 2	3, 3
Stage IIB: N, %	6, 15	25, 27 ***
Stage IIIA: N, %	4, 10	14, 15 *
Stage IIIB: N, %	1, 2	0, 0
Stage IV: N, %	0, 0	4, 4
Histological diagnosis		
SCC: N, %	4, 10	17, 19 **
Adenocarcinoma: N, %	30, 75	70, 75 ***
Others: N, %	6, 15	6, 7
Blood parameters		
Total leucocytes/μL	7.51 10^3 (2.46 10^3)	9.06 10^3 (2.94 10^3) **
Total neutrophils/μL	4.92 10^3 (2.55 10^3)	5.93 10^3 (2.61 10^3) *
Total lymphocytes/μL	1.76 10^3 (811.18)	2.30 10^3 (1.59 10^3) *
Albumin (g/dL)	4.28 (0.45)	4.11 (0.56) *
Total proteins (g/dL)	6.98 (0.63)	6.77 (0.79)
Fibrinogen (mg/dL)	424 (120)	450 (152)
CRP (mg/dL)	7.51 (8.54)	6.92 (12.74)
GSV (mm/h)	29 (14)	26 (16)
Body weight loss, kg		
0, N, %	37, 93	85, 91 ***
1-5, N, %	1, 2	3, 3
6-10, N, %	2, 5	5, 6

Continuous variables are presented as mean (standard deviation), while categorical variables are presented as the number of patients in each group and the percentage

in the study group total population. *Definition of abbreviations*: N, number; kg, kilograms; m, metres; BMI, body mass index; FEV_1, forced expiratory volume in the first second; pred. predicted; FVC, forced vital capacity; DL_{CO}, carbon monoxide transfer; K_{CO}, Krogh transfer factor; TNM, tumor, nodes, metastasis; CRP, C-reactive protein; GSV, globular sedimentation velocity; L, liter. *Statistical analyses and significance*: *, $p \leq 0.05$; **, $p \leq 0.01$; ***, $p \leq 0.001$ between LC-COPD patients and LC patients.

Table 4. Number of germinal centers in tertiary lymphoid structures.

	LC		**LC-COPD**	
	NT lung	T lung	NT lung	T lung
0, n (%)	14 (93)	10 (67)	46 (100)	36 (78) ***
>1, n (%)	1 (7)	5 (33) ***	0 (0)	10 (23) ***

Statistical analyses and significance: *** $p \leq 0.001$ between tumor and non-tumor lung specimens in either LC or LC-COPD group of patients. The digit 0 means absence of GCs in the samples

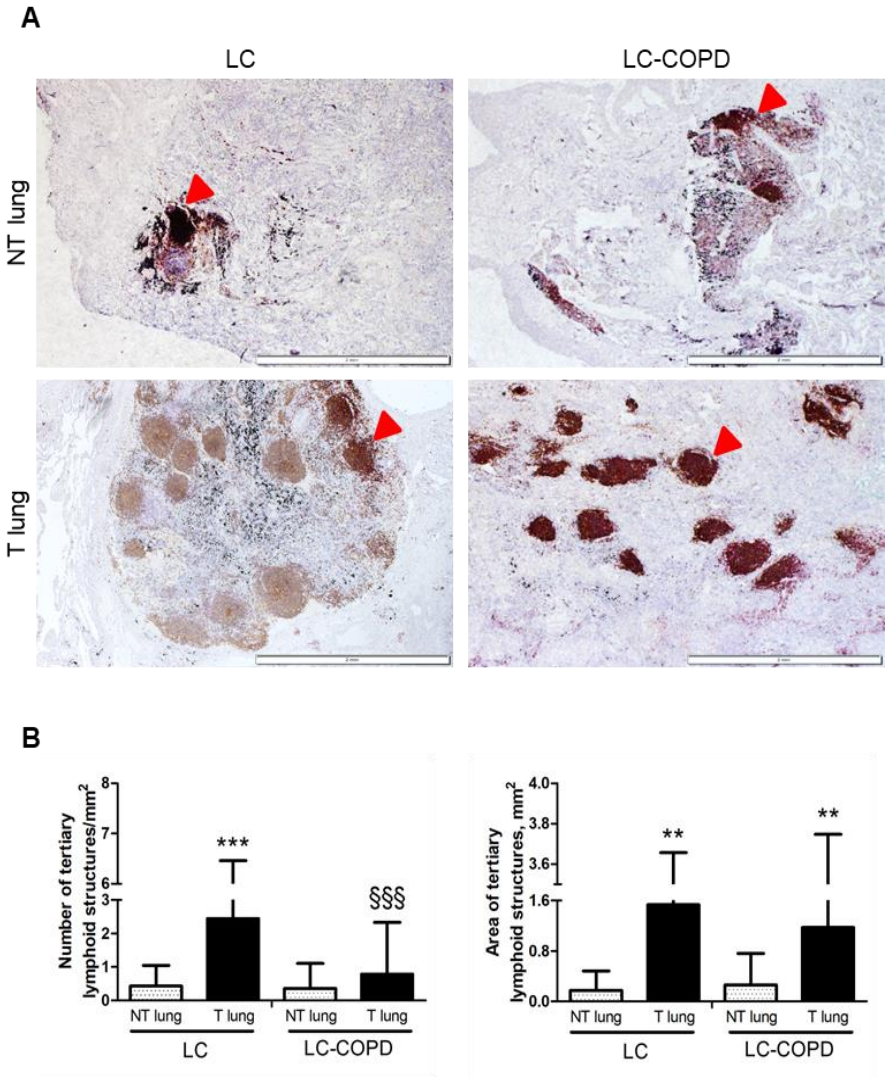

Figure 5. (A) Representative examples of double immunohistoquemical staining for TLSs pointed by red arrows. **(B)** Mean values and SD of number of TLS/mm^2 and area of TLSs (mm^2). Black stained regions correspond to anthracosis. As described in Methods, comparisons were made between the non-tumor (NT) and tumor (T) groups and the lung cancer (LC) and LC–chronic obstructive pulmonary disease (LC-COPD) groups. Statistical significance: *, $p \leq 0.05$; **, $p \leq 0.01$; ***, $p \leq 0.001$ between tumor and non-tumor lungs in either LC or LC-COPD patients. Definition of abbreviations: TLSs, tertiary lymphoid structures, CD, cluster of differentiation.

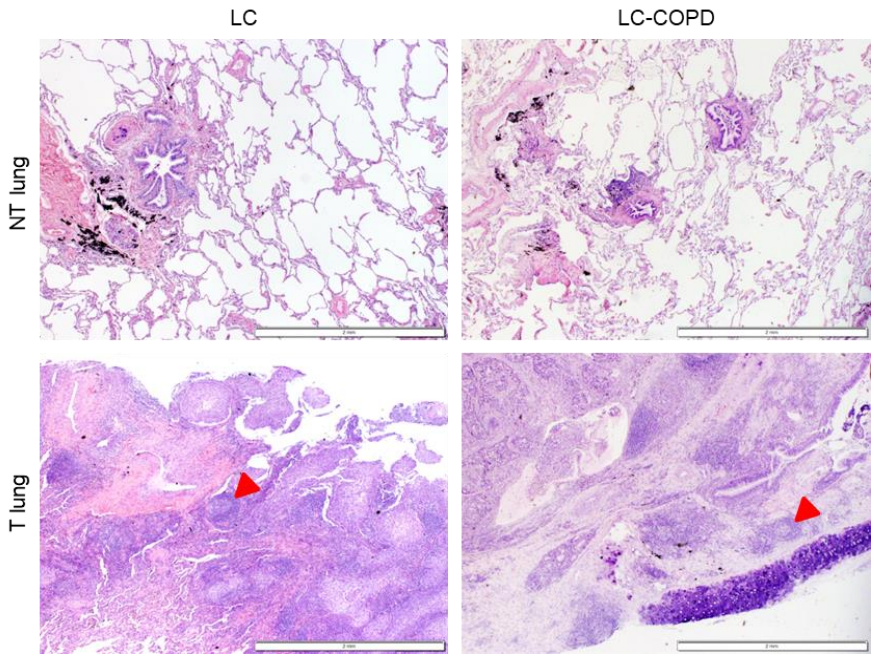

Figure 6. Representative examples of hematoxylin-eosin staining for GCs pointed by red arrows. Black stained regions correspond to anthracosis. Definition of abbreviations: GCs, germinal centers.

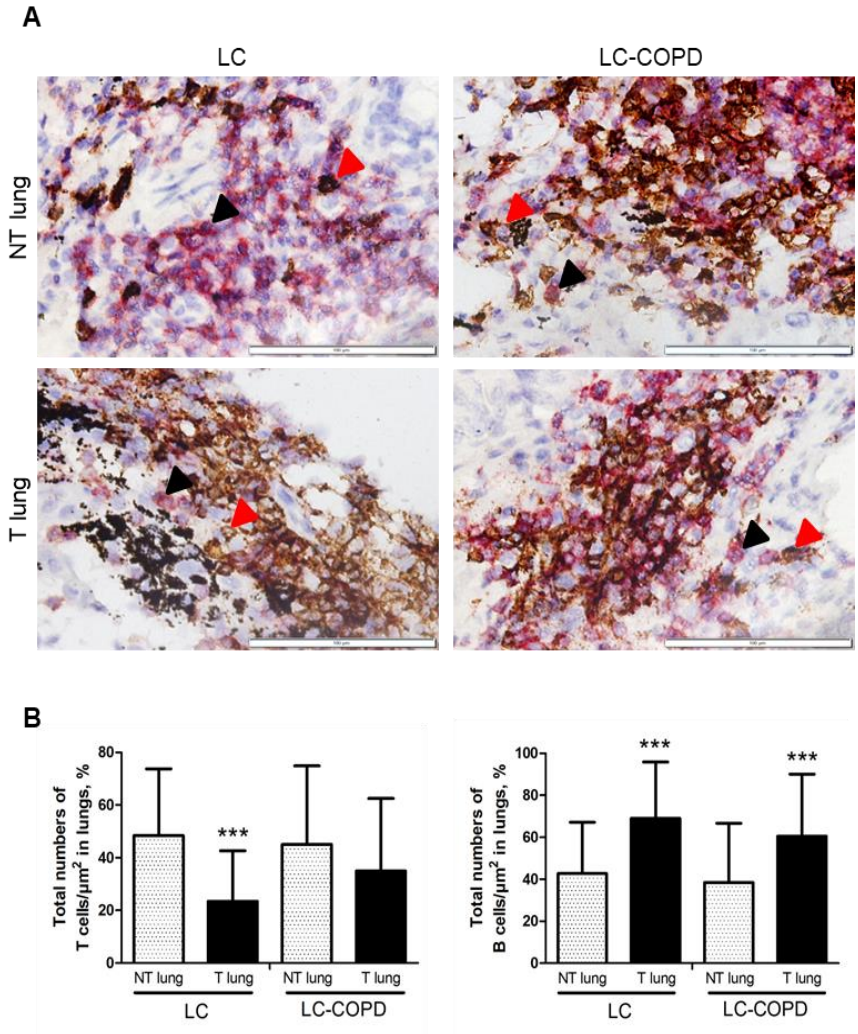

Figure 7. (A) Representative examples of double immunohistoquemical staining for T and B cells. Black arrows point towards T cells (CD3+) stained in red and red arrows point towards B cells (CD20+) stained in brown. **(B)** Mean values and SD of number of T and B cells/μm^2. Black stained regions correspond to anthracosis. As described in Methods, comparisons were made between the non-tumor (NT) and tumor (T) groups and the lung cancer (LC) and LC–chronic obstructive pulmonary disease (LC-COPD) groups. Statistical significance: *, $p \leq 0.05$; **, $p \leq 0.01$; ***, $p \leq 0.001$ between tumor and non-tumor lungs in either LC or LC-COPD patients. Definition of abbreviations: TLSs, tertiary lymphoid structures, CD, cluster of differentiation.

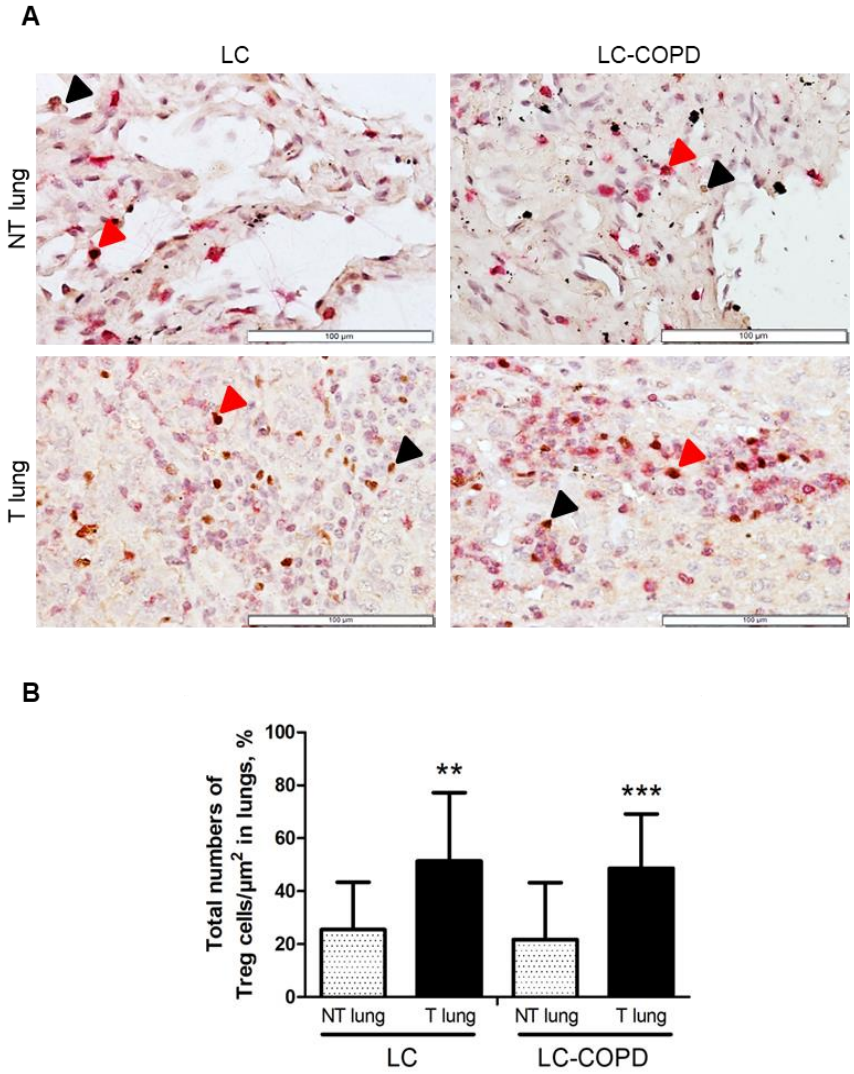

Figure 8. (A) Representative examples of double immunohistoquemical staining for Treg cells (CD3-FOXP3 positively stained T cells). All types of T cells (CD3+) are stained in only in brown (black arrow), while Treg cells (CD3+-FOXP3+) are specifically stained with both brown and red. **(B)** Mean values and SD of number of Treg cells/μm^2 and area (mm^2). Black stained regions correspond to anthracosis. As described in Methods, comparisons were made between the non-tumor (NT) and tumor (T) groups and the lung cancer (LC) and LC–chronic obstructive pulmonary disease (LC-COPD) groups. Statistical significance: **, $p \leq 0.01$; ***, $p \leq 0.001$ between tumor and non-tumor lungs in either LC or LC-COPD patients. Definition of abbreviations: CD, cluster of differentiation; FOXP3, forkhead box P3.

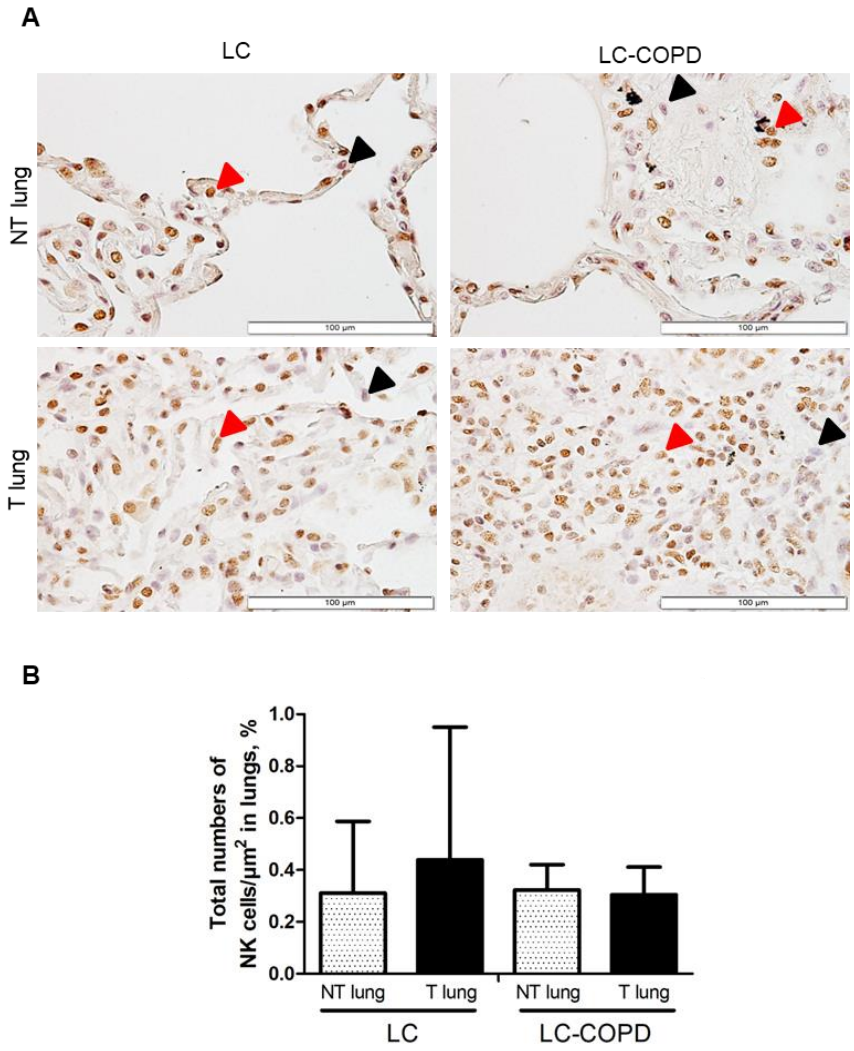

Figure 9. (A) Representative examples of immunohistoquemical staining for NK cells (NCR1+). Black arrows point towards NK cells negatively stained in red and red arrows point towards NK cells (NCR1+) stained in brown. **(B)** Mean values and SD of number of NK cells/µm2. Black stained regions correspond to anthracosis. As described in Methods, comparisons were made between the non-tumor (NT) and tumor (T) groups and the lung cancer (LC) and LC–chronic obstructive pulmonary disease (LC-COPD) groups. Statistical significance: **, $p \leq 0.01$; ***, $p \leq 0.001$ between tumor and non-tumor lungs in either LC or LC-COPD patients. Definition of abbreviations: NK, natural killer; NCR1, natural cytotoxicity triggering receptor 1.

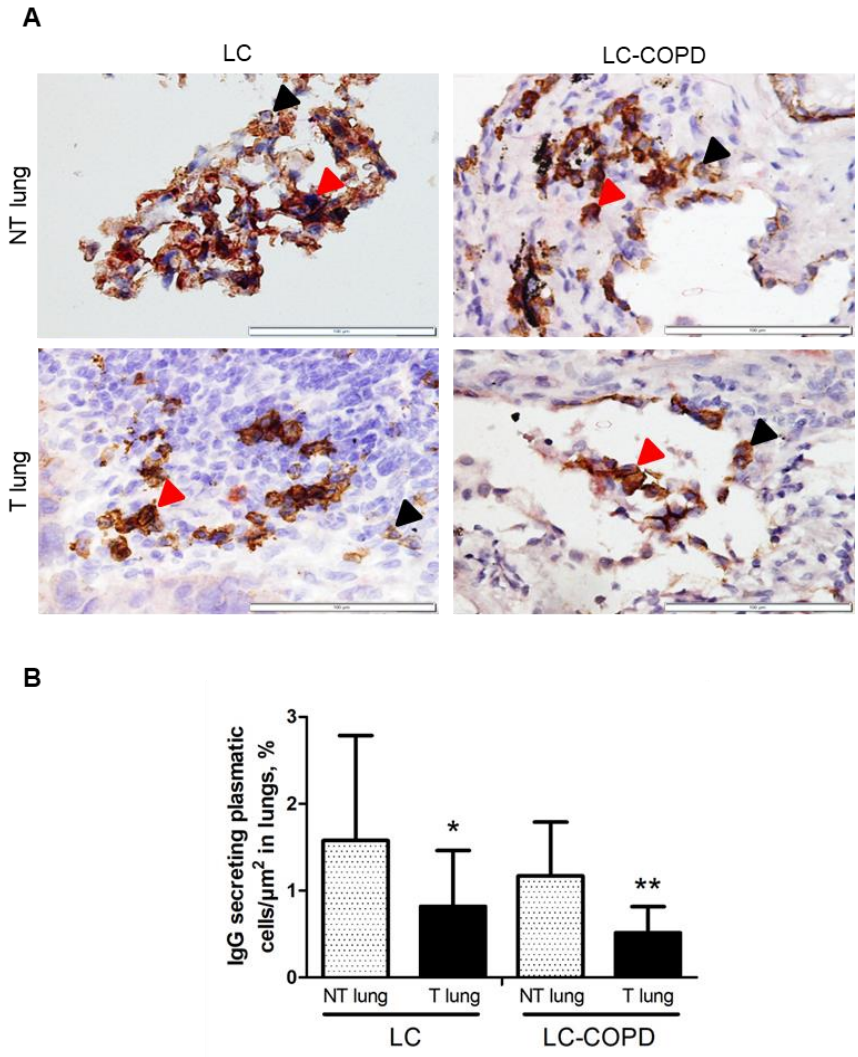

Figure 10. (A) Representative examples of double immunohistoquemical staining for IgG secreting plasma cells (CD138-IgG positively stained plasma cells). All types of plasma cells (CD138+) are stained in only in brown (black arrow), while IgG secreting plasma cells (CD138+-IgG+) are specifically stained with both brown and red. **(B)** Mean values and SD of number of IgG secreting plasma cells/μm^2. Black stained regions correspond to anthracosis. As described in Methods, comparisons were made between the non-tumor (NT) and tumor (T) groups and the lung cancer (LC) and LC–chronic obstructive pulmonary disease (LC-COPD) groups. Statistical significance: *, $p \leq 0.05$; **, $p \leq 0.01$ between tumor and non-tumor lungs in either LC or LC-COPD patients. Definition of abbreviations: CD, cluster of differentiation; Ig, immunoglobulin.

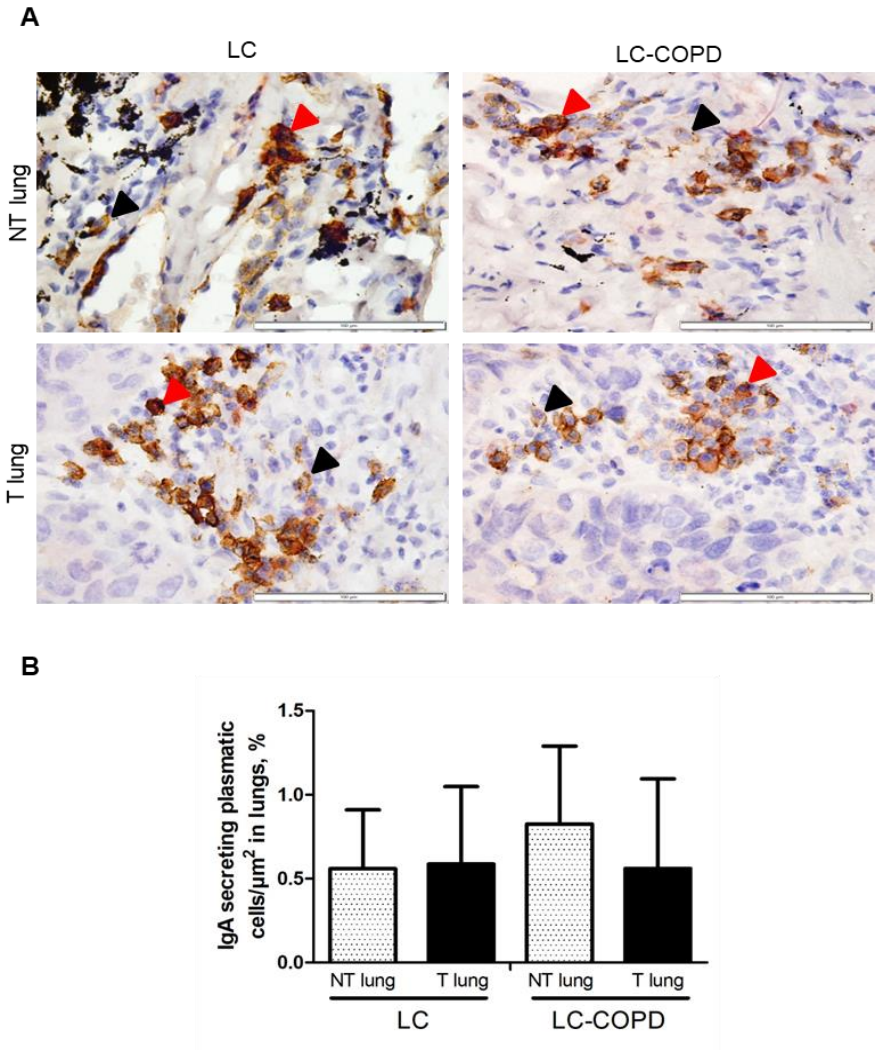

Figure 11. (A) Representative examples of double immunohistoquemical staining for IgG secreting plasma cells (CD138-IgA positively stained plasma cells). All types of plasma cells (CD138+) are stained in only in brown (black arrow), while IgA secreting plasma cells (CD138+-IgA+) are specifically stained with both brown and red. **(B)** Mean values and SD of number of IgA secreting plasma cells/μm^2. Black stained regions correspond to anthracosis. As described in Methods, comparisons were made between the non-tumor (NT) and tumor (T) groups and the lung cancer (LC) and LC–chronic obstructive pulmonary disease (LC-COPD) groups. Statistical significance: *, $p \leq 0.05$; **, $p \leq 0.01$ between tumor and non-tumor lungs in either LC or LC-COPD patients. Definition of abbreviations: CD, cluster of differentiation; Ig, immunoglobulin.

2. Study 2

2.1. Monoclonal antibodies administration reduces tumor burden and increases body weight in mice

As shown in **Table 5** and **Figure 19A**, at the end of the study protocol (day 30), compared to LC-control mice, the group of LC mice treated with the cocktail of mAbs experienced a significant improvement in the following variables: final body weight, body weight gain with and without tumor, tumor weight (34% reduction), and tumor area (64% reduction). Furthermore, levels of Ki-67 positively-stained nuclei were significantly lower (27%) in the tumors of LC-mAbs mice compared to those detected in the LC-control animals (**Table 5** and **Figure 19B**).

2.2. Immunomodulators increase immune cell levels in the tumor microenvironment

As shown in **Figures 25A** and **B**, compared to non-treated LC-control animals, treatment of the LC-mAbs mice with the combination of mAbs elicited a significant rise in the levels of T cells ($CD3^+$) and effector or cytotoxic T cells ($CD8^+$).

2.3. Immunomodulators enhance oxidative stress in the tumor microenvironment

Compared to the LC-control mice, levels of protein tyrosine nitration and total MDA-protein adducts (**Figures 20A** and **B**) and cytosolic

SOD1 (**Figure 21A**) were significantly increased in the subcutaneous tumors of mice treated with the mAbs, while no significant differences were detected in mitochondrial SOD2 or catalase protein levels between the two study groups (**Figures 21B** and **C**).

2.4. Increased levels of apoptosis and autophagy in response to immunomodulation

Compared to non-treated LC-control animals, mice from LC-mAbs group shown a significant rise in the protein levels of BAX, while any differences were found in the levels of BCL-2 in the subcutaneous tumors (**Figures 22A** and **B**). Furthermore, as depicted in **Figures 23A** and **B**, the levels of apoptosis measured by TUNEL show increased levels of apoptotic nuclei in the subcutaneous tumors of mice treated with immunomodulators (LC-mAbs group) compared to non-treated mice (LC-control group).

Protein levels of total LC3, as measured by the ratio of LC3-II to LC3-I, and the deacetylase sirtuin-1 significantly increased in the tumors of the mice treated with the mAbs compared to those seen in the non-treated control animals (**Figures 24A** and **B**).

Results

Table 5. Physiological and tumor characteristics in the study groups of mice.

Variables	LC-control	LC-mAbs
Initial body weight (g)	20.41 (1.22)	20.34 (0.79)
Final body weight (g)	19.35 (2.25)	21.39 (1.57), *
Body weight gain (%)	-4.27 (10.47)	+5.16 (6.33), *
Body weight gain without tumor (%)	-15.06 (11.28)	-2.66 (8.35), *
Tumor weight (g)	2.38 (0.75)	1.57 (0.89), *
Ki-67 positively-stained nuclei (%)	83.09 (13.34)	60.73 (8.28), ***

Variables are presented as mean (standard deviation). Statistical significance: *: $p \leq 0.05$, ***: $p \leq 0.001$ between the two study groups of mice.

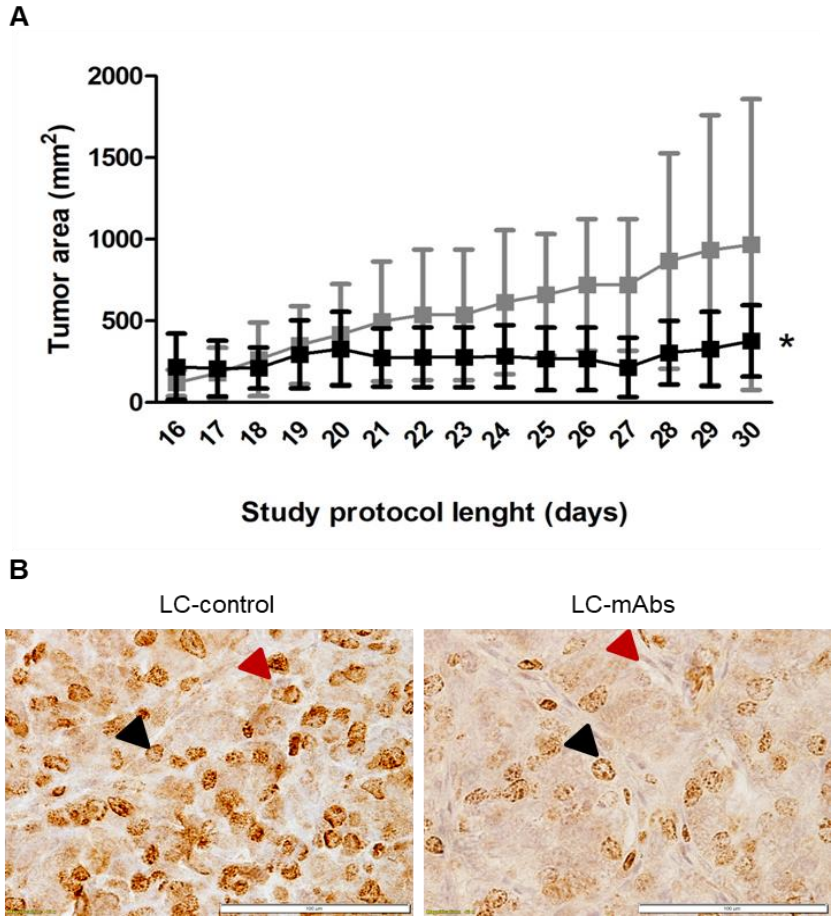

Figure 12. (A) Mean values and standard deviation of subcutaneous tumor area (mm^2) of non-treated control lung cancer group of mice (black color) and lung cancer mice treated with monoclonal antibodies group (red color) during the study protocol. Statistical significance: *: $p \leq 0.05$ between lung cancer group compared to lung cancer-monoclonal antibodies group. **(B)** Representative examples of Ki-67 immunostaining histological sections (40x) in the subcutaneous tumors of non-treated control group (left side) and treated lung cancer group (right side). Black arrowheads point towards Ki-67 positively-stained nuclei (brown color), while red arrowheads point towards Ki-67 negatively-stained nuclei (purple color).

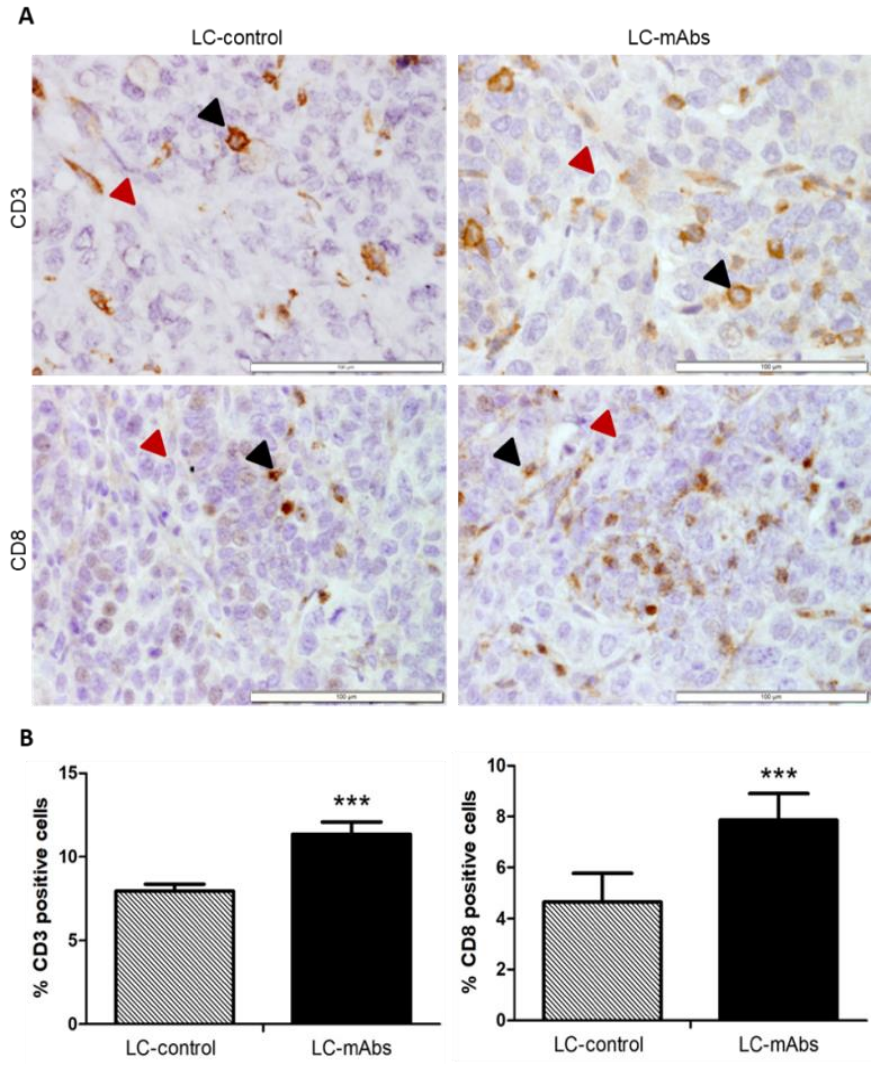

Figure 13. **(A)** Representative examples of CD3 and CD8 immunostaining histological sections (40x) in the subcutaneous tumors of LC-control group (left side) and LC-mAbs group (right side). Black arrowheads point towards CD3 and CD8 positively-stained nuclei (brown color), while red arrowheads point towards CD3 and CD8 negatively-stained nuclei (purple color). **(B)** Representative mean values and standard deviation of % of CD3-positive nuclei and CD8-positive nuclei. Statistical significance is represented as follows: n.s.: non-significant and *: $p \leq 0.05$ and **: $p \leq 0.01$ between non-treated controls and treated lung cancer.

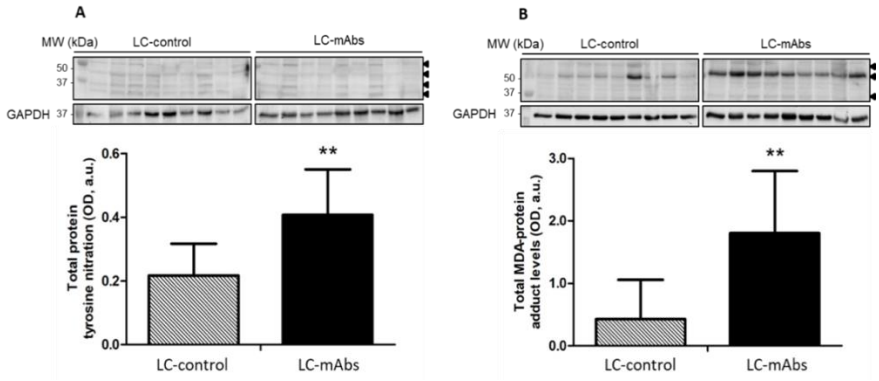

Figure 14. (A) Representative immunoblots and mean values and standard deviation of total tyrosine nitration protein levels in subcutaneous tumors of LC mice as measured by optical densities. **(B)** Representative immunoblots and mean values and standard deviation of total MDA-protein adduct levels in subcutaneous tumors of LC mice as measured by optical densities. Statistical significance is represented as follows: **: $p \leq 0.01$ between non-treated controls and treated lung cancer. Definition of abbreviations: MDA, malondialdehyde; GAPDH, glyceraldehyde-3-phospate dehydrogenase; OD, optical densities; a.u., arbitrary units.

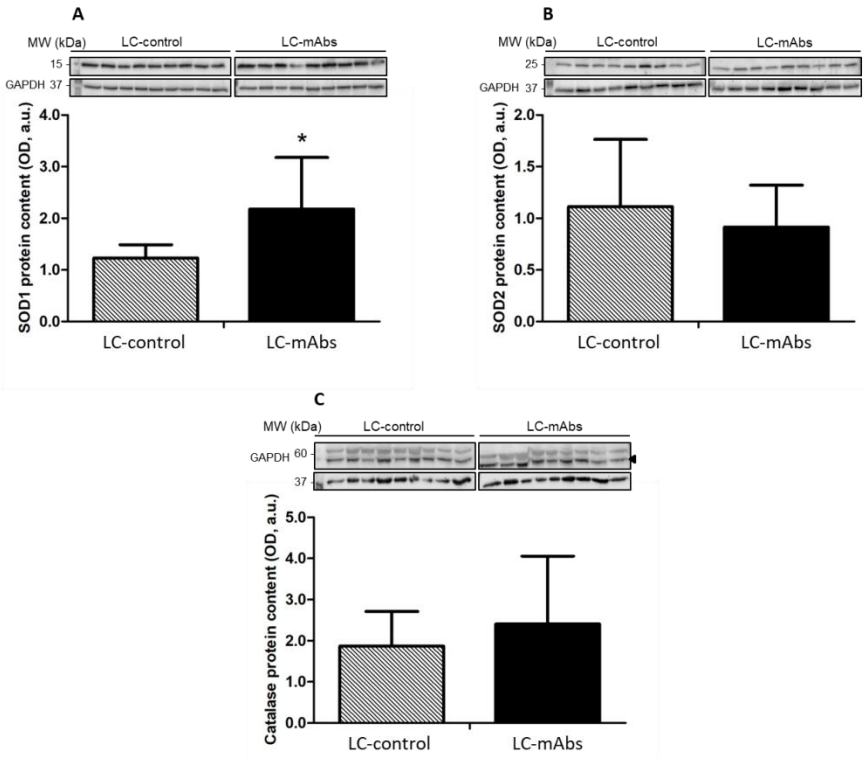

Figure 15. (A) Representative immunoblots and mean values and standard deviation of SOD1 protein levels in subcutaneous tumors of LC mice as measured by optical densities. **(B)** Representative immunoblots and mean values and standard deviation of SOD2 protein levels in subcutaneous tumors of LC mice as measured by optical densities. C) Mean values and standard deviation of catalase protein levels in subcutaneous tumors of LC mice as measured by optical densities. Statistical significance is represented as follows: *: $p \leq 0.05$ between non-treated controls and treated lung cancer. Definition of abbreviations: SOD1, CuZn-superoxide dismutase; SOD2, Mn-superoxide dismutase; GAPDH, glyceraldehyde-3-phospate dehydrogenase; OD, optical densities; a.u., arbitrary units.

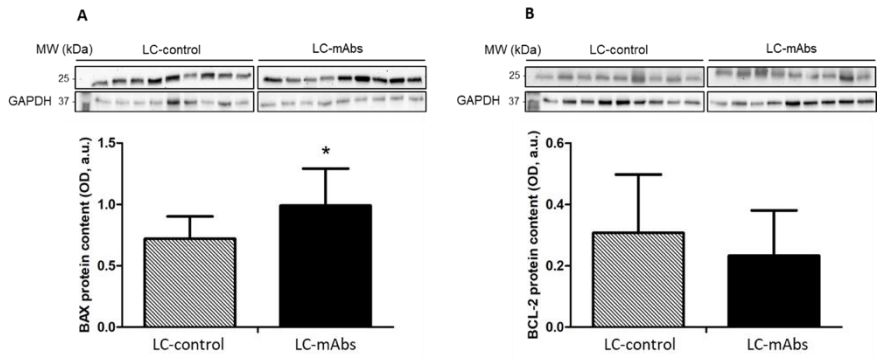

Figure 16. (A) Representative immunoblots and mean values and standard deviation of BAX protein levels in subcutaneous tumors of LC mice as measured by optical densities. **(B)** Representative immunoblots and mean values and standard deviation of BCL-2 levels in subcutaneous tumors of LC mice as measured by optical densities. Statistical significance is represented as follows: *: $p \leq 0.05$ between non-treated controls and treated lung cancer. Definition of abbreviations: BAX, BCL-2 associated X protein; BCL-2, b-cell lymphoma 2; GAPDH, glyceraldehyde-3-phospate dehydrogenase; OD, optical densities; a.u., arbitrary units.

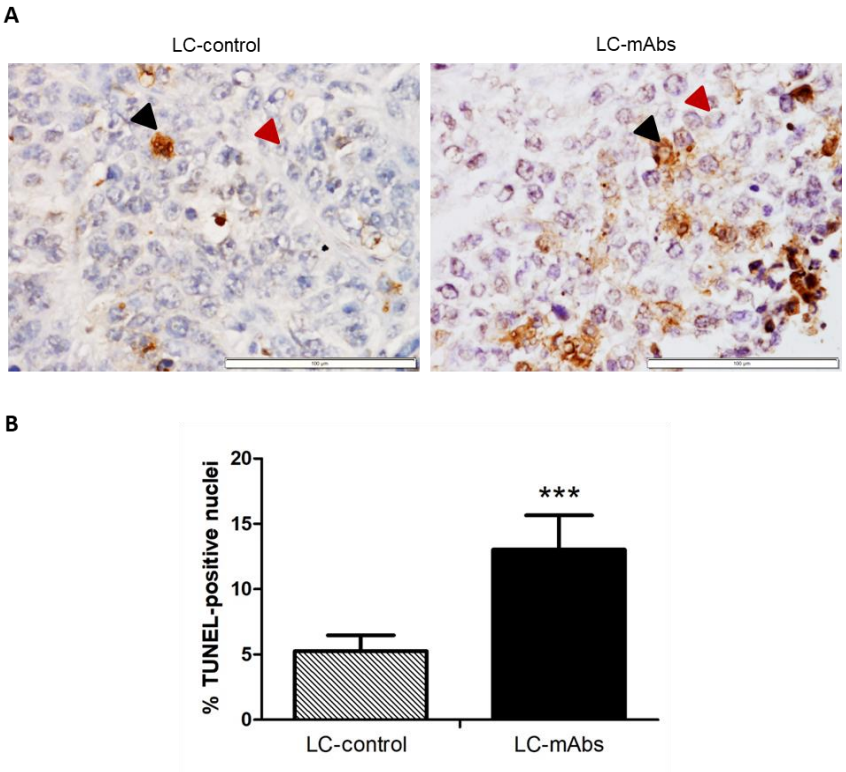

Figure 17. (A) Representative examples of TUNEL immunostaining histological sections (40x) in the subcutaneous tumors of LC-control group (left side) and LC-mAbs group (right side). Black arrowheads point towards TUNEL positively-stained nuclei (brown color), while red arrowheads point towards TUNEL negatively-stained nuclei (purple color). **(B)** Representative mean values and standard deviation of % of TUNEL-positive nuclei. Statistical significance is represented as follows: n.s.: non-significant and *: $p \leq 0.05$ and **: $p \leq 0.01$ between non-treated controls and treated lung cancer.

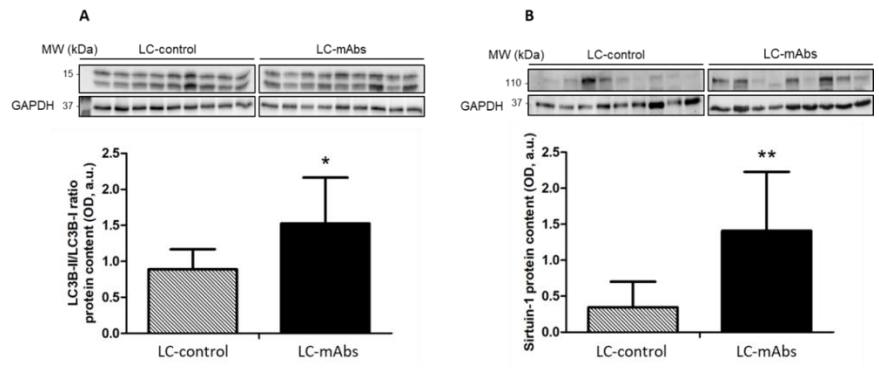

Figure 18. (A) Representative immunoblots and man values and standard deviation of total LC3-II/LC3-I protein levels in subcutaneous tumors of LC mice as measured by optical densities. **(B)** Representative immunoblots and mean values and standard deviation of sirtuin-1 protein levels in subcutaneous tumors of LC mice as measured by optical densities. Statistical significance is represented as follows: n.s.: non-significant and *: $p \leq 0.05$ and **: $p \leq 0.01$ between non-treated controls and treated lung cancer. Definition of abbreviations: LC3, light-chain 3; GAPDH, glyceraldehyde-3-phospate dehydrogenase; OD, optical densities; a.u., arbitrary units.

DISCUSSION

Differential immune profile between LC patients and LC patients underlying COPD

In line with previous publications (162,170,171,233) lymphoid aggregates or TLSs, as local priming and activation sites, were identified in the airways and parenchyma (associated with bronchi, pulmonary vessels or randomly placed in the pulmonary interstitium), as well as in the tumors or its vicinity of LC patients with and without COPD. The reported results revealed that increased numbers of TLSs, as well as the sizes of which, were found in the tumors of LC patients compared to those from lung parenchyma. These findings might imply that the location of this transient structures may be relevant in the context of immune surveillance.

Lymphoid neogenesis is a dynamic process by which immune cells congregate themselves (233). While secondary lymphoid organs (SLOs) arise in specific anatomical locations as part of a programmed process during ontogenesis, TLSs develop in response to *stimuli* (172). In addition, regardless synthesis *de novo* of TLSs shares analogical programs with SLOs, the formation of TLSs can be induced in absence of lymphotoxin and lymphoid tissue inducer cells through inflammatory cytokines (234). CS-induced bronchial epithelium irritation is known to lead to the release of antigens and promote TLS neogenesis *via* IL-4, IL-6, IL-13, and tumor necrosis factor α (TNF-α) in COPD (233,235). The induction of these pro-inflammatory factors may be triggered by local cross-talk between immune cells and resident stromal cells, such as fibroblasts and mese-

nchymal cells (234). Thus, the activation of local mesenchymal cells can be induced by lymphotoxin α (LTα) and TNF-α (162) and accumulation of antigens may be assisted by resident immune cells (236) and increased enzymatic degradation of tissue by activated neutrophils and macrophages in COPD lungs (237). Moreover, the expression of CCL19, CCL21, CXCL12, CXCL13, LTα3, LTβ, and TNF-α has been reported in either tumoral and non-tumoral lung tissues, suggesting that lymphoid neogenesis may comprehend a common program among different pathologies (169,172). However, other authors suggest that the initiating cues of TLS neogenesis may differ among cancer types (172), as CCL17 and CCL22 are reported to be overexpressed in LC-associated TLSs (238). Furthermore, LC-associated TLSs have been shown to rely on IL6, IL-16, IL-17A, and IL-23 expression (238–240). In addition, IL-17 have also been found to exhibit an important role in COPD-associated TLS formation, as the number of IL-17-producing cells correlates with airflow limitation (241,242) and lymphoid neogenesis in severe COPD is linked to IL-17 levels (243). Accordingly, in absence of follicular DCs, TLS neogenesis can be induced through IL-17-dependent expression of CXCL12 and CXCL13 by CD4+ T cells (244,245).

In the current thesis, the density of intratumoral TLSs was also found to be increased in the lung tumors of NSCLC patients with COPD compared to those without COPD. These differences may be explained as TLSs are reported to promote either protective or deleterious features depending on the nature of the pathology (171,172,233,234,246). Moreover, the supportive or suppressive role

of TLSs along disease progression may be determined by the composition, architecture, and localization of these structures, as well as the surrounding contexture (172).

The accumulation of immunosuppressive Treg cells and MDSCs may promote immune tolerance as their presence is correlated with short-term survival (171,172,234,247–249). In accordance, Treg cells depleted *in vivo* TLS-mediated antitumor immune responses in a mouse model of lung adenocarcinoma and abrogation of Treg cells lead to enhanced DC and T cell activity (51). Such immunosuppressive cells are recruited into TLSs *via* CCL2/CC chemokine receptor 4 (CCR4) axis and can be activated by mature DCs once within these structures (247). Furthermore, Treg cells are reported to mitigate HEV differentiation and thereby lymphoid neogenesis in several malignancies (172).

On one hand, our results revealed that levels of Treg cells were increased in the tumor specimens compared to non-tumor of NSCLC patients. However, cancer patients from this study underlying COPD were shown to not differ in Treg population levels. These findings highlight that other immunosuppressive mechanisms/agents, such as MSDCs, may account for reduced levels of TLSs. On the other hand, in another study, IL-10 levels were increased in the lung tumors of LC patients with COPD compared to tumor samples from LC patients without COPD (158). These findings might imply that cancer cells-mediated IL-10 production may be one example of the immunosuppr-

essive mechanisms overexpressed in NSCLC patients whom also underlie COPD.

Hence, TLSs highly resemble SLOs, although there is a lack of capsule in the former (172). This fact could be beneficial for antigen delivery (234), as B cells also act as antigen presenting cells (170). Like DCs, B cells recruit T cells and trigger T cell polarization with either positive or negative impact on T cell-mediated anti-tumor activity, depending on the co-stimulatory molecules secreted (170). B and plasmatic cells produce high-affinity antibodies against tumor cells, mostly IgG, which could license the activation of programmed cell death, antibody-dependent cell-mediated cytotoxicity and the release of immune-supportive cytokines (170). However, other Ig may take part in this role or even produce the contrary effect. For instance, the presence of IgA+ plasmatic cells correlate with immune scape and IgG4 production *in situ* is suggested to promote Th2 polarization (170). The results presented in the current investigation revealed that IgG+ plasmatic cells, which are suggested to be associated with both immune surveillance and immune scape, were reduced in the tumors of patients with NSCLC. Whereas, the levels of IgA+ plasmatic cells were not significant. Perhaps, the reduced levels in the number of these cell populations might imply that malignant cells could recur to other immunosuppressive mechanisms to evade immune surveillance. Reduced levels of IgG+ plasmatic cells may also suggest that these cells are responsible to aid tumor regression and tumor-mediated immunosuppressive mechanisms may be induced in the TME in order to tailor immune escape.

Nevertheless, it is far from clear whether these plasmatic cells may license tumor supportive features rather than tumor suppressive or *vice versa*.

Apart from Treg cells accumulation, B cell follicles can also exert an immunosuppressive role in several tumors (171). These cells with such behavior are considered as regulatory B (Breg) cells and induce the secretion of immunosuppressive molecules, such as IL-10, and thus expansion of Treg cells aiding tumor progression (170,250). Additionally, B cell-produced antibodies bind to their target antigens to form immune complexes in order to be then removed through phagocytosis by immune cells (233). Immune complexes are reported to aid tumorigenesis *via* MDSCs and angiogenesis activation (251). Previous reports also state whether these complexes also bind to the ECM, it could harness tissue integrity (233). Thereby, the production of auto-antibodies could lead to lung tissue destruction (251). Indeed, circulating immune complexes correlate with poor clinical outcome in human cancers (252).

B cell levels, as well as the number of GCs, were found to be increased in the tumor specimens from both LC and LC-COPD groups once compared to specimens from non-tumor lung parenchyma. These findings highlight the role of B cells in antitumoral adaptive immune responses. Nevertheless, any differences were found between both study groups, suggesting that these adaptive immune cells might not interfere in the reduced number of TLSs found in LC-COPD patients. In addition, the density

of GCs (175,253), as well as plasmatic cells (170,172,254), or IgG (254–260) correlates with survival in NSCLC patients. Moreover, the density of B cell-rich follicles has been correlated with the density of plasmatic cells, responsible to license humoral adaptive immunity directed against tumor-associated antigens (169,170). Conversely, as early discussed, levels of IgG+ (but not IgA+) plasmatic cells were decreased in the tumors of both LC and LC-COPD patients compared to non-tumor samples. These findings raise controversial reports in the link between GCs and plasmatic cells. However, GCs may be associated with other plasmatic populations rather than IgG+ plasmatic cells.

In line with the above discussed and according to previous investigations (172), it is feasible to state that considerable tumor-associated antigenic *stimuli* may be required in order to overcome immunosuppression and provide a favorable environment for TLS neogenesis. Moreover, some authors describe these structures as immunological micro-niches that foster hepatocellular progenitor cells, thereby driving cancer progression (261).

Taken together, these findings suggest that some tumor-associated TLSs may require to overcome profound immunosuppression within the TME to elicit an effective anti-tumor immune response and even may promote immunosuppression and tumor progression rather than immune activation (162,171,172,234). Perhaps, TLSs may initially license an anti-tumor immune response at early stages of disease, whereas this capability may be lost during cancer progression due to

a highly immunosuppressive TME leading to the loss of tumor immunogenicity (172).

TLSs are largely associated with favorable clinical outcome in different solid tumors including NSCLC (165,172). Regardless the presence of TLSs, the presence of intratumoral peripheral node addressin (PNAd)+ HEVs is also a strong prognostic factor (172). Hence, TLSs are found to shape T cell infiltration towards a Th1 response as NSCLC patients with high density of TLSs manifest high infiltrates of effector T cells and improved outcome (169). The density of CD4+ and CD8+ T cells, follicular T helper cells, dendritic cell-lysosomal-associated membrane protein (DC-Lamp)+ mature DCs, and follicular B cells also present prognostic value in NSCLC patients (170,172). In line with this, in a previous study, stratification of LC patients according to the density of mature DCs within the TLSs revealed increased levels of T cells in TLSs with high density of DCs in contrast with T cell scarcity present in TLSs with low densities of DCs (247). The recruitment of T cells in DCs-rich TLSs may be facilitated by CXCL10 and CXCL11 (166). These findings highlight the requirement of DCs in order to license T cell effector activity. Furthermore, TLSs rich in mature DCs overexpress Th1 immunity-associated genes (162), suggesting that TLSs may require a favorable TME in order to elicit effective tumor control.

In contrast with the above mentioned, our results manifested reduced T cell infiltration levels in the tumors of patients with NSCLC whom were not associated with airway obstruction. These data suggest that

a highly immunosuppressive TME may block tumor infiltration by T cells. A previous study reported increased levels of CD8+ T cells, but not CD4+ cells, in the tumor stroma of patients with NSCLC and COPD compared to NSCLC patients (262). Despite non-significant data was provided, our results manifest a likely tendency. Perhaps, such discrepancy may be due to both T cell types were measured at once, suggesting that once analyzed by separated, the results obtained would match with previous reports (262).

Despite large percentages of NK cells are contained in the lung (263), the results provided in the current investigation did not revealed any significant finding regarding the levels of NK cells. According with such findings, it could be hypothesized that NK cells may be hindered by malignant cells, which are reported to suppress NK cell activity through IL-10 or TFGβ among other immunosuppressive cytokines (264).

In contrast with chronic inflammatory environments, a highly immunosuppressive TME is present in cancer, therefore the heterogeneity of TLSs in structure or composition may arise according to several factors such as cancer type, disease progression, and anatomical locations (171,172). This heterogeneity may reflect the diversity of individual TME, ranging from more to less suppressive in regards with lymphoid neogenesis and immunity (166,247). Thereby, TLSs can vary from simple lymphoid aggregates to structures highly resembling SLOs (265–268) which might reflect a gradient of stages in the program of lymphoid neogenesis from naï-

ve to mature TLSs (166). However, some authors suggest that tumor-associated TLSs might not be essential for lymphocyte activation as lymphocytes may infiltrate the TME *via* tumor-draining lymphoid vessels and activation of lymphocytes may occur *in situ* through specific activating signals regardless the presence of organized lymphoid structures (172).

Nevertheless, it is widely agreed that TLSs consist of large B cell aggregates surrounded by both CD4+ and CD8+ T cells and DC-Lamp+ mature DCs (162,166,170,171,233,269). B cell follicles also include follicular DCs and macrophages to ensure B cell homeostasis and follicular T helper cells that assist B cell differentiation towards plasmatic cells (166,170,171). B cells encountered in GCs are mainly IgM+ and IgD- suggesting prior cell activation (170,233). Moreover, the majority of B cells are CD27+, which means they are memory B cells, and Ki-67+ in central clusters (270). Furthermore, CD138+ plasmatic cells are observed in the vicinity of these segregation (233).

Importantly, the levels of lymphocytes in the peripheral blood of LC-COPD patients was increased compared to LC patients without chronic pulmonary disease. These findings are in line with the above mentioned and could explain the reduced number of TLSs in LC-COPD patients compared to LC, as lymphocyte recall may be attenuated in the former patients. Accordingly, the presence of PNAd+ HEVs within or surrounding lymphoid aggregates is essential for the extravasation of immune cells from the peripheral blood that will congregate into TLSs (166,171,172,271).

Discussion

Peripheral blood immune cells are recruited *via* PNAd+ HEVs by CCL19, CCL21, TNFα or LTα3 secretion to form clusters (166,172). These cytokines might act on the tumor necrosis factor receptor (TNFR)+ of endothelial cells inducing differentiation towards HEVs (172). CCL21 and CCL19 are known to induce T cell-mediated LTα1β2 expression while CXCL13 induce the same effect in B cells (247,272). Hence, CXCL13 can also be expressed by follicular DCs as a positive feedback (238).

Although the exact mechanisms remain unclear, TNFα is reported to induce CCL21 and CXCL13 expression (240,273), whereas IL-22 and IL-17A induce CXCL12 and CXCL13 (244,245,274–276). Moreover, CXCL12, like CCL19, could participate in the recruitment of TLS-associated lymphocytes through LTα1β2 signaling, while CXCL13 and CCL21 may participate in the segregation of T and B cells (172). DC-Lamp+ mature DCs are suggested to contribute towards the maintenance of the lymphoid structure *via* CCL19-dependent recruitment of naïve and memory T cells as well as activated DCs (172). CXCL13 is also suggested to contribute towards the generation of humoral immune responses recruiting follicular helper T cells into the GCs (172). Moreover, a plethora of adhesion molecules, such as intercellular adhesion molecule (ICAM)2, ICAM3, vascular cell adhesion molecule 1 (VCAM1), mucosal vascular addressin cell adhesion molecule 1 (MAdCAM1) and PNAd, have been associated with HEVs-associated TLSs in NSCLC patients (166,238). ICAM2 and VCAM participate in the recruitment of circulating T cells (277,278). It is suggested that HEVs from LC-

associated TLSs may provide a differential adhesion molecule profile than nontumoral (247). However, ICAM2, VCAM1, and PNAd has also been observed in TLSs from non-inflamed lungs (279,280).

All these data reinforce the results disclaimed, as TLS are differentially sculped depending on the pathologic circumstances. In agreement with earlier reports (122,122,158,228), the present findings provide arguments in favor with the hypothesis that TME from LC patients differ from LC patients also underlying chronic respiratory conditions. Hence, the density of lymphoid aggregates in both airways or parenchyma have been correlated with COPD progression (233), suggesting a detrimental role in this pathology. Accordingly, TLS disruption may assist the arrest of COPD inflammatory progression (237). In addition, despite TLSs form in response to inflammatory *stimuli*, its function may persist in absence of *stimuli* and may generate autoimmune pathogenic reactions. Evidence highlights that TLSs may persist even after CS cessation and contribute to autoreactive antibodies (281). However, a wide range of heterogeneity exists among COPD patients in lymphoid neogenesis (237) and it is not fully understood whether TLSs may have deleterious or beneficial impact in COPD.

In addition, primary tumor may also play a relevant role in metastasis-associated TLSs, as infiltration of DC and T cells in the TLSs of lung metastases from colorectal carcinoma was associated with better prognosis in contrast with lung metastasis from renal cell carcinoma (282). These findings manifest that TLSs may depend on

the tumor type and stage and might dictate the immune response against cancer (172).

The assessment of TLSs, as a useful biomarker for inclusion criteria, may assist in the screening of patients whom would favor from immunotherapy or with high risk of relapse (166,170). In accordance with that, the induction of TLSs, alone or in combination with immunomodulatory agents, might be an interesting approach in the therapy for cancer patients. However, in order to achieve this goal, the ultimate role of TLSs during disease progression must be carefully identified, especially in LC patients underlying COPD.

Altered TME in LC-bearing mice after immunomodulatory monoclonal antibodies administration

In the present study, treatment with the cocktail of mAbs that specifically targeted immune checkpoints with both agonistic and antagonistic effects elicited a significant reduction of tumor burden in the lung cancer-bearing mice.

In the tumors of the mice treated with the cocktail of immunomodulators, the area of the subcutaneous tumors was significantly reduced (64%) at the end of the study period, as well as the weight of the tumors once extracted (34%). These relevant findings confirm the efficacy of this combination of immunomodulators in mice. The present results are in line with those previously reported (283), in which a complete regression of skin and

lung tumors in mice was achieved after several intratumoral adminitrations of the same cocktail of mAbs. Although, in the current investigation, the cocktail of mAbs was intraperitoneally administered with the aim to mimic the treatments applied to patients in the clinics, in whom drugs are usually administered systemically. Interestingly, proliferation rates of cancer cells, as measured by Ki-67, was also significantly reduced in the subcutaneous tumors of the mice treated with immunomodulators. These results suggest that cell cycle arrest may be probably induced through alterations in cyclin expression levels which may account for the reduced levels of Ki-67-positively stained nuclei encountered in the adenocarcinoma cells of the tumor-bearing mice treated with mAbs. These findings are also in agreement with previous studies in which expression levels of Ki-67 were significantly reduced in the tumors of mice treated with several selective inhibitors of cell survival pathways (230), in those from transgenic mice deficient for either poly (ADP-ribose) polymerases (PARP)1 and PARP2 enzymes (123), and in those of rodents treated with pharmacological inhibitors of PARP activity (284).

Taken together, these results are also very consistent with the above-mentioned reduced tumor area and weight seen in the tumor-bearing mice treated with the cocktail of immunomodulators at the end of the study period.

At the end of the study period, treatment with immunomodulators also elicited a significant body weight gain in mice, as mice from LC-

mAbs group shown an increased final body weight. These findings are in line with the reports published in previous studies (212,213) and suggest that the treatment in mice induced an improvement of the cancer-associated paraneoplastic syndromes commonly produced in these murine models such as body weight loss, weakness, poor performance statures, and cancer-induced cachexia. In addition, spleen enlargement and lung metastases were also found as reported in previous publications (212,213).

As shown in the current investigation, increased levels of immune cells (both CD3+ and CD8+ T cells) were found in the subcutaneous tumors of mice treated with immunomodulators. These findings suggest an effective activation of several pathways in the immunity cycle narrowed to the enhancement of anti-cancer activity. This raised immunity is attributed to mAbs administration, as reported by several previous studies through early described cascades of transduction signals (57,59,285–289). Indeed, the impairment of the negative regulatory feedback of PD-1 produced by the bound with antagonistic mAbs is reported to restore cytotoxic activity of the effector T cells, responsible of the elimination of cancer cells (57,286–288). These reports are in accordance with the results attained in the current investigation, where enhanced levels of T cells where observed.

Moreover, anti-CTLA-4 antagonistic mAbs are reported to mitigate the inhibitory role of this receptor and enhance antigen presentation by DCs and further activation of T cells (66,290). This was observed

in our study by increased levels of effector T cells in the established mouse tumors treated with immunomodulators. According with the reported results from the current investigation, previous studies with anti-CD-137 mAbs report that these co-stimulatory agonistic mAbs are reported to induce an enhanced proliferation of T cells through increased antigen presentation by DCs and repression of negative regulatory function of Treg cells (62).

Previous reports suggest that the addition of anti-CD19 to the cocktail of mAbs increases the immunomodulatory effects towards tumor rejection (283). Antagonistic mAbs anti-CD19 are reported to modulate the function of B cells (291,292). These cells are reported to display a controversial role in tumor progression with either pro-tumoral and anti-tumoral effects (64,293,294). Nevertheless, it is clear that the depletion of B cells in this animal models account for a significant effect against tumor progression suggesting a pro-tumoral role of B cells. However, ongoing experiments will shed light in the fate of this cells regarding tumorigenesis.

Raised levels of both oxidative and nitrosative stress, as detected by indirect markers, were found in the subcutaneous tumors of mice treated with immunomodulators. These results are in agreement with those previously observed in another investigation in which protein oxidation levels were also increased in the tumors of $PARP1^{-/-}$ and $PARP2^{-/-}$ mice (123).

Discussion

Oxidative and nitrosative stress in the tumor nests can be produced by increased levels of ROS and RNS respectively or deficiencies in the antioxidant system. Increased levels of these reactive species can be both induced directly by tumor cells and/or several inflammatory mediators released in the TME (295). Such chronic stress in the tumor niche is known to play a deleterious role in immune response (295,296). Indeed, such events are reported to harness T cell function, maturation and survival, especially by the presence of certain inflammatory components in the TME (295). However, despite a large amount of studies that have been carried in order to clarify the interplay between oxidative stress and immune function, controversial reports and an important lack of information are still present.

High levels of ROS are known to upregulate several oncogenic signaling pathways implicated in tumor cell proliferation, apoptosis-evasion and cell migration (297). Although, at advanced stages, a substantial reduction of ROS levels in tumor cells is observed along with tumor growth and metastasis promotion (298,299). This fact puts in manifest a strong association between ROS amounts and cancer stage. Furthermore, pro-angiogenic features become crucial in advanced hypoxic tumors such as LC. Angiogenesis may be dependent of oxidative stress in advanced stages as VEGF upregulates hypoxia-inducible factor-1α (HIF-1α), which in turn decreases ROS amounts and further promotes tumor progression (300).

Several reports suggest that T cell suppression and Th1/Th2 polarization are triggered by tumor-induced oxidative stress, as Th2 phenotype aids tumor progression (295,301,302). In several studies, this detrimental role in immune response has been reported to be induced by a decrease in cytokine levels, including IFNγ and IL-2 (303). Nevertheless, many other intermediates such as IL-6 may also be crucial in Th2 polarization (304).

Importantly, in the current investigation, protein levels of protein tyrosine nitration, as well as total MDA-protein adducts were significantly greater in the tumors of mice administered with mAbs. In absence of antigen-presenting cells such as DCs, reactive carbonyls including MDA, are reported to assist Th1 differentiation towards a Th2 phenotype (305). As T cells are more vulnerable to oxidative stress than tumor cells (304), a highly inflammatory and oxidative environment in tumor beds confers substantial tumor dominance (295). However, costimulatory immune checkpoint receptors such as CD137, may have an important intervention in the reduction of oxidative stress through decreased levels of ROS (306).

Apart from cancer cells, ROS can be released in the TME by tumor associated macrophages, MDSCs, and Treg cells (295,296), contributing in conjunction to a highly immunosuppressive environment. In contrast, modest levels of ROS are shown to assist in T cell differentiation, proliferation, activation, and effector function (295,296). This fact suggests that regulation of T cells by ROS may be dose dependent. For instance, T cell receptor activation

produces ROS, but in turn, ROS can further mitigate T cell role through dysfunctional recognition in the major histocompatibility complex (MHC)/T cell receptor (TCR) axis (296). However, the exact ROS-mediated mechanisms by which T cell fate is modulated remain unclear, but it is in agreement that it depends on the balance between production and consumption of ROS (296). Nevertheless, some studies suggest that intracellular ROS levels in T cells might be regulated by NADPH oxidase (NOX), as well as mitochondrial activity and antioxidants synthesis (307–309). In addition, the immunosuppressive role of Treg cells seems to be dependent of ROS levels, as Treg cells are more resistant to ROS-induced cell death and TGF-β secreted by Tregs activates the NOXs to produce ROS (296). Moreover, ROS induces indoleamine 2,3-dioxygenase (IDO) expression in Treg cells engaging immune tolerance (310). Immunosuppressive activity of MDSCs by ROS induction seems to be mediated by cyclooxygenase-2 (COX-2), inducible nitric oxide synthase (iNOS), and arginase-1 (311).

Taken together, oxidative and nitrosative stress levels are expected to be elevated in the TME, especially in hypoxic tumors such as LC. Oxidative and nitrosative stress levels were higher in the subcutaneous tumors when administered with immunomodulators. These findings might imply that cancer cells may recur to chronic stress conditions in order to counter enhanced immunity exerted by immunomodulators and restore immune tolerance and aid tumor growth. However, levels of CD3+ and CD8+ T cells were increased in the tumors of mice administered with mAbs, suggesting that oxide-

tive and nitrosative stress levels were not enough to harness T cell populations and cancer cells were still surrogated under host immunity.

The role of antioxidants in ROS-mediated tumor promotion and ROS-mediated T cell function are major focus of study. Antioxidants are reported to regulate key signaling pathways affecting survival, plasticity and invasiveness of tumor cells as well as T cell function and survival (295). In the present investigation, levels of the antioxidant enzyme SOD1 were significantly greater in the tumors of the LC-bearing mice treated with immunomodulators. These results are in line with those encountered in the tumors of mice treated with the proteasome inhibitor bortezomib (230).

The rise in the expression of cytosolic SOD1 levels may have been in response to counterbalance the deleterious effects produced by increased oxidative stress as previously suggested (230). However, cancer cells constitutively show elevated intrinsic oxidative environment and effective mechanisms to counter it (312,313), so increasing the pool of available antioxidants may actually assist the tumor cells to sustain the cellular microenvironment that drives redox-dependent survival signals (295).

The role of antioxidants as enhancers of immune surveillance has been manifested in several reports. As mentioned above, T cell intrinsic ROS levels might be regulated by antioxidants as several studies report increased levels of T cell intracellular ROS accompanied by decreased levels of catalase and SODs (314), along

with protection against ROS-mediated cell death conferred by catalase in T cells (315). Indeed, SODs are known to mitigate the TCR-induced ROS-mediated oxidant effect in T cells, assisting survival, maturation and function (316,317). Moreover, catalase is suggested to impair immunosuppressive effects of MDSCs on T cell proliferation (318). Additionally, IL-2 and IL-4 are recognized as mediators in the regulation of T cell activation by mitochondrial ROS (319).

ROS are mainly produced in the TME by tumor cells and immunosuppressive cells, manifesting a crucial intervention in the activation, proliferation, differentiation and survival of T cells (296). Considering the ROS-mediated immunosuppressive mechanisms, an important implication in the therapeutic approach of LC may include targeting ROS and immune tolerance by the combined effect of antioxidants with immunomodulatory mAbs. Nevertheless, in spite of remarkable advances in the recent years, the action of ROS regarding T cell fate still remains unclear. Development of effective strategies combining ROS and T cells warrants further investigations. Oxidative stress may also trigger several important cellular pathways such as cell death, apoptosis, and autophagy. For instance, in the tumors of mice treated with the cocktail of immunomodulators, levels of pro-apoptotic BAX were significantly greater, while those of the anti-apoptotic BCL-2 were not significantly different than in the non-treated rodents. These results are consistent with those obtained in previous investigations (123,230). The increase in apoptotic markers

of cancer cells was also demonstrated in previous investigations in which the animals were treated with inhibitors of PARP (284,320). Increased levels of oxidative stress in the TME can also induce apoptosis in T cells. As discussed above, ROS are delicate regulators of T cell function and survival. A ROS-enriched environment can induce a tolerogenic response and trigger the elimination of activated T cells (295,296). Hence, T cell hyporesponsiveness is reported in cancer patients due to ROS-mediated oxidative stress (321).

In T cells, ROS are essential for the expression of Fas ligand (FasL), an important mediator of activation-induced cell death (AICD) (307,317,322). AICD is an apoptotic process that mediates T cell homeostasis and seems to be tightly regulated by antioxidant SODs (322,323) as well as crosstalk between mitochondrial dynamics and autophagy (324). Apart from ROS, tumor cells can also induce FasL expression in T cells and thus promote AICD in order to limit immune surveillance (325). TCR-ROS crosstalk in T cells serves as a regulator of FasL-mediated proapoptotic pathway and ERK-mediated proliferative pathway and both are crucial for T cell function and survival (296).

ROS-mediated FasL expression upregulates NOX-2 and AKT while downregulates MEK (326). Interestingly, some subsets of T cells may show AICD resistance along with increased effector activity (327). Some subsets of T cells have shown differential susceptibility to oxidative stress-induced apoptosis (125) and it is likely that effector T cells can become insensitive to ROS-mediated death (296).

Discussion

Differences in the expression of oxidative stress-related genes and the metabolism of ROS in subsets of T cells have been implicated in the regulation of oxidative stress susceptibility (322).

In addition, recent studies have shown that epigenetic regulation may play a relevant role in AICD, as miRNA-146a is suggested to act as an anti-apoptotic factor that targets Fas (328). However, another immune escape mechanism has been seen in some colorectal cancers, where tumor cells express TNF-related apoptosis-inducing ligand (TRAIL) while the effector T cells express its cognate receptor (TRAIL-R1) and its interaction derives in T cell death (329).

Effector immune cells can undergo apoptosis through programmed cell death or AICD (322). However, programmed cell death inhibition was elicited in regard to anti-PD1 mAbs and AICD does not seem to dampen T cells as CD3+ and CD8+ T cell levels were increased upon immunomodulation. These findings suggest that mainly cancer cells underwent apoptosis as a result of enhanced anti-cancer immune cytotoxic activity. In line with this, cancer cells might get eliminated by immunogenic cell death (ICD), a non-silent cell death that activates immune system (330). Regardless the ICD action mechanism is not fully understood, it is reported to cause stress in the endoplasmic reticulum and thus translocation of pre-apoptotic calreticulin to the cancer cell surface (331). In line with our results, this translocation activates pro-apoptotic proteins such as caspase-8 and BAX (332) leading cancer cells to ultimately death.

A rise in autophagy, as measured by LC3B, was observed in the tumors of mice treated with immunomodulators compared to control rodents. These results imply that autophagy may also mediate the reduced tumor burden observed in the mice that received the cocktail of monoclonal antibodies. In fact, similar results were previously demonstrated in the tumors of mice that were genetically deficient for either PARP1 and 2 (123). Furthermore, the deacetylase sirtuin-1 may play a role in autophagy as a result of its upstream regulation of LC3B (333). In the current study, along with increased levels of LC3B, a significant rise in protein levels of sirtuin-1 was detected in the tumors of the mice treated with mAbs.

Autophagy is a conserved catabolic pathway that allows the lysosomal degradation of own cellular components in order to maintain cell homeostasis (334) and adapt to stressful environments such as nutrients deprivation (335). Autophagy is prevalent in many cancers and is recognized to exert a dual role in tumorigenesis, acting as a tumor suppressor or tumor promoter in regards of the tumor type, stage, and genetic context (334,336). A paradoxical dual role is stablished in autophagy as a suppressor in nascent tumors and promoter in developed tumors. Tumor suppressing activity of autophagy relies on its ability to scavenge damaged cellular components and thereby prevent ROS accumulation and genomic instability (334,336). However, in advanced tumors, autophagic tumor promoter activity allows tumor cells to overcome stress conditions produced by hypoxia (336,337).

Discussion

Emerging evidence drives attention to the prominent role of autophagy to modulate immune response. Both innate and adaptive immune responses are upregulated by autophagy. Innate immunity recognizes pathogens thereby triggering inflammatory cytokines release and inducing pathogen removal through autophagy (335,338). On the other hand, autophagy promotes adaptive anti-tumor immunity by enhanced processing and presentation of tumor-related antigens during cross-presentation or immune recognition (331,336,338). However, hypoxic tumors are recognized to shed tumor-related antigens (336), and this hypoxic TME may revert the role of autophagy (334). Moreover, several reports suggest that autophagy modulates tumor cell secretome and proteome after hypoxic stress and cell death (336). Such modulations allow tumor cells to communicate with nearby cells present in the TME (336). Indeed, under such stress conditions, autophagy is reported to induce immunosuppression through impairment of T and NK cells and MDSCs activation (331,334,336–338).

Autophagy may also act as an intrinsic mechanism of resistance evolved by tumor cells to overcome immune cell-mediated effects (334). Previous studies showed that hypoxia-induced autophagy acts as a mechanism of immune scape mediated by STAT3 (334,339,340). Although the clear link between the activation of autophagy and STAT3 signaling remains to be elucidated, it has been clearly established that represents an important mediator in the crosstalk between tumor and immune milieu (341). However, STAT3 signalling in tumor cells is suggested to suppress the expression of

pro-inflammatory IFNγ, TNFα, and CXCL10, and also induce the expression of immunosuppressive VEGF, IL-10 (342). In addition, attenuation of IL-1 can induce autophagy in tumor cells and impair tumor growth (343,344). Moreover, IL-1 is produced by T and NK cells and can trigger autophagy in endothelial cells and hepatocytes, while IFNγ can induce apoptosis in epithelial, immune and tumor cells (337).

NK cell exerts its anti-tumor effects by induction of apoptosis, secretion of IFNγ, and inhibition of tumor metabolism. However, recent reports demonstrate that NK cells can induce autophagy in tumor cells thus facilitating their survival, suggesting that autophagy can be deterrent in immune surveillance (345). In line with this, hypoxia-induced autophagy triggers Granzyme B degradation, an essential pro-apototic protein in NK cells-mediated killing and aids cancer immune scape (334,336,338). Other reports revealed that autophagy inhibition in cancer cells elicited a significant reduction in tumor volume by improved functionality of NK cells (346).

Conversely, cancers with upregulated autophagy, as indicated by accumulation LC3B, exhibit major density of CD8+ T cells along with lower density of Treg cells in the tumor niche (347). Thus, enhanced autophagy is correlated with anti-tumor immune activity, and its downregulation may aid immune scape (331,336). However, patients with high levels of autophagy in their tumors were associated with poor clinical outcome (348). Such evidences highlight that auto-

phagy activation in immune cells exposed to hypoxic stress in TME, is a key component of the immune response (334).

In the context of tumor immunity, it is clearly stablished that autophagy may influence the crosstalk between cancer and immune cells, thereby leading to either immune-suppression or immune-activation (334). Whether the activation of autophagy in hypoxic TME helps or hinders immune surveillance remains to be elucidated. To this end, a deeper understanding of the physiological impact of autophagy in the TME is needed to tailor therapies selectively targeted against suppression pathways in order to reinforce antitumor immunity (334). In the context of cancer immunotherapy, strategies aiming to target autophagy could be an asset for the improvement of immune surveillance (334). However, autophagy manipulation is not an easy command in order to target the autophagy machinery directly or selectively given that may affect multiple targets (331).

CONCLUSIONS

Conclusions

1. A differential immune profile is present between LC patients and LC patients with COPD.

2. LC patients with COPD may lack in the recruitment of blood peripheral lymphocites for the congregation of TLSs.

3. The combination of agonistic and antagonistic immuno-modulatory mAbs effectively attenuates tumor growth.

4. Reduction of tumor burden in response to immunomodulation exerted by mAbs elicited the overexpression of immunity-related mechanisms such as oxidative stress and autophagy.

FUTURE PERSPECTIVES

Future research will be devoted with the aim to explore the mechanisms that may induce a differential expression in the immune profile between LC patients and LC patients with COPD. In order to achieve this end, other immune markers should be explored, especially those implicated with immunosuppressive pathways.

Moreover, survival analyses should be performed to assess the role of the TLSs and assess whether they are tumor promoter rather than tumor controller. Otherwise, it would be of substantial interest to explore the response to treatment according to the immune profiles registered, with main interest in those patients whom received immunotherapy.

Furthermore, as the relevance manifested by other biological mechanisms such as oxidative stress and autophagy regarding immunity, it would be interesting to assess new therapeutic strategies with the combination of immunomodulatory mAbs and agents targeting oxidative stress and autophagy.

BIBLIOGRAPHY

1. Netter FH. Sistema Respiratorio. 2nd ed. Brass A, editor. Barcelona: Masson S.A.; 1972. 326 p.
2. Ira S. Human Physiology. 12th ed. New York: McGraw-Hill; 2010. 749 p.
3. Guyton AC, Hall JE. Textbook Medical Physiology. Textbook of Medical Physiology. 2006. 1011-1018 p.
4. Peracchia C, Anaizi NH. Lung Function in Health and Disease: Basic Concepts of Respiratory Physiology and Pathophysiology. Sharjah: Bentham Science Publishers Ltd; 2015.
5. Agustí À, Celli B. Enfermedad Pulmonar Obstructiva Crónica. Barcelona: Masson S.A.; 2005. 311 p.
6. Gerald LB, Bailey WC. Global Initiative for Chronic Obstructive Lung Disease. J Cardiopulm Rehabil. 2018; 22 (4): 234–44.
7. West JB, Luks AM. Fisiopatología pulmonar. 9th ed. Mendoza C, Estrada K, editors. Philadelphia: Wolters Kluwer; 2017. 251 p.
8. Nathell L, Nathell M, Malmberg P, Larsson K. COPD diagnosis related to different guidelines and spirometry techniques. Respir Res. 2007; 8: 1–7.
9. Goedhart D, Zanen P, Lammers J. Relevant and redundant lung function parameters in discriminating asthma from COPD. COPD. 2006; 3 (1): 33–9.
10. Shivakumar J, Shenoy JP, Karne SL, Biradar SS, Muniyappanavar NS, Nayak GH. Reference models of lung function parameters from FVC maneuver for south Indian male early adolescent population. Natl J Physiol Pharm Pharmacol. 2015; 5 (3): 181–4.
11. Castellsagué J, Burgos F, Sunyer J, Barberà JA, Roca J. Prediction equations for forced spirometry from European origin populations. Barcelona Collaborative Group on Reference Values for Pulmonary Function Testing and the Spanish Group of the European Community Respiratory Health Survey. Respir Med. 1998; 92 (3): 401–7.
12. Roca J, Sanchis J, Agusti-Vidal A, Segarra F, Navajas D, Rodriguez-Roisin R, et al. Spirometric reference values from a Mediterranean population. Bull Eur Physiopathol Respir. 1986; 22 (3): 217–24.
13. García-Río F, Pino JM, Dorgham A, Alonso A, Villamor J. Spirometric reference equations for European females and males aged 65-85 yrs. Eur Respir J. 2004; 24 (3): 397–405.
14. American Cancer Society. Cancer Facts and Figures 2018. Am Cancer Soc. 2018; 1–71.
15. Dela Cruz CS, Tanoue LT, Matthay R a. Lung Cancer: epidemiology, etiology and prevention. Clin Chest Med. 2011; 32 (4): 1–61.
16. Siegel RL, Miller KD, Jemal A. Cancer statistics, 2018. CA Cancer J Clin. 2018; 68 (1): 7–30.
17. Malvezzi M, Carioli G, Bertuccio P, Boffetta P, Levi F, La Vecchia C, et al. European cancer mortality predictions for the year 2017, with focus on lung cancer. Ann Oncol Off J Eur Soc Med Oncol. 2017; 28 (5): 1117–23.

Bibliography

18. Latimer K. Lung Cancer: Clinical Presentation and Diagnosis. FP Essent. 2018; 464: 23–6.
19. Tamura T, Kurishima K, Nakazawa K, Kagohashi K, Ishikawa H, Satoh H, et al. Specific organ metastases and survival in metastatic non-small-cell lung cancer. Mol Clin Oncol. 2014; 217–21.
20. Riihimäki M, Hemminki A, Fallah M, Thomsen H, Sundquist K, Sundquist J, et al. Lung Cancer Metastatic sites and survival in lung cancer. Lung Cancer. 2014; 86 (1): 78–84.
21. del Cielo A, Franchi P, Contegiacomo A, Cicchetti G, Bonomo L, Larici AR. Missed lung cancer: when, where, and why? Diagn Interv Radiol. 2017; 23: 118–26.
22. Barreiro E, Bustamante V, Curull V, Gea J, López-Campos JL, Muñoz X. Relationships between chronic obstructive pulmonary disease and lung cancer: Biological insights. J Thorac Dis. 2016; 8 (10): E1122–35.
23. European Lung Foundation. Lung factsheets. European Respiratory Society. 1–4 p.
24. Roth JA, Hong WK, Cox JD. Lung Cancer. 3rd Edition. Medical Oncology. 2008; 480 p.
25. Akopyan G, Bonavida B. Understanding tobacco smoke carcinogen NNK and lung tumorigenesis. Int J Oncol. 2006; 29 (4): 745–52.
26. Didkowska J, Wojciechowska U, Mańczuk M, Łobaszewski J. Lung cancer epidemiology: contemporary and future challenges worldwide. Ann Transl Med. 2016; 4 (8): 150.
27. Hanna JM, Onaitis MW. Cell of origin of lung cancer. J Carcinog. 2013; 12 (1): 6.
28. Tanoue LT, Tanner NT, Gould MK, Silvestri GA. Lung cancer screening. Am J Respir Crit Care Med. 2015; 191 (1): 19–33.
29. Kanwal M, Ding X, Cao Y. Familial risk for lung cancer. Oncol Lett. 2017; 13 (2): 535–42.
30. National Library of Medicine - National Institutes of Health. Genetics Home Reference - Lung Cancer. 2018; 1–3 p.
31. Wang J, Liu Q, Yuan S, Xie W, Liu Y, Xiang Y, et al. Genetic predisposition to lung cancer: Comprehensive literature integration, meta-analysis, and multiple evidence assessment of candidate-gene association studies. Sci Rep. 2017; 7 (1): 1–13.
32. Cooper WA, Lam DCL, O'Toole SA, Minna JD. Molecular biology of lung cancer. J Thorac Dis. 2013; Suppl 5: S479-90.
33. Herbst RS, Morgensztern D, Boshoff C. The biology and management of non-small cell lung cancer. Nature. 2018; 553 (7689): 446–54.
34. Travis WD, Brambilla E, Nicholson AG, Yatabe Y, Austin JHM, Beasley MB, et al. The 2015 World Health Organization Classification of Lung Tumors: Impact of Genetic, Clinical and Radiologic Advances since the 2004 Classification. J Thorac Oncol. 2015; 10 (9): 1243–60.

35. Giangreco A, Groot KR, Janes SM. Lung cancer and lung stem cells: Strange bedfellows? Am J Respir Crit Care Med. 2007; 175 (6): 547–53.
36. Goldstraw P. New Guidelines for the Classification and Staging of Lung Cancer : TNM Descriptor and Classification Changes in the 8th Edition . 2010; 5 p.
37. Detterbeck FC, Boffa DJ, Kim AW, Tanoue LT. The Eighth Edition Lung Cancer Stage Classification. Chest. 2018; 151 (1): 193–203.
38. Detterbeck FC. The eighth edition TNM stage classification for lung cancer: What does it mean on main street? J Thorac Cardiovasc Surg. 2018; 155 (1): 356–9.
39. Goldstraw P, Chansky K, Crowley J, Rami-Porta R, Asamura H, Eberhardt WEE, et al. The IASLC lung cancer staging project: Proposals for revision of the TNM stage groupings in the forthcoming (eighth) edition of the TNM Classification for lung cancer. J Thorac Oncol. 2016; 11 (1): 39–51.
40. AJCC. American Joint Comittee on Cancer Staging rules 8 th Edition. Cancer staging. 2018; 8: 1.
41. Pallis AG. A Review of Treatment in Non-small-cell Lung Cancer. Eur Oncol Haematol. 2012; 8 (4): 208.
42. Zappa C, Mousa SA. Non-small cell lung cancer: current treatment and future advances. Transl Lung Cancer Res. 2016; 5 (3): 288–300.
43. Cooper S, Spiro SG. Small cell lung cancer : Treatment review. Respirology. 2006; 11 (3): 241–8.
44. Huang C-Y, Ju D-T, Chang C-F, Muralidhar Reddy P, Velmurugan BK. A review on the effects of current chemotherapy drugs and natural agents in treating non–small cell lung cancer. BioMedicine. 2017; 7 (4): 23.
45. Popper HH. Progression and metastasis of lung cancer. Cancer Metastasis Rev. 2016; 35 (1): 75–91.
46. Morgensztern D, Campo MJ, Dahlberg SE, Doebele RC, Garon E, Gerber DE, et al. Molecularly Targeted Therapies in Non-Small Cell Lung Cancer Annual Update 2014. J Thorac Oncol. 2015; 10: S1-63 p.
47. Thomas A, Rajan A, Giaccone G. Tyrosine Kinase Inhibitors in Lung Cancer. Hematol Oncol Clin North Am. 2012; 26 (3): 589–605.
48. Ansari J, Palmer D, Rea D, Hussain S. Role of Tyrosine Kinase Inhibitors in Lung Cancer. Anticancer Agents Med Chem. 2009; 9 (5): 569–75.
49. Morabito A, De Maio E, Di Maio M, Normanno N, Perrone F. Tyrosine Kinase Inhibitors of Vascular Endothelial Growth Factor Receptors in Clinical Trials: Current Status and Future Directions. Oncologist. 2006; 11 (7): 753–64.
50. Frezzetti D, Gallo M, Maiello MR, D'Alessio A, Esposito C, Chicchinelli N, et al. VEGF as a potential target in lung cancer. Expert Opin Ther Targets. 2017; 21 (10): 959–66.
51. Sahu A, Prabhash K, Noronha V, Joshi A, Desai S. Crizotinib: a comprehensive review. South Asian J Cancer. 2013; 2 (2): 91–7.

52. Forde P, Rudin C. Crizotinib in the treatment of non-small-cell lung cancer. Expert Opin Pharmacother. 2012; 13 (8): 1195–201.
53. Chuang JC, Neal JW. Crizotinib as first line therapy for advanced ALK-positive non-small cell lung cancers. Transl Lung Cancer Res. 2015; 4 (5): 639–41.
54. Kowanetz M, Ferrara N. Vascular endothelial growth factor signaling pathways: therapeutic perspective. Clin Cancer Res. 2006; 12 (17): 5018–22.
55. Byrne WL, Mills KH, Lederer JA, O'Sullivan GC. Targeting Regulatory T cells in Cancer. Cancer Res. 2011; 71 (22): 6915–20.
56. Puig-Kröger A, Sierra-Filardi E, Domínguez-Soto A, Samaniego R, Corcuera MT, Gómez-Aguado F, et al. Folate receptor β is expressed by tumor-associated macrophages and constitutes a marker for M2 anti-inflammatory/regulatory Macrophages. Cancer Res. 2009; 69 (24): 9395–403.
57. Zhu H-F, Li Y. Small-Molecule Targets in Tumor Immunotherapy. Nat Products Bioprospect. 2018; 8 (4): 297–301.
58. Coe D, Begom S, Addey C, White M, Dyson J, Chai J-G. Depletion of regulatory T cells by anti-GITR mAb as a novel mechanism for cancer immunotherapy. Cancer Immunol Immunother. 2010; 59 (9): 1367–77.
59. Massarelli E, Papadimitrakopoulou V, Welsh J, Tang C, Tsao AS. Immunotherapy in lung cancer. Transl lung cancer Res. 2014; 3 (1): 53–63.
60. Rijavec E, Genova C, Alama A, Barlett G, Sini C, Pronzato P, et al. Role of immunotherapy in the treatment of advanced non-small-cell lung cancer. Futur Oncol. 2014; 10 (1): 79–90.
61. Dal Bello M, Alama A, Coco S, Vanni I, Grossi F. Understanding the checkpoint blockade in lung cancer immunotherapy. Drug Discov Todat. 2017; 22 (8): 1266–73.
62. Yonezawa A, Dutt S, Chester C, Kim J, Kohrt HE. Boosting cancer immunotherapy with anti-CD137 antibody therapy. Clin Cancer Res. 2015; 21 (14): 3113–20.
63. Schreiber RD, Old LJ, Smyth MJ. Cancer Immunoediting: Integrating Immunity's Roles in Cancer Suppression and Promotion. Science. 2011; 331 (6024): 1565–70.
64. Tsou P, Katayama H, Ostrin EJ, Hanash SM. The emerging role of b cells in tumor immunity. Cancer Res. 2016; 76 (19): 5591–601.
65. Ohaegbulam KC, Assal A, Lazar-Molnar E, Yao Y, Zang X. Human cancer immunotherapy with antibodies to the PD-1 and PD-L1 pathway. Trends Mol Med. 2015; 21 (1): 24–33.
66. Blank CU, Enk A. Therapeutic use of anti-CTLA-4 antibodies. Int Immunol. 2015; 27 (1): 3–10.

67. Boesteanu AC, Katsikis PD. Memory T cells need CD28 costimulation to remember. Semin Immunol. 2009; 21 (2): 69–77.
68. Conway EM, Pikor LA, Kung SHY, Hamilton MJ, Lam S, Lam WL, et al. Macrophages, inflammation, and lung cancer. Am J Respir Crit Care Med. 2016; 193 (2): 116–30.
69. Wao H, Mhaskar R, Kumar A, Miladinovic B, Djulbegovic B. Survival of patients with non-small cell lung cancer without treatment: a systematic review and meta-analysis. Syst Rev. 2013; 2 (1): 10.
70. Tas F, Ciftci R, Kilic L, Karabulut S. Age is a prognostic factor affecting survival in lung cancer patients. Oncol Lett. 2013; 6 (5): 1507–13.
71. Franceschini JP, Jamnik S, Santoro IL. Survival in a cohort of patients with lung cancer: the role of age and gender in prognosis. J Bras Pneumol. 2017; 43 (6): 431–6.
72. Moumtzi D, Lampaki S, Zarogoulidis P, Porpodis K, Lagoudi K, Hohenforst-Schmidt W, et al. Prognostic factors for long term survival in patients with advanced non-small cell lung cancer. Ann Transl Med. 2016; 4 (9): 161–161.
73. Yang P. Epidemiology of Lung Cancer Prognosis: Quantity and Quality of Life. Methods Mol Biol. 2009; 471: 469–86.
74. Sagerup CMT, Småstuen M, Johannesen TB, Helland Å, Brustugun OT. Sex-specific trends in lung cancer incidence and survival: A population study of 40 118 cases. Thorax. 2011; 66 (4): 301–7.
75. Janssen-Heijnen MLG, Smulders S, Lemmens VEPP, Smeenk FWJM, Van Geffen HJAA, Coebergh JWW. Effect of comorbidity on the treatment and prognosis of elderly patients with non-small cell lung cancer. Thorax. 2004; 59 (7): 602–7.
76. Brundage M, Davies D, Mackillop W. Prognostic factors in non-small cell lung cancer: a decade of progress. Chest. 2002; 122 (3): 1037–57.
77. Woodard G, Jones K, Jablons D. Lung Cancer Staging and Prognosis. Cancer Treat Res. 2016; 170: 47–75.
78. Xie S, Wang K, Zhang W, Xiao K, Yan P, Li Y, et al. Immunodeficiency in Patients with Acute Exacerbation of Chronic Obstructive Pulmonary Disease. Inflammation. 2018; 41 (5): 1582-89.
79. McGrath JJC, Stampfli MR. The immune system as a victim and aggressor in chronic obstructive pulmonary disease. J Thorac Dis. 2018; 10 (Suppl 17): S2011–7.
80. Devine JF. Chronic obstructive pulmonary disease: an overview. Am Heal drug benefits. 2008; 1 (7): 34–42.
81. Tuder RM, Petrache I. Pathogenesis of chronic obstructive pulmonary disease. J Clin Invest. 2012; 122 (8): 2749–55.
82. MacNee W. Pathogenesis of Chronic Obstructive Pulmonary Disease. Proc Am Thorac Soc. 2005; 2 (4): 258–66.

83. Brozyna S, Ahern J, Hodge G, Nairn J, Holmes M, Reynolds PN, et al. Chemotactic mediators of Th1 T-cell trafficking in smokers and COPD patients. COPD J Chronic Obstr Pulm Dis. 2009; 6 (1): 4–16.
84. O'Donnell R, Breen D, Wilson S, Djukanovic R. Inflammatory cells in the airways in COPD. Thorax. 2006; 61 (5): 448–54.
85. Barnes PJ. The cytokine network in asthma and chronic obstructive pulmonary disease. J Clin Invest. 2008; 118 (11): 3546–56.
86. Barnes PJ. Inflammatory mechanisms in patients with chronic obstructive pulmonary disease. J Allergy Clin Immunol. 2016; 138 (1): 16–27.
87. Marçôa R, Rodrigues D, Dias M, Ladeira I, Vaz A, Lima R, et al. Classification of Chronic Obstructive Pulmonary Disease (COPD) according to the new Global Initiative for Chronic Obstructive Lung Disease (GOLD) 2017: Comparison with GOLD 2011. COPD. 2018; 15 (1): 21–6.
88. Högman M, Sulku J, Ställberg B, Janson C, Bröms K, Hedenström H, et al. 2017 Global Initiative for Chronic Obstructive Lung Disease reclassifies half of COPD subjects to lower risk group. Int J Chron Obs Pulmon Dis. 2018; 13: 165–73.
89. Hernández M, García G, Falco J, García AR, Martín V, Ibarrola M, et al. Impact of using the new GOLD classification on the distribution of COPD severity in clinical practice. Int J Chron Obs Pulmon Dis. 2018; 13: 351–6.
90. Mittal R, Chhabra S. GOLD Classification of COPD: Discordance in Criteria for Symptoms and Exacerbation Risk Assessment. COPD. 2017; 14 (1): 1–6.
91. Tockman M, Anthonisen N, Wright E, Donithan M. Airways obstruction and the risk for lung cancer. Ann Intern Med. 1987; 106 (4): 512–8.
92. Skillrud D, Offord K, Miller R. Higher risk of lung cancer in chronic obstructive pulmonary disease. A prospective, matched, controlled study. Ann Intern Med. 1986; 105 (4): 503–7.
93. Young RP, Hopkins RJ, Christmas T, Black PN, Metcalf P, Gamble GD. COPD prevalence is increased in lung cancer, independent of age, sex and smoking history. Eur Respir J. 2008; 34 (2): 380–6.
94. De-Torres JP, Wilson DO, Sanchez-Salcedo P, Weissfeld JL, Berto J, Campo A, et al. Lung cancer in patients with chronic obstructive pulmonary disease: Development and validation of the COPD lung cancer screening score. Am J Respir Crit Care Med. 2015; 191 (3): 285–91.
95. Sekine Y, Katsura H, Koh E, Hiroshima K, Fujisawa T. Early detection of COPD is important for lung cancer surveillance. Eur Respir J. 2012; 39 (5): 1230–40.
96. Wilson DO, Weissfeld JL, Balkan A, Schragin JG, Fuhrman CR, Fisher SN, et al. Association of radiographic emphysema and airflow obstruction with lung cancer. Am J Respir Crit Care Med. 2008; 178 (7): 738–44.

97. Koshiol J, Rotunno M, Consonni D, Pesatori AC, De Matteis S, Goldstein AM, et al. Chronic obstructive pulmonary disease and altered risk of lung cancer in a population-based case-control study. PLoS One. 2009; 4 (10): e7380.
98. Kurishima K, Satoh H, Ishikawa H, Yamashita YT, Homma T, Ohtsuka M, et al. Lung cancer patients with chronic obstructive pulmonary disease. Oncol Rep. 2001; 8 (1): 63–5.
99. Zulueta JJ, Wisnivesky JP, Henschke CI, Yip R, Farooqi AO, McCauley DI, et al. Emphysema scores predict death from COPD and lung cancer. Chest. 2012; 141 (5): 1216–23.
100. Sin DD, Anthonisen NR, Soriano JB, Agustí AG. Mortality in COPD: The role of comorbidities. Chronic Obstr Pulm Dis Co-Morbidities Syst Consequences. 2012; 28 (6): 1–13.
101. Li Y, Swensen SJ, Karabekmez LG, Marks RS, Stoddard SM, Jiang R, et al. Effect of emphysema on lung cancer risk in smokers: A computed tomography-based assessment. Cancer Prev Res. 2011; 4 (1): 43–50.
102. De Torres JP, Bastarrika G, Wisnivesky JP, Alcaide AB, Campo A, Seijo LM, et al. Assessing the relationship between lung cancer risk and emphysema detected on low-dose CT of the chest. Chest. 2007; 132 (6): 1932–8.
103. Mouronte-Roibás C, Leiro-Fernández V, Ruano-Raviña A, Ramos-Hernández C, Abal-Arca J, Parente-Lamelas I, et al. Chronic Obstructive Pulmonary Disease in Lung Cancer Patients: Prevalence, Underdiagnosis, and Clinical Characterization. Respiration. 2018; 95 (6): 414-21.
104. Rivera-Ortega P, Sigel K, Ezer N, Marín JM, Casanova C, Cote C, et al. Severity of the Chronic Obstructive Pulmonary Disease (COPD) and the risk of Lung Cancer (LC): A Competing-Risks Analysis. Monogr Arch Bronconeumol. 2015; 2 (3): 69.
105. Mannino DM, Aguayo SM, Petty TL, Redd SC. Low Lung Function and Incident Lung Cancer in the United States: data From the First National Health and Nutrition Examination Survey follow-up. Arch Intern Med. 2003; 163(12): 1475–80.
106. De Torres JP, Marín JM, Casanova C, Cote C, Carrizo S, Cordoba-Lanus E, et al. Lung cancer in patients with chronic obstructive pulmonary disease: Incidence and predicting factors. Am J Respir Crit Care Med. 2011; 184 (8): 913–9.
107. Hashimoto N, Matsuzaki A, Okada Y, Imai N, Iwano S, Wakai K, et al. Clinical impact of prevalence and severity of COPD on the decision-making process for therapeutic management of lung cancer patients. BMC Pulm Med. 2014; 14 (1): 1–9.
108. Bishawi M, Moore W, Bilfinger T. Severity of emphysema predicts location of lung cancer and 5-y survival of patients with stage i nonesmall cell lung cancer. J Surg Res. 2013; 184 (1): 1–5.

109. Van Gestel YRBM, Hoeks SE, Sin DD, Hüzeir V, Stam H, Mertens FW, et al. COPD and cancer mortality: The influence of statins. Thorax. 2009; 64 (11): 963–7.
110. López-Encuentra A, Astudillo J, Cerezal J, González-Aragoneses F, Novoa N, Sánchez-Palencia A. Prognostic value of chronic obstructive pulmonary disease in 2994 cases of lung cancer. Eur J Cardiothorac Surg. 2005; 27 (1): 8–13.
111. Papi A, Casoni G, Caramori G, Guzzinati I, Boschetto P, Ravenna F, et al. COPD increases the risk of squamous histological subtype in smokers who develop non-small cell lung carcinoma. Thorax. 2004; 59 (8): 679–81.
112. Tuder RM, Petrache I. Review series Pathogenesis of chronic obstructive pulmonary disease. J Clin Invest. 2012; 122 (8): 2749–55.
113. Herbst RS, Heymach J V, Lippman SM. Lung cancer. N Engl J Med. 2008; 359: 1367.
114. Barreiro E. EPOC y cáncer de pulmón. Arch Bronconeumol. 2008; 44 (8): 399–401.
115. Sosa V, Moliné T, Somoza R, Paciucci R, Kondoh H, Lleonart ME. Oxidative stress and skin cancer: An overview. Aging Res Rev. 2013; 12: 376–90.
116. Noda N, Wakasugi H. Cancer and Oxidative Stress. J Japan Med Assoc. 2001; 44 (12): 1571–4.
117. Gill JG, Piskounova E, Morrison SJ. Cancer, Oxidative Stress, and Metastasis. Cold Spring Harbo Symp Quant Biol. 2016; 81: 163-75.
118. Grimm EA, Sikora AG, Ekmekcioglua S. Molecular Pathways: Inflammation-associated nitric-oxide production as a cancer-supporting redox mechanism and a potential therapeutic target. Clin Cancer Res. 2013; 19 (20): 5557–63.
119. Miar A, Hevia D, Muñoz-Cimadevilla H, Astudillo A, Velasco J, Sainz R, et al. Manganese superoxide dismutase (SOD2/MnSOD)/catalase and SOD2/GPx1 ratios as biomarkers for tumor progression and metastasis in prostate, colon, and lung cancer. Free Radic Biol Med. 2015; 85: 45–55.
120. Masri FA, Comhair SAA, Koeck T, Xu W, Janocha A, Ghosh S, et al. Abnormalities in nitric oxide and its derivatives in lung cancer. Am J Respir Crit Care Med. 2005; 172 (5): 597–605.
121. Barreiro E, Fermoselle C, Mateu-Jimenez M, Sánchez-Font A, Pijuan L, Gea J, et al. Oxidative stress and inflammation in the normal airways and blood of patients with lung cancer and COPD. Free Radic Biol Med. 2013; 65: 859–71.
122. Mateu-Jiménez M, Sánchez-Font A. Redox Imbalance in Lung Cancer of Patients with Underlying Chronic Respiratory Conditions. Mol Med. 2016; 22 (1): 1.

123. Mateu-Jiménez M, Cucarull-Martínez B, Yelamos J, Barreiro E. Reduced tumor burden through increased oxidative stress in lung adenocarcinoma cells of PARP-1 and PARP-2 knockout mice. Biochimie. 2016; 121: 278–86.
124. Filaire E, Dupuis C, Galvaing G, Aubreton S, Laurent H, Richard R, et al. Lung cancer: What are the links with oxidative stress, physical activity and nutrition. Lung Cancer. 2013; 82 (3): 383–9.
125. Mehrotra S, Mougiakakos D, Christian Johansson C, Voelkel-Johnson C, Kiessling R. Oxidative stress and lymphocyte persistence. Implications in immunotherapy. 1st ed. Vol. 102, Advances in Cancer Research. Elsevier Inc.; 2009. 197-227 p.
126. Esme H, Cemek M, Sezer M, Saglam H, Demir A, Melek H, et al. High levels of oxidative stress in patients with advanced lung cancer. Respirology. 2008; 13 (1): 112–6.
127. Anderson GP, Bozinovski S. Acquired somatic mutations in the molecular pathogenesis of COPD. Trends Pharmacol Sci. 2003; 24 (2): 71–6.
128. Genova C, Rijavec E, Grossi F. Tumor microenvironment as a potential source of clinical biomarkers in non-small cell lung cancer: Can we use enemy territory at our advantage? J Thorac Dis. 2017; 9 (11): 4300–4.
129. Wang M, Zhao J, Zhang L, Wei F, Lian Y, Wu Y, et al. Role of tumor microenvironment in tumorigenesis. J Cancer. 2017; 8 (5): 761–73.
130. Flanagan DJ, Hodder MC, Sansom OJ. Microenvironmental cues in cancer stemness. Nat Cell Biol. 2018; 20 (10): 1102–4.
131. Spill F, Reynolds DS, Kamm RD, Zaman MH. Impact of the physical microenvironment on tumor progression and metastasis. Curr Opin Biotechnol. 2016; 40: 41–8.
132. Kerbel RS. A Decade of Experience in Developing Preclinical Models of Advanced- or Early-Stage Spontaneous Metastasis to Study Antiangiogenic Drugs, Metronomic Chemotherapy, and the Tumor Microenvironment. Cancer J (United States). 2015; 21 (4): 274–83.
133. Pickup MW, Mouw JK, Weaver VM. The extracellular matrix modulates the hallmarks of cancer. EMBO Rep. 2014; 15 (12): 1243–53.
134. Chen DS, Mellman I. Elements of cancer immunity and the cancer-immune set point. Nature. 2017; 541 (7637): 321–30.
135. Denys H, Braems G, Lambein K, Pauwels P, Hendrix A, De Boeck A, et al. The extracellular matrix regulates cancer progression and therapy response: implications for prognosis and treatment. Curr Pharm Des. 2009; 15 (12): 1373–84.
136. Kalluri R, Zeisberg M. Fibroblasts in cancer. Nat Rev Cancer. 2006; 6 (5): 392–401.

137. Tanaka K, Miyata H, Sugimura K, Fukuda S, Kanemura T, Yamashita K, et al. miR-27 is associated with chemoresistance in esophageal cancer through transformation of normal fibroblasts to cancer-associated fibroblasts. Carcinogenesis. 2015; 36 (8): 894–903.
138. Min A, Zhu C, Peng S, Shuai C, Sun L, Han Y, et al. Downregulation of MicroRNA-148a in Cancer-Associated Fibroblasts from Oral Cancer Cell Migration and Invasion by Targeting Wnt10b. J Biochem Mol Toxicol. 2016; 30 (4): 186-91
139. Wiseman BS, Werb Z. Stromal effects on mammary gland development and breast cancer. Science. 2002; 296 (5570): 1046–9.
140. Hlatky L, Tsionou C, Hahnfeldt P, Coleman CN. Mammary Fibroblasts May Influence Breast Tumor Angiogenesis Via Hypoxia-Induced Vascular Endothelial Growth Factor Up-Regulation And Protein Expression. Cancer Res. 1994; 54 (23): 6083–6.
141. Fukui H, Zhang X, Sun C, Hara K, Kikuchi S, Yamasaki T, et al. IL-22 produced by cancer-associated fibroblasts promotes gastric cancer cell invasion via STAT3 and ERK signaling. Br J Cancer. 2014; 111 (4): 763–71.
142. Saussez S, Decaestecker C, Cludts S, Ernoux P, Chevalier D, Smetana K, et al. Adhesion/growth-regulatory tissue lectin galectin-1 in relation to angiogenesis/lymphocyte infiltration and prognostic relevance of stromal up-regulation in laryngeal carcinomas. Anticancer Res. 2009; 29 (1): 59–65.
143. He XJ, Tao HQ, Hu ZM, Ma YY, Xu J, Wang HJ, et al. Expression of galectin-1 in carcinoma-associated fibroblasts promotes gastric cancer cell invasion through upregulation of integrin β1. Cancer Sci. 2014; 105 (11): 1402–10.
144. Feig C, Jones J, Kraman M, Wells R, Deonarine A, Chan D, et al. Targeting CXCL12 from FAP-expressing carcinoma-associated fibroblasts synergyzes with anti-PD-L1 immunotherapy in pancreatic cancer. PNAS. 2013; 110 (50): 20212–7.
145. Yu X, Graves DT. Fibroblasts, mononuclear phagocytes, and endothelial cells express monocyte chemoattractant protein-1 (MCP-1) in inflamed human gingiva. J Periodontol. 1995; 66 (1): 80–8.
146. Zucali JR, Dinarello CA, Oblon DJ, Gross MA, Anderson L, Weiner RS. Interleukin 1 stimulates fibroblasts to produce granulocyte-macrophage colony-stimulating activity and prostaglandin E2. J Clin Invest. 1986; 77 (6): 1857–63.
147. Yashiro M, Matsuoka T. Fibroblast growth factor receptor signaling as therapeutic targets in gastric cancer. World J Gastroenterol. 2016; 22 (8): 2415–23.

148. Ding N, Yu RT, Subramaniam N, Sherman MH, Rao R, Leblanc M, et al. A vitamin D receptor/SMAD genomic circuit gates hepatic fibrotic response. Cell. 2013; 153 (3): 601–13.
149. Allavena P, Garlanda C, Borrello MG, Sica A, Mantovani A. Pathways connecting inflammation and cancer. Curr Opin Genet Dev. 2008; 18 (1): 3–10.
150. Tran Janco JM, Lamichhane P, Karyampudi L, Knutson KL. Tumor-infiltrating dendritic cells in cancer pathogenesis. 2015; 194 (7): 2985–91.
151. Maeda H, Akaike T. Nitric oxide and oxygen radicals in infection, inflammation, and cancer. Biochemistry. 1998; 63 (7): 854–65.
152. Chae YK, Chang S, Ko T, Anker J, Agte S, Iams W, et al. Epithelial-mesenchymal transition (EMT) signature is inversely associated with T-cell infiltration in non-small cell lung cancer (NSCLC). Sci Rep. 2018; 8 (1): 2–9.
153. Balkwill FR, Capasso M, Hagemann T. The tumor microenvironment at a glance. J Cell Sci. 2012; 125 (23): 5591–6.
154. Karin M. Nuclear factor-kappaB in cancer development and progression. Nature. 2006; 441 (7092): 431–6.
155. H Y, Kortylewski M, Pardoll D. Crosstalk between cancer and immune cells: role of STAT3 in the tumour microenvironment. Nat Rev Immunol. 2007; 7 (1): 41–51.
156. O'Callaghan D, O'Donnell D, O'Connell F, O'Byrne K. The role of inflammation in the pathogenesis of non-small cell lung cancer. J Thorac Oncol. 2010; 5 (12): 2024–36.
157. Meaney CL, Zingone A, Brown D, Yu Y, Cao L, Ryan BM. Identification of serum inflammatory markers as classifiers of lung cancer mortality for stage I adenocarcinoma. Oncotarget. 2017; 8 (25): 40946–57.
158. Mateu-Jimenez M, Curull V, Pijuan L, Sánchez-Font A, Rivera-Ramos H, Rodríguez-Fuster A, et al. Systemic and Tumor Th1 and Th2 Inflammatory Profile and Macrophages in Lung Cancer: Influence of Underlying Chronic Respiratory Disease. J Thorac Oncol. 2017; 12 (2): 235–48.
159. Angell H, Galon J. From the immune contexture to the Immunoscore: the role of prognostic and predictive immune markers in cancer. Curr Opin Immunol. 2013; 25 (2): 261–7.
160. Butt A, Mills K. Immunosuppressive networks and checkpoints controlling antitumor immunity and their blockade in the development of cancer immunotherapeutics and vaccines. Oncogene. 2014; 33 (38): 4623–31.
161. Domagala-Kulawik J, Osinska I, Hoser G. Mechanisms of immune response regulation in lung cancer. Transl lung cancer Res. 2014; 3 (1): 15–22.
162. Goc J, Fridman WH, Sautès-Fridman C, Dieu-Nosjean MC. Characteristics of tertiary lymphoid structures in primary cancers. Oncoimmunology. 2013; 2 (12): 1–9.

Bibliography

163. Dieu-Nosjean M, Antoine M, Danel C, Heudes D, Wislez M, Poulot V, et al. Long-term survival for patients with non-small-cell lung cancer with intratumoral lymphoid structures. J Clin Oncol. 2008; 26 (27): 4410–7.
164. Randall TD, Kern JA. Tertiary lymphoid structures target the antitumor immune response to lung cancer. Am J Respir Crit Care Med. 2014; 189 (7): 767–9.
165. Sautïs-Fridman C, Lawand M, Giraldo NA, Kaplon H, Germain C, Fridman WH, et al. Tertiary lymphoid structures in cancers: Prognostic value, regulation, and manipulation for therapeutic intervention. Front Immunol. 2016; 7: 407.
166. Dieu-Nosjean MC, Giraldo NA, Kaplon H, Germain C, Fridman WH, Sautès-Fridman C. Tertiary lymphoid structures, drivers of the anti-tumor responses in human cancers. Immunol Rev. 2016; 271 (1): 260–75.
167. Tang H, Zhu M, Qiao J, Fu YX. Lymphotoxin signalling in tertiary lymphoid structures and immunotherapy. Cell Mol Immunol. 2017; 14 (10): 809–18.
168. Pimenta EM, Barnes BJ. Role of tertiary lymphoid structures (TLS) in anti-tumor immunity: Potential tumor-induced cytokines/chemokines that regulate TLS formation in epithelial-derived cancers. Cancers. 2014; 6 (2): 969–97.
169. Dieu-Nosjean MC, Goc J, Giraldo NA, Sautès-Fridman C, Fridman WH. Tertiary lymphoid structures in cancer and beyond. Trends Immunol. 2014; 35 (11): 571–80.
170. Teillaud JL, Dieu-Nosjean MC. Tertiary lymphoid structures: An anti-tumor school for adaptive immune cells and an antibody factory to fight cancer? Front Immunol. 2017; 8: 830.
171. Engelhard VH, Rodriguez AB, Mauldin IS, Woods AN, Peske JD, Slingluff CL. Immune Cell Infiltration and Tertiary Lymphoid Structures as Determinants of Antitumor Immunity. J Immunol. 2018; 200 (2): 432–42.
172. Colbeck EJ, Ager A, Gallimore A, Jones GW. Tertiary lymphoid structures in cancer: Drivers of antitumor immunity, immunosuppression, or Bystander Sentinels in disease? Front Immunol. 2017; 8: 1830.
173. Silina K, Soltermann A, Attar FM, Casanova R, Uckeley ZM, Thut H, et al. Germinal centers determine the prognostic relevance of tertiary lymphoid structures and are impaired by corticosteroids in lung squamous cell carcinoma. Cancer Res. 2018; 78 (5): 1308–20.
174. Lee HJ, Park IA, Song IH, Shin SJ, Kim JY, Yu JH, et al. Tertiary lymphoid structures: Prognostic significance and relationship with tumour-infiltrating lymphocytes in triple-negative breast cancer. J Clin Pathol. 2016; 69 (5): 422–30.

175. Germain C, Gnjatic S, Tamzalit F, Knockaert S, Remark R, Goc J, et al. Presence of B cells in tertiary lymphoid structures is associated with a protective immunity in patients with lung cancer. Am J Respir Crit Care Med. 2014; 189 (7): 832–44.
176. Warth A, Penzel R, Lindenmaier H, Brandt R, Stenzinger A, Herpel E, et al. EGFR, KRAS, BRAF and ALK gene alterations in lung adenocarcinomas: patient outcome, interplay with morphology and immunophenotype. Eur Respir J. 2014; 43 (3): 872–83.
177. Evan G, Vousden K. Proliferation, cell cycle and apoptosis in cancer. Nature. 2001; 411 (6835): 342–8.
178. Yin P, Peng R, Peng H, Yao L, Sun Y, Wen L, et al. MiR-451 suppresses cell proliferation and metastasis in A549 lung cancer cells. Mol Biotechnol. 2015; 57 (1): 1–11.
179. Bihl M, Tamm M, Nauck M, Wieland H, Perruchoud A, Roth M. Proliferation of human non-small-cell lung cancer cell lines: role of interleukin-6. Am J Respir Cell Mol Biol. 1998; 19 (4): 606–12.
180. Warth A, Cortis J, Soltermann A, Meister M, Budczies J, Stenzinger A, et al. Tumour cell proliferation (Ki-67) in non-small cell lung cancer: a critical reappraisal of its prognostic role. Br J Cancer. 2014; 111: 1222–9.
181. Zahel T, Krysa S, Herpel E, Stenzinger A, Goeppert B, Schirmacher P, et al. Phenotyping of pulmonary carcinoids and a Ki-67-based grading approach. Virchows Arch. 2012; 460 (3): 299–308.
182. Warth A, Fink L, Fisseler-Eckhoff A, Jonigk D, Keller M, Ott G, et al. Interobserver agreement of proliferation index (Ki-67) outperforms mitotic count in pulmonary carcinoids. Virchows Arch. 2013; 462 (5): 507–13.
183. Urruticoechea A, Smith I, Dowsett M. Proliferation marker Ki-67 in early breast cancer. J Clin Oncol. 2005; 23 (28): 7212–20.
184. Viale G, Giobbie-Hurder A, Regan M, Coates A, Mastropasqua M, Dell'Orto P, et al. Prognostic and predictive value of centrally reviewed Ki-67 labeling index in postmenopausal women with endocrine-responsive breast cancer: results from Breast International Group Trial 1-98 comparing adjuvant tamoxifen with letrozole. J Clin Oncol. 2008; 26 (34): 5569–75.
185. Pollack A, DeSilvio M, Khor L, Li R, Al-Saleem T, Hammond M, et al. Ki-67 staining is a strong predictor of distant metastasis and mortality for men with prostate cancer treated with radiotherapy plus androgen deprivation: Radiation Therapy Oncology Group Trial 92-02. J Clin Oncol. 2004; 22 (11): 2133–40.
186. Martin B, Paesmans M, Mascaux C, Berghmans T, Lothaire P, Meert A, et al. Ki-67 expression and patients survival in lung cancer: systematic review of the literature with meta-analysis. Br J Cancer. 2004; 91 (12): 2018–35.

187. Yamashita S, Moroga T, Tokuishi K, Miyawaki M, Chujo M, Yamamoto S, et al. Ki-67 labeling index is associated with recurrence after segmentectomy under video-assisted thoracoscopic surgery in stage I non-small cell lung cancer. Ann Thorac Cardiovasc Surg. 2011; 17 (4): 341–6.
188. Poleri C, Morero J, Nieva B, Vázquez M, Rodríguez C, de Titto E, et al. Risk of recurrence in patients with surgically resected stage I non-small cell lung carcinoma: histopathologic and immunohistochemical analysis. Chest. 2003; 123 (6): 1858–67.
189. Sofocleous C, Garg S, Cohen P, Petre E, Gonen M, Erinjeri J, et al. Ki 67 is an independent predictive biomarker of cancer specific and local recurrence-free survival after lung tumor ablation. Ann Surg Oncol. 2013; 20 (3): 676–83.
190. Wong RSY. Apoptosis in cancer: From pathogenesis to treatment. J Exp Clin Cancer Res. 2011; 30 (1): 87.
191. Lowe SW, Lin AW. Apoptosis in cancer. Carcinogenesis. 2000; 21 (3): 485–95.
192. Pore MM, Hiltermann JN, Kruyt FA. Targeting apoptosis pathways in lung cancer. Cancer Lett. 2013; 332: 359–68.
193. Shivapurkar N, Reddy J, Chaudhary PM, Gazdar AF. Apoptosis and lung cancer: A review. J Cell Biochem. 2003; 88: 885–98.
194. Hengartner M. The biochemistry of apoptosis. Nature. 2000; 407 (6805): 770–6.
195. Hannahan D, Weinberg R. The hallmarks of cancer. Cell. 2000; 100 (1): 57–70.
196. Brown JM, Attardi LD. The role of apoptosis in cancer development and treatment response. Nat Rev Cancer. 2005; 5: 231–7.
197. Levine A. p53, the cellular gatekeeper for growth and division. Cell. 1997; 88 (3): 323–31.
198. Vousden H, Lu X. Live or let die: the cell's response to p53. Nat Rev Cancer. 2002; 2 (8): 594–604.
199. Kaminskyy VO, Piskunova T, Zborovskaya IB, Tchevkina EM, Zhivotovsky B. Suppression of basal autophagy reduces lung cancer cell proliferation and enhances caspase-dependent and -independent apoptosis by stimulating ROS formation. Autophagy. 2012; 8 (7): 1032–44.
200. Rao S, Tortola L, Perlot T, Wirnsberger G, Novatchkova M, Nitsch R, et al. A dual role for autophagy in a murine model of lung cancer. Nat Commun. 2014; 5.
201. Liu G, Pei F, Yang F, Li L, Amin AD, Liu S, et al. Role of autophagy and apoptosis in non-small-cell lung cancer. Int J Mol Sci. 2017; 18 (2).
202. Mariño G, Niso-Santano M, Baehrecke E, Kroemer G. Self-consumption: the interplay of autophagy and apoptosis. Nat Rev Mol Cell Biol. 2014; 15 (2): 91–4.

203. Wei Y, Pattingre S, Sinha S, Bassik M, Levine B. JNK1-mediated phosphorylation of Bcl-2 regulates starvation-induced autophagy. Mol Cell. 2008; 30 (6): 678–88.
204. Jaboin JJ, Hwang M, Lu B. Autophagy in lung cancer. Methods Enzym. 2009; 453: 287–304.
205. Rello-Varona S, Lissa D, Shen S, Niso-Santano M, Senovilla L, Mariño G, et al. Autophagic removal of micronuclei. Cell Cycle. 2012; 11: 170–6.
206. Kuo T, Chen C, D B, Onder T, Loewer S, Almeida S, et al. Midbody accumulation through evasion of autophagy contributes to cellular reprogramming and tumorigenicity. Nat Cell Biol. 2011; 13 (10): 1214–23.
207. Karantza-Wadsworth V, Patel S, Kravchuk O, Chen G, Mathew R, Jin S, et al. Autophagy mitigates metabolic stress and genome damage in mammary tumorigenesis. Genes Dev. 2007; 21 (13): 1621–35.
208. Meuwissen R, Berns A. Mouse models for human lung cancer. Genes Dev. 2005; 19 (6): 643–64.
209. Safari R, Meuwissen R. Practical use of advanced mouse models for lung cancer. Methods Mol Biol. 2015; 1267: 93–124.
210. Sanmamed MF, Chester C, Melero I, Kohrt H. Defining the optimal murine models to investigate immune checkpoint blockers and their combination with other immunotherapies. Ann Oncol. 2016; 27 (7): 1190–8.
211. Kwon M, Berns A. Mouse models for lung cancer. Mol Oncol. 2013; 7 (2): 165–77.
212. Urtreger AJ, Diament MJ, Ranuncolo S, Vidal M, Puricelli L, Klein S. New Murine Cell Line Derived From a Spontaneous Lung Tumor Induces Paraneoplastic Syndromes. Int J Oncol. 2001; 18 (3): 639–347.
213. Diament MJ, Garcia C, Stillitani I, Saavedra VM. Spontaneous murine lung adenocarcinoma (P07): a new experimental model to study paraneoplastic syndromes of lung cancer. Int J Mol Med. 1998; 2: 45–50.
214. Mateu-Jimenez M, Fermoselle C, Rojo F, Mateu J, Pena R, Urtreger AJ, et al. Pharmacological Approaches in an Experimental Model of Non-Small Cell Lung Cancer: Effects on Tumor Biology. Curr Pharm Des. 2016; 22 (34): 5300-5310.
215. Chacon-Cabrera A, Mateu-Jiménez M, Langohr K, Fermoselle C, García-Arumí E, Andreu AL, et al. Role of PARP activity in lung cancer-induced cachexia: Effects on muscle oxidative stress, proteolysis, anabolic markers and phenotype. J Cell Physiol. 2017; 232 (12): 3744–61.
216. Chacon-Cabrera A, Fermoselle C, Urtreger AJ, Mateu-Jimenez M, Diament MJ, de Kier Joffé EDB, et al. Pharmacological Strategies in Lung Cancer-Induced Cachexia: Effects on Muscle Proteolysis, Autophagy, Structure, and Weakness. J Cell Physiol. 2014; 229 (11): 1660–72.
217. Jett JR, Schild SE, Kesler KA, Kalemkerian GP. Treatment of Small Cell Lung Cancer. Chest. 2013; 143 (5): e400S–e419S.

218. Kowozer BD, Larner JM, Detterbeck FC, Jones DR. Special Treatment Issues in Non-small Cell Lung Cancer. Chest. 2013; 143 (5): e369S–e399S.
219. Detterbeck FC, Boffa DJ, Kim AW, Tanoue LT. The Eighth Edition Lung Cancer Stage Classification. Chest. 2017; 151 (1): 193–203.
220. Miravitlles M, Calle M, Soler-Cataluna JJ. Clinical Phenotypes of COPD: Identification, Definition and Implications for Guidelines [Spanish] Fenotipos clinicos de la EPOC. Identificacion, definicion e implicaciones para las guias de tratamiento. Arch Bronconeumol. 2012; 48 (3): 86–98.
221. Miravitlles M, Soler-Cataluña JJ, Calle M, Molina J, Almagro P, Quintano JA, et al. Guía española de la EPOC (GesEPOC). Actualización 2014. Arch Bronconeumol. 2014; 50, Supple (Supl 1): 1–16.
222. Ohri C, Shikotra A, Green R, Waller D, Bradding P. Macrophages within NSCLC tumour islets are predominantly of a cytotoxic M1 phenotype associated with extended survival. Eur Respir J. 2009; 33 (1): 118–26.
223. Feldman A, Wolfe D. Tissue processing and hematoxylin and eosin staining. Methods Mol Biol. 2014; 1180: 31–43.
224. Welsh T, Green R, Richardson D, Waller D, O'Byrne K, Bradding P. Macrophage and mast-cell invasion of tumor cell islets confers a marked survival advantage in non-small-cell lung cancer. J Clin Oncol. 2005; 23 (35): 8959–67.
225. Mateu-Jimenez M, Curull V, Pijuan L, Sánchez-Font A, Rivera-Ramos H, Rodríguez-Fuster A, et al. Systemic and Tumor Th1 and Th2 Inflammatory Profile and Macrophages in Lung Cancer: Influence of Underlying Chronic Respiratory Disease. J Thorac Oncol. 2017; 12 (2): 235–48.
226. De Silva NS, Klein U. Dynamics of B cells in germinal centres. Nat Rev Immunol. 2015; 15 (3): 137–48.
227. Siliņa K, Soltermann A, Movahedian Attar F, Casanova R, Uckeley ZM, Thut H, et al. Germinal Centers Determine the Prognostic Relevance of Tertiary Lymphoid Structures and Are Impaired by Corticosteroids in Lung Squamous Cell Carcinoma. Cancer Res. 2018; 78 (5): 1308–20.
228. Mateu-Jimenez M, Curull V, Rodríguez-Fuster A, Aguiló R, Sánchez-Font A, Pijuan L, et al. Profile of epigenetic mechanisms in lung tumors of patients with underlying chronic respiratory conditions. Clin Epigenetics. 2018; 10 (1): 1–11.
229. Mateu-Jiménez M, Cucarull-Martínez B, Yelamos J, Barreiro E. Reduced tumor burden through increased oxidative stress in lung adenocarcinoma cells of PARP-1 and PARP-2 knockout mice. Biochimie. 2016; 121: 278–86.
230. Mateu-Jiménez M, Fermoselle C, Rojo F, Mateu J, Peña R, Urtreger AJ, et al. Pharmacological Approaches in an Experimental Model of Non-Small Cell Lung Cancer: Effects on Tumor Biology. Curr Pharm Des. 2016; 22 (34): 5300–10.

231. Chen DS, Mellman I. Oncology meets immunology: The cancer-immunity cycle. Immunity. 2013; 39 (1): 1–10.
232. Fermoselle C, Rabinovich R, Ausín P, Puig-Vilanova E, Coronell C, Sanchez F, et al. Does oxidative stress modulate limb muscle atrophy in severe COPD patients? Eur Respir J. 2012; 40 (4): 851–62.
233. Brusselle GG, Demoor T, Bracke KR, Brandsma CA, Timens W. Lymphoid follicles in (very) severe COPD: Beneficial or harmful? Eur Respir J. 2009; 34 (1): 219–30.
234. Pipi E, Nayar S, Gardner DH, Colafrancesco S, Smith C, Barone F. Tertiary lymphoid structures: Autoimmunity goes local. Front Immunol. 2018; 9: 1952.
235. Kirkham PA, Caramori G, Casolari P, Papi AA, Edwards M, Shamji B, et al. Oxidative stress-induced antibodies to carbonyl-modified protein correlate with severity of chronic obstructive pulmonary disease. Am J Respir Crit Care Med. 2011; 184 (7): 796–802.
236. Henson PM, Vandivier RW, Douglas IS. Cell Death, Remodeling, and Repair in Chronic Obstructive Pulmonary Disease? Proc Am Thorac Soc. 2006; 3 (8): 713–7.
237. Yadava K, Bollyky P, Lawson MA. The formation and function of tertiary lymphoid follicles in chronic pulmonary inflammation. Immunology. 2016; 149 (3): 262–9.
238. De Chaisemartin L, Goc J, Damotte D, Validire P, Magdeleinat P, Alifano M, et al. Characterization of chemokines and adhesion molecules associated with T cell presence in tertiary lymphoid structures in human lung cancer. Cancer Res. 2011; 71 (20): 6391–9.
239. Pikor NB, Astarita JL, Summers-Deluca L, Galicia G, Qu J, Ward LA, et al. Integration of Th17- and Lymphotoxin-Derived Signals Initiates Meningeal-Resident Stromal Cell Remodeling to Propagate Neuroinflammation. Immunity. 2015; 43 (6): 1160–73.
240. Goya S, Matsuoka H, Mori M, Morishita H, Kida H, Kobashi Y, et al. Sustained interleukin-6 signalling leads to the development of lymphoid organ-like structures in the lung. J Pathol. 2003; 200 (1): 82–7.
241. Zhang J, Chu S, Zhong X, Lao Q, He Z, Liang Y. Increased expression of CD4+IL-17+ cells in the lung tissue of patients with stable chronic obstructive pulmonary disease (COPD) and smokers. Int Immunopharmacol. 2013; 15 (1): 58–66.
242. Di Stefano A, Caramori G, Gnemmi I, Contoli M, Vicari C, Capelli A, et al. T helper type 17-related cytokine expression is increased in the bronchial mucosa of stable chronic obstructive pulmonary disease patients. Clin Exp Immunol. 2009; 157 (2): 316–24.
243. Roos AB, Mori M, Gura HK, Lorentz A, Bjermer L, Hoffmann HJ, et al. Increased IL-17RA and IL-17RC in End-Stage COPD and the Contribution to Mast Cell Secretion of FGF-2 and VEGF. Respir Res. 2017; 18(1): 3–6.

244. Rangel-Moreno J, Carragher D, de la Luz Garcia-Hernandez M, Hwang J, Kusser K, Hartson L. The development of inducible bronchus-associated lymphoid tissue depends on IL-17. Nat Immunol. 2011; 12: 639–46.
245. Fleige H, Ravens S, Moschovakis GL, Bölter J, Willenzon S, Sutter G, et al. IL-17–induced CXCL12 recruits B cells and induces follicle formation in BALT in the absence of differentiated FDCs. J Exp Med. 2014; 211 (4): 643–51.
246. Barua S, Fang P, Sharma A, Fujimoto J, Wistuba I, Rao AUK, et al. Spatial interaction of tumor cells and regulatory T cells correlates with survival in non-small cell lung cancer. Lung Cancer. 2018; 117:73–9.
247. Goc J, Fridman W-H, Hammond SA, Sautès-Fridman C, Dieu-Nosjean M-C. Tertiary lymphoid structures in human lung cancers, a new driver of antitumor immune responses. Oncoimmunology. 2014; 3 (6): e28976.
248. Kotsakis A, Koinis F, Katsarou A, Gioulbasani M, Aggouraki D, Kentepozidis N, et al. Prognostic value of circulating regulatory T cell subsets in untreated non-small cell lung cancer patients. Sci Rep. 2016; 6: 1–11.
249. Tao H, Mimura Y, Aoe K, Kobayashi S, Yamamoto H, Matsuda E, et al. Prognostic potential of FOXP3 expression in non-small cell lung cancer cells combined with tumor-infiltrating regulatory T cells. Lung Cancer. 2012; 75 (1): 95–101.
250. Wang S si, Liu W, Ly D, Xu H, Qu L, Zhang L. Tumor-infiltrating B cells: their role and application in anti-tumor immunity in lung cancer. Cell Mol Immunol. 2019; 16 (1): 6–18.
251. Yuen GJ, Demissie E, Pillai S. B lymphocytes and cancer: a love-hate relationship. Trends Cancer. 2016; 2 (12): 747–57.
252. Tan TT, Coussens LM. Humoral immunity, inflammation and cancer. Curr Opin Immunol. 2007; 19 (2): 209–16.
253. Germain C, Gnjatic S, Dieu-Nosjean MC. Tertiary lymphoid structure-associated B cells are key players in anti-tumor immunity. Front Immunol. 2015; 6: 1–14.
254. Lohr M, Edlund K, Botling J, Hammad S, Hellwig B, Othman A, et al. The prognostic relevance of tumour-infiltrating plasma cells and immunoglobulin kappa C indicates an important role of the humoral immune response in non-small cell lung cancer. Cancer Lett. 2013; 333 (2): 222–8.
255. Yasuda M, Mizukami M, Hanagiri T, Shigematsu Y, Fukuyama T, Nagata Y. Antigens recognized by IgG derived from tumor-infiltrating B lymphocytes in human lung cancer. Anticancer Res. 2006; 26 (5): 3601–11.
256. Mizukami M, Hanagiri T, Shigematsu Y, Baba T, Fukuyama T, Nagata Y. Effect of IgG produced by tumor-infiltrating B lymphocytes on lung tumor growth. Anticancer Res. 2006; 26 (3): 1827–31.

257. Mizukami M, Hanagiri T, Yasuda M, Kuroda K, Shigematsu Y, Baba T, et al. Antitumor effect of antibody against a SEREX-defined antigen (UOEH-LC-1) on lung cancer xenotransplanted into severe combined immunodeficiency mice. Cancer Res. 2007; 67 (17): 8351–7.
258. Siliņa K, Rulle U, Kalniņa Z, Linē A. Manipulation of tumour-infiltrating B cells and tertiary lymphoid structures: A novel anti-cancer treatment avenue? Cancer Immunol Immunother. 2014; 63 (7): 643–62.
259. Schmidt M, Hellwig B, Hammad S, Othman A, Lohr M, Chen Z, et al. A comprehensive analysis of human gene expression profiles identifies stromal immunoglobulin κ C as a compatible prognostic marker in human solid tumors. Clin Cancer Res. 2012; 18 (9): 2695–703.
260. Nagalla S, Chou J, Willingham M, Ruiz J, Vaughn J, Dubey P, et al. Interactions between immunity, proliferation and molecular subtype in breast cancer prognosis. Genome Biol. 2013; 14 (4): 1-11.
261. Finkin S, Yuan D, Stein I, Taniguchi K, Weber A, Unger K, et al. Ectopic lymphoid structures function as microniches for tumor progenitor cells in hepatocellular carcinoma. Nat Immunol. 2016; 16 (12): 1235–44.
262. Jackute J, Žemaitis M, Pranys D, Šitkauskiene B, Miliauskas S, Bajoriunas V, et al. Distribution of CD4+and CD8+T cells in tumor islets and stroma from patients with non-small cell lung cancer in association with COPD and smoking. Med. 2015; 51 (5): 263–71.
263. Hesker P, Krupnick A. The role of natural killer cells in pulmonary immunosurveillance. Front Biosci (Schol Ed). 2011; 2011 (4): 986491.
264. Aktaş ON, Öztürk AB, Erman B, Erus S, Tanju S, Dilege Ş. Role of natural killer cells in lung cancer. J Cancer Res Clin Oncol. 2018; 144 (6): 997–1003.
265. Neyt K, Perros F, GeurtsvanKessel CH, Hammad H, Lambrecht BN. Tertiary lymphoid organs in infection and autoimmunity. Trends Immunol. 2012; 33 (6): 297–305.
266. Lu TT, Browning JL. Role of the lymphotoxin/LIGHT system in the development and maintenance of reticular networks and vasculature in lymphoid tissues. Front Immunol. 2014; 5: 47.
267. Aloisi F, Pujol-Borrell R. Lymphoid neogenesis in chronic inflammatory diseases. Nat Rev Immunol. 2006; 6 (3): 205–17.
268. Carragher D, Rangel-Moreno J, Randall TD. Ectopic lymphoid tissues and local immunity. October. 2008; 20 (1): 26–42.
269. Bremnes RM, Busund LT, Kilver TL, Andersen S, Richardsen E, Paulsen EE, et al. The role of tumor-infiltrating lymphocytes in development, progression, and prognosis of non-small cell lung cancer. J Thorac Oncol. 2016; 11 (6): 789–800.
270. Zubler RH. Naive and memory B cells in T-cell-dependent and T-independent responses. Springer Semin Immunopathol. 2001; 23 (4): 405–19.

Bibliography

271. Weinstein AM, Storkus WJ. Biosynthesis and functional significance of peripheral node addressin in cancer-associated TLO. Front Immunol. 2016; 7: 301.
272. Litsiou E, Semitekolou M, Galani IE, Morianos I, Tsoutsa A, Kara P, et al. CXCL13 production in B cells via toll-like receptor/lymphotoxin receptor signaling is involved in lymphoid neogenesis in chronic obstructive pulmonary disease. Am J Respir Crit Care Med. 2013; 187 (11): 1194–202.
273. Johnson LA, Jackson DG. Inflammation-induced secretion of CCL21 in lymphatic endothelium is a key regulator of integrinmediated dendritic cell transmigration. Int Immunol. 2010; 22 (10): 839–49.
274. Barone F, Nayar S, Campos J, Cloake T, Withers DR, Toellner K-M, et al. IL-22 regulates lymphoid chemokine production and assembly of tertiary lymphoid organs. Proc Natl Acad Sci. 2015; 112 (35): 11024–9.
275. Hsu HC, Yang PA, Wang J, Wu Q, Myers R, Chen J, et al. Interleukin 17-producing T helper cells and interleukin 17 orchestrate autoreactive germinal center development in autoimmune BXD2 mice. Nat Immunol. 2008; 9 (2): 166–75.
276. Gopal R, Rangel-moreno J, Slight S, Lin Y, Nawar HF. Interleukin-17–dependent CXCL13 mediates mucosal vaccine-induced immunity against tuberculosis. Mucosal Immunol. 2013; 6 (5): 972–84.
277. Miyasaka M, Tanaka T. Lymphocyte trafficking across high endothelial venules: Dogmas and enigmas. Nat Rev Immunol. 2004; 4 (5): 360–70.
278. DeNucci CC, Mitchell JS, Shimizu Y. Integrin Function in T-Cell Homing to Lymphoid and Nonlymphoid Sites: Getting There and Staying There. Crit Rev Immunol. 2009; 29 (2): 87–109.
279. Kawamata N, Xu B, Nishijima H, Aoyama K, Kusumoto M, Takeuchi T, et al. Expression of endothelia and lymphocyte adhesion molecules in bronchus-associated lymphoid tissue (BALT) in adult human lung. Respir Res. 2009; 10: 1–11.
280. Xu B, Wagner N, Pham LN, Magno V, Shan Z, Butcher EC, et al. Lymphocyte Homing to Bronchus-associated Lymphoid Tissue (BALT) Is Mediated by L-selectin/PNAd, α_4 β_1 Integrin/VCAM-1, and LFA-1 Adhesion Pathways. J Exp Med. 2003; 197 (10): 1255–67.
281. Morissette MC, Jobse BN, Thayaparan D, Nikota JK, Shen P, Labiris NR, et al. Persistence of pulmonary tertiary lymphoid tissues and anti-nuclear antibodies following cessation of cigarette smoke exposure. Respir Res. 2014; 15 (1): 1–10.
282. Remark R, Alifano M, Cremer I, Lupo A, Dieu-Nosjean MC, Riquet M, et al. Characteristics and clinical impacts of the immune environments in colorectal and renal cell carcinoma lung metastases: Influence of tumor origin. Clin Cancer Res. 2013; 19 (15): 4079–91.

283. Dai M, Yip YY, Hellstrom I, Hallstrom KE. Curing mice with large tumors by locally delivering combinations of immunomodulatory antibodies. Clin Cancer Res. 2015; 21 (5): 1127–38.
284. Albert JM, Cao C, Kwang WK, Willey CD, Geng L, Xiao D, et al. Inhibition of poly(ADP-ribose) polymerase enhances cell death and improves tumor growth delay in irradiated lung cancer models. Clin Cancer Res. 2007; 13 (10): 3033–42.
285. Chen DS, Mellman I. Oncology Meets Immunology: The Cancer-Immunity Cycle. Immunity. 2013; 39: 1–10.
286. Qin A, Coffey DG, Warren EH, Ramnath N. Mechanisms of immune evasion and current status of checkpoint inhibitors in non-small cell lung cancer. Cancer Med. 2016; 5 (9): 2567–78.
287. Ott PA, Hodi FS, Kaufman HL, Wigginton JM, Wolchok JD. Combination immunotherapy: A road map. J Immunother Cancer. 2017; 5 (1): 1–15.
288. Marshall R, Popple A, Kordbacheh T, Honeychurch J, Faivre-Finn C, Illidge T. Immune Checkpoint Inhibitors in Lung Cancer – An Unheralded Opportunity? Clin Oncol. 2017; 29 (4): 207–17.
289. Haanen JBAG, Robert C. Immune Checkpoint Inhibitors. Prog tumor Res. 2015; 42: 55–66.
290. Assal A, Kaner J, Pendurti G, Zang X. Emerging targets in cancer immunotherapy: Beyond CTLA-4 and PD-1. Immunotherapy. 2015; 7 (11): 1169–86.
291. Wang K, Wei G, Liu D. CD19: a biomarker for B cell development, lymphoma diagnosis and therapy. Exp Hematol Oncol [Internet]. 2012; 1 (36): 1–7.
292. Del Nagro CJ, Otero DC, Anzelon AN, Omori SA, Kolla R V, Rickert RC. CD19 Function in Central and Peripheral B-Cell Development. Immunol Res. 2005; 31 (2): 119–31.
293. De Visser KE, Eichten A, Coussens LM. Paradoxical roles of the immune system during cancer development. Nat Rev Cancer. 2006; 6 (1): 24–37.
294. Sarvaria A, Madrigal JA, Saudemont A. B cell regulation in cancer and anti-tumor immunity. Cell Mol Immunol. 2017; 14 (8): 662–74.
295. Bhattacharyya S, Saha J. Tumour, Oxidative Stress and Host T Cell Response: Cementing the Dominance. Scand J Immunol. 2015; 82 (6): 477–88.
296. Chen X, Song M, Zhang B, Zhang Y. Reactive Oxygen Species Regulate T Cell Immune Response in the Tumor Microenvironment. Oxid Med Cell Longev. 2016; 2016: 11–6.
297. Liou G-Y, Storz P. Reactive oxygen species in cancer. Free Radic Res. 2010; 44 (5): 479–92.
298. De Nicola GM, Karreth FA, Humpton TJ, Gopinathan A, Wei C, Frese K, et al. Oncogene-induced Nrf2 transcription promotes ROS detoxification and tumorigenesis. Nature. 2011; 475: 106–9.

299. Piskounova E, Agathocleous M, Murphy MM, Hu Z, Huddlestun SE, Zhao Z, et al. Oxidative stress inhibits distant metastasis by human melanoma cells. Nature. 2015; 527: 186–91.
300. Nishida N, Yano H, Nishida T, Kamura T, Kojiro M. Angiogenesis in cancer. Vasc Heal Risk Manag. 2006; 2 (3): 213–9.
301. King M, Ismail A, Davis L, Karp D. Oxidative stress promotes polarization of human T cell differentiation toward a T helper 2 phenotype. J Immunol. 2006; 176 (5): 2765–72.
302. Malmberg K, Arulampalam V, Ichihara F, Petersson M, Seki K, Andersson T, et al. Inhibition of activated/memory (CD45RO(+)) T cells by oxidative stress associated with block of NF-kappaB activation. J Immunol. 2001; 167 (5): 2595–601.
303. Bhattacharyya S, Md Sakib Hossain D, Mohanty S, Sankar Sen G, Chattopadhyay S, Banerjee S, et al. Curcumin reverses T cell-mediated adaptive immune dysfunctions in tumor-bearing hosts. Cell Mol Immunol. 2010; 7 (4): 306–15.
304. Lucey DR, Clerici M, Shearer GM. Type 1 and Type 2 Cytokine Dysregulation in Human Infectious, Neoplastic, and Inflammatory Diseases. Clin Microbiol Rev. 1996; 9 (4): 532–62.
305. Moghaddam A, Gartlan K, Kong L, Sattentau Q. Reactive carbonyls are a major Th2-inducing damage-associated molecular pattern generated by oxidative stress. J Immunol. 2011; 187 (4): 1626–33.
306. Kwajah S, Schwarz H. CD137 ligand signaling induces human monocyte to dendritic cell differentiation. Eur J Immunol. 2010; 40 (7): 1938–49.
307. Kaminski M, Kiessling M, Suss D, Krammer PH, Gulow K. Novel Role for Mitochondria: Protein Kinase C-Dependent Oxidative Signaling Organelles in Activation-Induced T-Cell Death. Mol Cell Biol. 2007; 27 (10): 3625–39.
308. Jackson S, Devadas S, Kwon J, Pinto L, Williams M. T cells express a phagocyte-type NADPH oxidase that is activated after T cell receptor stimulation. Nat Immunol. 2004; 5 (8): 818–27.
309. Kwon J, Shatynski K, Chen H, Morand S, de Deken X, Miot F, et al. The nonphagocytic NADPH oxidase Duox1 mediates a positive feedback loop during T cell receptor signaling. Sci Signal. 2010; 3 (133): ra59.
310. Kim HR, Lee A, Choi EJ, Hong MP, Kie JH, Lim W, et al. Reactive oxygen species prevent imiquimod-induced psoriatic dermatitis through enhancing regulatory T cell function. PLoS One. 2014; 9 (3): 1–14.
311. Greten TF, Manns MP, Korangy F. Myeloid derived suppressor cells in human diseses. Int Immunopharmacol. 2011; 11 (7): 802–7.
312. Church SL, Grant JW, Ridnour LA, Oberley LW, Swanson PE, Meltzer PS, et al. Increased manganese superoxide dismutase expression suppresses the malignant phenotype of human melanoma cells. Proc Natl Acad Sci. 1993; 90 (7): 3113–7.

313. Freuhauf J, Trapp V. Reactive oxygen species: an Achilles' heel of melanoma? Expert Rev Anticancer Ther. 2008; 8 (11): 1751–7.
314. Bhattacharyya S, Mandal D, Sen GS, Pal S, Banerjee S, Lahiry L, et al. Tumor-induced oxidative stress perturbs nuclear factor-κB activity-augmenting tumor necrosis factor-α-mediated T-cell death: Protection by curcumin. Cancer Res. 2007; 67 (1): 362–70.
315. Ando T, Mimura K, Johansson CC, Hanson MG, Mougiakakos D, Larsson C, et al. Transduction with the Antioxidant Enzyme Catalase Protects Human T Cells against Oxidative Stress. J Immunol. 2008; 181 (12): 8382–90.
316. Case AJ, McGill JL, Tygrett LT, Shirasawa T, Spitz DR, Waldschmidt TJ, et al. Elevated mitochondrial superoxide disrupts normal T-cell development to impair adaptive immune responses to an influenza challenge. Free Radic Biol Med. 2011; 50 (3): 448–58.
317. Kamiński MM, Röth D, Sass S, Sauer SW, Krammer PH, Gülow K. Manganese superoxide dismutase: A regulator of T cell activation-induced oxidative signaling and cell death. Biochim Biophys Acta Mol Cell Res. 2012; 1823 (5): 1041–52.
318. Liu Y, Wei J, Zhou J. Norepinephrine-induced myeloid-derived suppressor cells block T-cell responses via generation of reactive oxygen species. Immunopharmacol Immunotoxicol. 2015; 37 (4): 359–65.
319. Kaminski MM, Sauer SW, Klemke CD, Suss D, Okun JG, Krammer PH, et al. Mitochondrial Reactive Oxygen Species Control T Cell Activation by Regulating IL-2 and IL-4 Expression: Mechanism of Ciprofloxacin-Mediated Immunosuppression. J Immunol. 2010; 184 (9): 4827–41.
320. Gangopadhyay N, Luketich J, Opest A, Visus C, Meyer E, Landreneau R, et al. Inhibition of poly(ADP-ribose) polymerase (PARP) induces apoptosis in lung cancer cell lines. Cancer Invest. 2011; 29 (9): 608–16.
321. Cemerski S, Cantagrel A, Van Meerwijk JP, Romagnoli P. Reactive Oxygen Species Differentially Affect T Cell Receptor-signalling Pathways. J Biol Chem. 2002; 277 (22): 19585–93.
322. K. Murali A, Mehrotra S. Apoptosis – an Ubiquitous T cell Immunomodulator. J Clin Cell Immunol. 2012; S3 (2): 1–17.
323. Devadas S, Zaritskaya L, Rhee SG, Oberley L, Williams MS. Discrete Generation of Superoxide and Hydrogen Peroxide by T Cell Receptor Stimulation. J Exp Med. 2002; 195 (1): 59–70.
324. Simula L, Nazio F, Campello S. The mitochondrial dynamics in cancer and immune-surveillance. Semin Cancer Biol. 2017; 47: 29–42.
325. Maher S, Toomey D, Condron C, Bouchier-Hayes D. Activation-induced cell death: the controversial role of Fas and Fas ligand in immune privilege and tumour counterattack. Immunol Cell Biol. 2002; 80 (2): 131–7.

326. Li-Weber M, Weigand MA, Giaisi M, Süss D, Treiber MK, Baumann S, et al. Vitamin E inhibits CD95 ligand expression and protects T cells from activation-induced cell death. J Clin Invest. 2002; 110 (5): 681–90.
327. Tabbekh M, Franciszkiewicz K, Haouas H, Lecluse Y, Benihoud K, Raman C, et al. Rescue of Tumor-Infiltrating Lymphocytes from Activation-Induced Cell Death Enhances the Antitumor CTL Response in CD5-Deficient Mice. J Immunol. 2011; 187 (1): 102–9.
328. Curtale G, Citarella F, Carissimi C, Goldoni M, Carucci N, Fulci V. An emerging player in the adaptive immune response : microRNA-146a is a modulator of IL-2 expression and activation-induced cell death in T lymphocytes. Blood. 2010; 115 (2): 265–74.
329. Grimm M, Kim M, Rosenwald A, Von Raden B, Tsaur I, Meier E, et al. Tumour-mediated TRAIL-Receptor expression indicates effective apoptotic depletion of infiltrating CD8+ immune cells in clinical colorectal cancer. Eur J Cancer. 2010; 46 (12): 2314–23.
330. Bezu L, Gomes-da-Silva LC, Dewitte H, Breckpot K, Fucikova J, Spisek R, et al. Combinatorial strategies for the induction of immunogenic cell death. Front Immunol. 2015; 6 (187): 1–11.
331. Zhong Z, Sanchez-Lopez E, Karin M. Autophagy, Inflammation, and Immunity: A Troika Governing Cancer and Its Treatment. Cell. 2016; 166 (2): 288–98.
332. Kepp O, Senovilla L, Vitale I, Vacchelli E, Adjemian S, Agostinis P, et al. Consensus guidelines for the detection of immunogenic cell death. Oncoimmunology. 2014; 3 (9): e955691.
333. Huang R, Xu Y, Wan W, Shou X, Qian J, You Z, et al. Deacetylation of nuclear LC3 drives autophagy initiation under starvation. Mol Cell. 2015; 57 (3): 456–67.
334. Janji B, Viry E, Moussay E, Paggetti J, Arakelian T, Mgrditchian T, et al. The multifaceted role of autophagy in tumor evasion from immune surveillance. Oncotarget. 2016; 7 (14): 17591–607.
335. Jin Y, Hong Y, Park CY, Hong Y. Molecular interactions of autophagy with the immune system and cancer. Int J Mol Sci. 2017; 18 (1694): 1–10.
336. Viry E, Noman MZ, Arakelian T, Lequeux A, Chouaib S, Berchem G, et al. Hijacker of the Antitumor Immune Response: Autophagy Is Showing Its Worst Facet. Front Oncol. 2016; 6 (246): 1–10.
337. Li C-J, Wan-Ting L, Meng-Yu W, Pei-Yi C. New insights into the role of autophagy in tumor immune microenvironment. Int J Mol Sci. 2017; 18 (1566): 1–14.
338. Pan H, Chen L, Xu Y, Han W, Lou F, Fei W, et al. Autophagy-associated immune responses and cancer immunotherapy. Oncotarget. 2015; 7 (16): 21235–46.

339. Noman MZ, Janji B, Kaminska B, Van Moer K, Pierson S, Przanowski P, et al. Blocking hypoxia-induced autophagy in tumors restores cytotoxic T-cell activity and promotes regression. Cancer Res. 2011; 71 (18): 5976–86.
340. Noman MZ, Buart S, Van Pelt J, Richon C, Hasmim M, Leleu N, et al. The Cooperative Induction of Hypoxia-Inducible Factor-1 and STAT3 during Hypoxia Induced an Impairment of Tumor Susceptibility to CTL-Mediated Cell Lysis. J Immunol. 2009; 182 (6): 3510–21.
341. Yu H, Kortylewski M, Pardoll D. Crosstalk between cancer and immune cells: role of STAT3 in the tumour microenvironment. Nat Immunol. 2007; 7: 41–51.
342. Wang T, Niu G, Kortylewski M, Burdelya L, Shain K, Zhang S, et al. Regulation of the innate and adaptive immune responses by Stat-3 signaling in tumor cells. Nat Med. 2003; 10: 48–54.
343. Borthwick LA. The IL-1 cytokine family and its role in inflammation and fibrosis in the lung. Semin Immunopathol. 2016; 38 (4): 517–34.
344. Iannitti RG, Napolioni V, Oikonomou V, De Luca A, Galosi C, Pariano M, et al. IL-1 receptor antagonist ameliorates inflammasome-dependent inflammation in murine and human cystic fibrosis. Nat Commun. 2016; 7.
345. Buchser WJ, Laskow TC, Pavlik PJ, Lin H-M, Lotze MT. Cell-mediated Autophagy Promotes Cancer Cell Survival. Cancer Res. 2012; 72 (12): 2970–9.
346. Baginska J, Viry E, Berchem G, Poli A, Noman MZ, van Moer K, et al. Granzyme B degradation by autophagy decreases tumor cell susceptibility to natural killer-mediated lysis under hypoxia. Proc Natl Acad Sci. 2013; 110 (43): 17450–5.
347. Ladoire S, Enot D, Senovilla L, Ghiringhelli F, Poirier-Colame V, Chaba K, et al. The presence of LC3B puncta and HMGB1 expression in malignant cells correlate with the immune infiltrate in breast cancer. Autophagy. 2016; 12 (5): 864–75.
348. Ma X, Piao S, Wang D, Mcafee Q, Nathanson KL, Lum JJ, et al. Measurements of tumor cell autophagy predict invasiveness, resistance to chemotherapy, and survival in melanoma. Clin Cancer Res. 2011; 17 (10): 3478–89.